The Role of the Myelin and Lymphocyte Protein (MAL) in Breast and Ovarian Cancer

by

Hisani N. Horne

Department of Pathology
Duke University

Date:_____

Approved:

_____
Jeffrey R. Marks, PhD, Supervisor

_____
Gerard C. Blobe, MD, PhD

_____
Mark W. Dewhirst, DVM, PhD

_____
Joseph Geradts, MD, MA

_____
Laura P. Hale, MD, PhD

Dissertation submitted in partial fulfillment of
the requirements for the degree of Doctor
of Philosophy in the Department of
Pathology in the Graduate School
of Duke University

2010

ABSTRACT

The Role of the Myelin and Lymphocyte Protein (MAL) in Breast and Ovarian Cancer

by

Hisani N. Horne

Department of Pathology
Duke University

Date:_____

Approved:

_____
Jeffrey R. Marks, PhD, Supervisor

_____
Gerard C. Blobe, MD, PhD

_____
Mark W. Dewhirst, DVM, PhD

_____
Joseph Geradts, MD, MA

_____
Laura P. Hale, MD, PhD

An abstract of a dissertation submitted in partial
fulfillment of the requirements for the degree
of Doctor of Philosophy in the Department of
Pathology in the Graduate School
of Duke University

2010

Abstract

MAL (myelin and lymphocyte protein), has been implicated in several malignancies including esophageal, gastric, and cervical cancers. We have demonstrated that the MAL protein is expressed in the normal breast epithelium, and aberrantly expressed in breast cancer. Bisulfite sequencing of the MAL promoter CpG island revealed hypermethylation in breast cancer cell lines and 69% of primary tumors analyzed compared with normal breast epithelial cells. Differential methylation between normal and cancer DNA was confined to the proximal promoter region. In a subset of breast cancer cell lines, promoter methylation correlated with transcriptional silencing that was reversible with the methylation inhibitor decitabine. Furthermore, exogenous expression of MAL in breast cancer cell lines resulted in decreased cell proliferation, motility, reduced cell invasion through Matrigel and suppressed anchorage-independent growth in soft agar. In a cohort of 122 primary breast tumors, immunohistochemical analysis revealed that the MAL protein was an independent predictor of benefit from adjuvant chemotherapy. Moreover, overexpression of MAL in triple-negative MDA-MB-468 and BT20 breast cancer cell lines was sufficient to confer sensitivity to epidermal growth factor receptor (EGFR)-tyrosine kinase inhibition and was associated with reduced phosphatidylinositol-3 kinase (PI3K)/Akt signaling. Immunohistochemistry studies conducted on 144 late-stage serous ovarian cancers

showed that MAL expression was a significant predictor of survival. Knockdown of MAL expression in the SKOV8 ovarian cancer cell line reduced cell proliferation and resulted in increased sensitivity to the chemotherapeutic drug carboplatin. Thus, we have identified the MAL gene as a novel epigenetically regulated gene in breast cancer with implications for response to chemotherapy in both breast and ovarian cancer. Furthermore, we have shown that the MAL protein has predictive and prognostic value in breast and ovarian cancers, respectively.

Dedication

To my beloved little sister Aina Horne, although you are absent in body your beautiful spirit continues to brighten my day. My work is dedicated to you.

Table of Contents

Abstract iv

List of Tables xi

List of Figures xii

Abbreviations xv

Acknowledgements xvi

1. Introduction 1

    1.1 Breast cancer background 1

    1.2 Myelin and lymphocyte (MAL) protein 3

    1.3 Role of MAL in cancer development 4

    1.4 Membrane rafts or "lipid rafts" 6

    1.5 Intracellular signaling through membrane rafts 7

2. Experimental Procedures 10

    2.1 Cell Culture 10

    2.2 Generating Stable and Transient Transfectants 11

    2.3 Cell Treatments 12

        2.3.1 Reactivation with DAC 12

        2.3.2 Serum Starvation and EGF Stimulation 13

        2.3.3 EGFR Inhibition with AG1478 13

    2.4 Methylation Analyses 13

    2.5 Quantitative RT-PCR 16

2.6 Laser Capture Microdissection 17
2.7 Immunohistochemical Analysis 17
2.7.1 Breast Tissue 17
2.7.2 Ovarian Tissue 19
2.8 Immunoblot Analysis 20
2.9 Detergent Extraction Procedures 20
2.10 In Vitro Wound-Healing Assay 21
2.11 Soft Agar Assay 21
2.12 Cell Cycle Analysis 22
2.13 Proliferation Assay 22
2.14 Growth Response in AG1478 23
2.15 3-D Culturing of MCF10A Cells 23
2.16 Immunofluorescence 23
2.17 Caspase 3/7 Luminescence Assay 25
2.18 Matrigel Invasion Assay 25
2.19 Antibodies Utilized 27
3. MAL is a Novel Epigenetically Regulated Gene in Breast Cancer 28
3.1 Introduction 28
3.2 Results 31
3.2.1 The MAL promoter is commonly methylated in breast cancer cell lines. 31
3.2.2 Methylation of the MAL promoter in primary breast tumors 34

3.2.3 Methylation-specific PCR confirms methylation in both breast cancer cell lines and primary tumor samples 40

3.2.4 Differential methylation in the MAL promoter is confined to the proximal promoter region 43

3.2.5 MAL promoter methylation is associated with gene silencing 47

3.2.6 MAL mRNA expression in primary breast tumors is variable and does not directly correlate with promoter methylation status 53

3.3 Discussion 57

4. Biological Consequences of Aberrant MAL Expression in Breast Cancer 66

4.1 Introduction 66

4.2 Results 69

4.2.1 Stable breast cell lines utilized in MAL functional studies 69

4.2.2 Sub-cellular localization of the MAL-V5 protein 74

4.2.3 Effect of MAL expression on cell growth and cell cycle progression 77

4.2.4 Exogenous expression of MAL decreases anchorage independent growth in soft agar 82

4.2.5 Expression of MAL reduces cell migration and invasion through Matrigel 84

4.2.6 MAL overexpression disrupts acinar structure in MCF10A cells grown in three-dimensional Matrigel culture 88

4.2.7 The MAL protein is expressed in normal breast tissue 90

4.2.8 MAL protein expression has predictive value in primary breast cancer 95

4.3 Discussion 101

5. Role of the MAL Protein in Cancer-Related Cell Signaling 109

5.1 Introduction 109

5.2 Results 112

5.2.1 Expression of MAL results in altered membrane raft composition 112

5.2.2 EGF drives migration of MAL-V5 both in and out of membrane rafts 114

5.2.3 Expression of MAL sensitizes breast cancer cell lines to the EGFR inhibitor AG1478 118

5.2.4 MAL expression does not enhance AG1478 anti-tumor effects in MCF10A cells 131

5.2.5 MAL expression in membrane rafts coincides with the exclusion of signaling molecules 134

5.3 Discussion 137

6. Examining the Consequences of Aberrant MAL Expression in Ovarian Cancer 144

6.1 Introduction 144

6.2 Results 147

6.2.1 MAL protein expression is an independent predictor of poor survival in advance serous ovarian cancer 147

6.2.2 Characterizing the effects of altered MAL expression in ovarian cancer cell lines 150

6.3 Discussion 152

7. Summary 156

References 161

Biography 174

List of Tables

Table 1. Clinico-pathologic features of patients by methylation status 38

Table 2. Clinico-pathologic features of patients by MAL IHC 98

Table 3. Clinico-pathologic features of patients stratified by chemotherapy received ... 100

Table 4. Cox multivariate analysis by survival in advanced ovarian cancer 149

List of Figures

Figure 3-1. Methylation of the MAL promoter region in breast cancer and reactivation of expression by DAC 32

Figure 3-2. Methylation of the MAL promoter region in primary breast tumors 36

Figure 3-3. Profile of MAL promoter methylation in ductal carcinoma in situ (DCIS) samples 39

Figure 3-4. Methylation-specific PCR confirms bisulfite sequencing analysis in breast cell lines 41

Figure 3-5. Methylation-specific PCR analysis of the MAL promoter region 42

Figure 3-6. Profile of MAL promoter methylation at the transition point 44

Figure 3-7. Cancer-related methylation confined to the proximal MAL promoter region 46

Figure 3-8. Dose-dependent reactivation of MAL expression with DAC 49

Figure 3-9. Reactivation of MAL expression with DAC in a panel of breast cell lines 50

Figure 3-10. Expression analysis of the basal levels of MAL mRNA 52

Figure 3-11. MAL mRNA expression in primary tumors 55

Figure 3-12. Comparing MAL mRNA levels to the levels of T cell-specific genes 56

Figure 4-1. Overexpression of MAL-V5 in breast epithelial cells 72

Figure 4-2 Knockdown of MAL expression in DU99 cells 73

Figure 4-3. MAL-V5 subcellular localization in MCF7 cells 75

Figure 4-4. MAL-V5 localizes to membrane rafts 76

Figure 4-5. Effect of MAL expression on cell cycle progression 79

Figure 4-6. Effect of MAL overexpression on the rate of cell growth 81

Figure 4-7. MAL expression reduces anchorage-independent growth 83

Figure 4-8. MAL overexpression reduces cell migration 85

Figure 4-9. MAL expression reduced cell invasion through Matrigel 87

Figure 4-10. Effect of MAL on acini formation in MCF10A cells 89

Figure 4-11. The MAL protein is expressed in normal breast tissue 91

Figure 4-12. MAL protein expression and survival analysis in breast cancer patients 97

Figure 4-13. Survival analysis of breast cancer patients by adjuvant chemotherapy treatment 99

Figure 5-1. MAL expression alters membrane raft composition 113

Figure 5-2. EGF induces MAL-V5 migration out of membrane raft fractions in MCF10A cells 116

Figure 5-3. EGF induces MAL-V5 accumulation in membrane raft fractions in MCF7 cells 117

Figure 5-4. Exogenous MAL expression decreases the baseline levels of activated Akt 124

Figure 5-5. MAL expression increases the sensitivity of MD468 breast cancer cells to AG1478 125

Figure 5-6. MAL-dependent decrease in phosphorylated-Akt with low dose AG1478 treatment 127

Figure 5-7. MAL expression increases the sensitivity of BT20 breast cancer cells to AG1478 129

Figure 5-8. No effect of MAL expression on MCF10A response to AG1478 132

Figure 5-9. MAL expression in membrane raft fractions coincides with the exclusion of signaling molecules 134

Figure 6-1. Immunodetection of MAL protein in primary ovarian tissues and relation to disease outcome 148

Figure 6-2. Variable MAL protein levels in ovarian cancer cell lines 151

Abbreviations

MAL = myelin and lymphocyte protein

PI3K = phosphatidylinositol-3 kinase

EGFR = epidermal growth factor receptor

DAC = 5-Aza-2'-deoxycytidine/decitabine

MSP = methylation-specific PCR

HMEC = human mammary epithelial cells

PBS = phosphate buffered saline

DSF = detergent soluble fraction

DIF = detergent insoluble fraction

SD = sub-diploid

LCM = laser capture microdissection

WB = western blot

bp = base pair

kDa = kiloDalton

Acknowledgements

I am truly grateful to everyone who has played a part in helping me accomplish this momentous task of completing my graduate studies. The Marks/Olson lab members have been a great source of knowledge and personal support. I would like to thank my advisor Dr. Jeffrey Marks, for his wisdom and guidance throughout my tenure at Duke. I would also like to personally thank Gudrun Huper who taught me a great deal of my lab techniques and was a constant source of encouragement and support; and Nancy Glover who provided assistance with the immunohistochemical studies.

I am extremely fortunate to have a wide network of family and friends who are a constant source of support. My parents, Carol and Danny Horne, my sisters NiGia, Maati, and Aina, and my brothers Christian and Ira; without them none of this would be possible. I am also grateful to my best friend Ernest Madison who has never doubted my ability to succeed. Also, a huge thank you to my daughter Ania Madison who is a daily reminder of the important things in life. To everyone who baby sat Ania allowing me to make late night trips to the lab, I owe you an enormous amount of gratitude.

I would also like to thank my committee members Dr. Gerard Blobe, Dr. Mark Dewhirst, Dr. Joseph Geradts, and Dr. Laura Hale for their academic guidance during my studies and willingness to provide constructive criticism. I must also extend a special thank you to Dr. Susan Murphy who has been an invaluable resource.

1. Introduction

1.1 Breast cancer background

According to the National Cancer Institute, the breast is the number one site of cancer occurrence in women. In 2009, there were an estimated 192,000 new cases in women with over 40,000 deaths in the United States alone (1). These statistics speak to the gravity of breast cancer and why it is such a significant health problem with regards to both incidence and mortality. Consequently, researchers are focused on elucidating novel early detection and treatment methods that will lessen the burden of cancer on society while working toward the ultimate goal of a cure.

One model for the progression of breast cancer involves it's initiation as the premalignant stage of atypical ductal hyperplasia, progression into the preinvasive stage of ductal carcinoma *in situ*, and culminating in the potentially lethal stage of invasive ductal carcinoma (2). The molecular basis underlying the progression of breast cancer from premalignant to invasive is still being actively investigated. Using microarray analysis to analyze the transcriptome of premalignant, preinvasive and invasive stages of breast cancer, Ma *et al.* found that the three distinct stages are highly similar to each other at the level of the transcriptome (3). Their finding supports the idea that genes conferring invasive growth are active in the preinvasive stages. Therefore, it is critical to identify and characterize genes that are altered early in the transformation process.

No single genetic mutation can initiate cancer progression; on the contrary, neoplasia is a multi-step process resulting in the accumulation of various genetic and/or epigenetic events. A simplified view of cancer development can be summed up as an imbalance between the rate of cell growth and programmed cell death or apoptosis. The expression of tumor suppressor genes and oncogenes are frequently altered during cancer development and progression. Tumor suppressor genes are involved in slowing down cell growth and inducing apoptosis while oncogenes facilitate uncontrolled proliferation. Both loss-of-function mutations in tumor suppressor genes and gain-of-function mutations in oncogenes contribute to the malignant phenotype (4)

There are a score of molecular gatekeepers charged with maintaining the delicate balance between cell proliferation and cell death in breast tissue. Several of these proteins are found in signaling pathways commonly mutated in breast cancer including but not limited to PI3K/Akt (5), p53 (6), and Ras/Raf/MAPK (7) pathways. Furthermore, receptor tyrosine kinases (RTKs) such as EGFR lie upstream of these pathways and are often altered during cancer progression. Bearing in mind the plasma membrane association of RTKs and other signaling molecules, the role of membrane dynamics in cancer progression is increasingly relevant.

Given the heterogeneous nature of breast cancer, designing effective therapies is complicated by the uncertainty of which patients will respond to a given treatment. The traditional chemotherapeutics are becoming less appealing for clinical use due to their

global cell death properties and subsequent toxicity issues. As a consequence research funds are being allocated to designing novel targeted cancer therapies, many of which are in clinical trials or currently FDA approved (8). Targeted therapies are designed to act directly against cancer cells, sparing their normal counterparts from cell death. An understanding of the varied molecular background of cancer patients has facilitated the design of these drugs. However, identifying novel molecular targets for breast cancer detection, diagnosis, and response to therapy is vital.

1.2 Myelin and lymphocyte (MAL) protein

The gene under investigation in this study, myelin and lymphocyte protein (MAL) was first identified in a screen for genes differentially expressed during T cell development (9). The MAL gene encodes a 17 kDa transmembrane domain protein selectively found in glycolipid enriched membrane (GEM) rafts or lipid rafts where it mediates the formation of apical transport vesicles (10-12). The myelin and lymphocyte protein is an itinerant protein, cycling between the trans-golgi network (TGN) and the plasma membrane (13). MAL contains a MARVEL (MAL and related proteins for vesicle trafficking and membrane link) domain which is shared by proteins associated with membrane juxtaposition events (14). Knockout mice for the MAL protein were viable, had a normal life span and appeared grossly normal. However, a closer examination revealed defects in axon-glia interactions in the central nervous system (15). Initially MAL was thought to be a T cell specific protein but was subsequently demonstrated to

be expressed in a wide range of human cell types (16). Although this particular study did not investigate MAL expression in human breast epithelial cells, our studies have confirmed that it is expressed in this tissue as well.

MAL's known function is in GEM-mediated apical sorting of membrane and secretory proteins in polarized epithelial cells (17, 18). However, the mechanism of MAL function in lipid-raft mediated apical sorting is unknown. Increased MAL expression in polarized Madin-Darby canine kidney cells resulted in increased apical delivery where as RNAi directed against MAL caused accumulation of protein in the Golgi, impaired apical transport, and/or loss of polarity (17, 19). In renal epithelial cells, MAL was shown to increase the phosphorylation state and apical surface expression of aquaporin-2 by attenuating its internalization (20) indicating the involvement of MAL in the cell surface retention of apical membrane proteins.

1.3 Role of MAL in cancer development

Several studies have implicated MAL in the etiology of various human cancer types. Hatta and colleagues reported down-regulation of MAL mRNA in seventy percent of primary cervical squamous cell cancers tested when compared to corresponding non-cancerous uterine squamous cells suggesting that MAL plays an important role in cervical cancer development (21). A more recent study published in 2009 identified promoter methylation as the cause of MAL gene silencing in cervical cancer, demonstrating a direct correlation between methylation and reduced MAL

mRNA expression (22). In esophageal cancer MAL has been suggested to be a tumor suppressor gene based on studies which showed that MAL expression repressed the formation of tumors induced by TE3 cells in nude mice, inhibited cell motility, and produced apoptosis (23). MAL gene expression is frequently downregulated in head and neck squamous cell carcinomas and was recently identified as a candidate metastasis suppressor gene in this cancer type (24). Alterations in the expression and/or subcellular distribution of MAL was observed in renal and thyroid neoplasms implying that MAL expression may not have to be completely extinguished to contribute to the cancer phenotype but aberrant protein localization may be a factor as well (16). These findings taken together demonstrate a critical role for MAL in the development and progression of a variety of cancer types.

Of late, several labs have identified MAL as an important prognostic and predictive factor in various cancers. Tracey and colleagues found that MAL was overexpressed in T cell lymphoma cells resistant to interferon-alpha therapy (25). Furthermore, MAL expression was associated with longer time to complete remission in T cell lymphoma patients. In Hodgkin's lymphoma, MAL protein expression identified a sub-set of patients with poor prognosis (26). On the other hand, MAL promoter hypermethylation is a prognostic marker in gastric cancer as well as a marker of early colon tumorigenesis (27, 28). A recent study published out of our lab found that elevated MAL expression was accompanied by promoter hypomethylation and platinum

resistance in ovarian cancer (29). Therefore, both MAL expression and MAL gene promoter methylation are relevant prognostic and predictive factors.

Interest in the MAL gene in our laboratory arose from a microarray study demonstrating that MAL was the most differentially expressed transcript between serous ovarian cancers with good versus poor outcome (30). This finding led us to examine MAL transcriptional regulation in ovarian (31) and breast cancer. Our findings confirm that high levels of MAL expression are characteristic of ovarian cancer while loss of expression is associated with breast cancer. Consistent with the manuscripts reviewed above, it appears that the manner in which MAL expression is disrupted in cancer is tissue- and cell-type specific.

1.4 Membrane rafts or "lipid rafts"

The lipid raft hypothesis was formulated over twenty years ago (32-35) originating from studies on epithelial cell polarity; its central theme was the existence of lipid rafts, areas of the plasma membrane enriched in cholesterol and sphingolipids. Membrane rafts are further defined as small (10-200 nm), heterogeneous, highly dynamic, sterol- and sphingolipid-enriched domains that compartmentalize cellular processes (36). In the literature, lipid rafts are referred to by many different names: detergent-insoluble glycolipid-rich domains (DIGs), glycolipid-enriched membranes (GEMs), and low-density Triton-insoluble (LDTI) complexes (37). In a Keystone symposium in 2006 dedicated to defining lipid rafts and their cellular functions, the term

"lipid raft" was discarded in favor of the term "membrane raft"(36). Thus, for the remainder of the dissertation, we will use the term membrane rafts when referring to these structures. Functionally, membrane rafts facilitate selective protein-protein interactions by selectively excluding or including proteins at the membrane (38). Experimentally, membrane rafts are characterized by resistance to solubilization in non-ionic detergents such as Triton X-100 at low temperatures and are often referred to as detergent-resistant membrane domains (39).

The existence and biological importance of these structures has long been controversial (40) although recently widely accepted (35, 41), in principal because it has been difficult to prove definitively their presence in living cells. However, using a novel fluorescence correlation spectroscopy strategy, Lasserre and colleagues were able to identify highly dynamic nanoscale membrane organizations in live cells (42). Their study confirmed the existence of membrane nanodomains in both the inner and outer leaflets of the plasma membrane. Furthermore, they found that nanodomains play a crucial role in triggering the PI3K/Akt signaling pathway, by facilitating Akt recruitment and activation upon phosphatidylinositol-3,4,5-triphosphate (PIP_3) accumulation in the plasma membrane (42).

1.5 Intracellular signaling through membrane rafts

It has long been accepted that the plasma membrane is a crucial component of intracellular signaling pathways. The membrane houses key signaling molecules such as

receptor tyrosine kinases and heterotrimeric G-proteins, facilitating ligand-receptor and protein-protein interactions. Similar to the bulk plasma membrane, the integrity of specialized membrane rafts is also critical to regulating signal transduction pathways. Membrane rafts are thought to function as platforms for signal transduction. Moreover, several signaling molecules relevant to carcinogenesis have been shown to localize to these domains including the epidermal growth factor receptor (EFGR) (43), Src family tyrosine kinases, HRAS and platelet-derived growth factor receptor (PDGF-R) (37). Disruption of membrane rafts via membrane cholesterol depletion (44-46) or inhibition of sterol and sphingolipid synthesis (42) were shown to have marked effects on cell signaling via EGFR. Also, the integrity of membrane rafts was critical for membrane EGFR levels (47) and EGF-induced chemotaxis (48) in human breast cancer cells.

As stated previously, the MAL protein resides in membrane rafts and facilitates the formation of transport vesicles. Several studies in T cells have highlighted the importance of MAL in signaling processes. MAL was shown to physically associate with src-like kinases including Fyn and Lck, both key components in T cell signaling (11). More importantly, MAL was shown to mediate the targeting of Lck to the plasma membrane by allowing recruitment of Lck to specialized intracellular membrane rafts and the formation of specific transport carriers for Lck targeting (49). This novel transport pathway involving the MAL protein is crucial for T cell receptor mediated signaling.

Our previous microarray analysis in advanced serous ovarian cancers identified the MAL transcript as the most differentially expressed when comparing short-term and long-term survivors. This initial finding has served as the basis of my thesis work in which I have studied the role that the MAL gene plays in both breast and ovarian carcinogenesis. The following body of work will begin by examining the transcriptional regulation of the MAL gene in breast cancer. We then progress to *in vitro* studies that explore the biological consequences of aberrant MAL expression in a panel of breast cell lines. Also, additional *in vitro* experiments will examine the role of the MAL protein in response to chemotherapy. Finally, our clinical studies in both breast and ovarian cancer investigate the prognostic and predictive value of the MAL protein.

2. Experimental Procedures

2.1 Cell Culture

All of the cell lines were maintained in a 37°C incubator with 5% CO_2. The human breast cancer cell lines MCF7, MDA-MB-468 (MD468), T47D, ZR75-1, BT474, HCC1937 and BT-20 were obtained from the American Type Culture Collection and maintained in RPMI 1640 medium supplemented with 10% heat-inactivated fetal bovine serum (FBS) (Life Technologies, Inc.; Grand Island, NY) and 1% penicillin/streptomycin. Benign breast epithelial cultures and lines were also used in these studies and were cultured in DFCI medium (50). Primary human mammary epithelial cells (HMEC) were obtained from women undergoing reduction mammoplasty with no evidence of cancer. The 26NC cell line is a chemically immortalized (dimethylbenzanthracene) derivative of the 26N primary culture and has been maintained in our laboratory for over 10 years (51). The BE20E6 line was immortalized by stable transfection of a plasmid expressing the human papillomavirus (HPV) E6 gene (provided by Ray White, University of Utah) and MCF10A are spontaneously immortalized adherent mammary epithelial cells obtained from the Michigan Cancer Foundation. DU99 cells are telomerase immortalized human mammary epithelial cells derived at Duke University Medical Center.

The human ovarian cancer cell lines SKOV8 and SKOV4 were a kind gift from of Dr. Susan K. Murphy (Duke University Medical Center, Durham, NC). They were

maintained in RPMI 1640 medium supplemented with 10% heat-inactivated fetal bovine serum (FBS) (Life Technologies, Inc.) and 1% penicillin/streptomycin.

2.2 Generating Stable and Transient Transfectants

For stable transfection of MAL, the MAL coding sequence (bases 60-518, accession #NM002371) was PCR-amplified, sequence-verified and inserted into the Gateway entry vector pDONR 221 (Invitrogen; Carlsbad, CA). Once in pDONR 221 the coding region was sub-cloned into pDEST 40, a C-terminal V5-tagged Gateway expression vector (Invitrogen) using the LR recombination reaction following the manufacturer's protocol. Transfection of pDEST40-MALV5 into MCF7, MCF10A and MDA-MB-468 cells was performed using Lipofectin (Invitrogen) or GenePORTER (Genlantis, Inc.; San Diego, CA) following the supplier's protocol. Control cell lines were established by transfecting an empty expression plasmid, pcDNA 3.1(+) (Invitrogen), into the respective parental cell lines. The efficiency for each transfection was analyzed by a GFP-containing plasmid. The selection of positive clones was carried out with 500-800 μg G418 sulfate (CellGro; Manassas, VA). After 3 weeks, several clones of MCF7, MCF10A, and MDA-MB-468 cells expressing MAL-V5 were isolated by cloning cylinders and expanded under continued selection. For transiently transfected cells, the transfection was performed as above and cells were harvested 48 h after transfection.

For stable knockdown of MAL expression, we obtained a MAL shRNA clone (Clone ID: V2HS_151541) from The Hannon-Elledge human retroviral shRNA collection,

which has been previously described (52) and is distributed by Open Biosystems (Huntsville, AL). Transfection of DU99 cells was performed using Lipofectin (Invitrogen), following the supplier's protocol. Control cell lines were established by transfecting a non-silencing shRNA control vector (Open Biosystems; Cat No. RHS1703) into the respective parental cell lines. The efficiency for each transfection was analyzed using a GFP-containing vector. Selection of positive clones was carried out with 1 μg/mL puromycin (Sigma; St. Louis, MO). Isolation and expansion of stable clones was done as described above.

The ovarian cancer cell lines SKOV8 and SKOV4 were stably transfected with shMAL and MAL-V5 respectively, using Lipofectin (Invitrogen) following the supplier's protocol. The selection of positive clones was done as described above using G418 for the MAL-V5 clones and puromycin for the shMAL clones.

2.3 Cell Treatments

2.3.1 Reactivation with DAC

Both benign and cancer cells were treated with 5 μM DAC (Decitabine/5-Aza-2'-deoxycytidine, Sigma) from a 200 mM stock dissolved in 50% acetic acid for 24 h. All treatments were carried out in complete medium with cells in logarithmic growth phase. Control cultures were treated with the vehicle only. Following treatment, cells were harvested and total RNA extracted using the Qiagen RNeasy Mini Kit (Qiagen; Valencia, CA).

2.3.2 Serum Starvation and EGF Stimulation

To examine the effects of EGF stimulation for short periods (0-1 h), cells were serum-starved overnight and then stimulated at the indicated time points in a 37°C incubator with 50 ng/mL EGF. After stimulation with EGF, cells were washed twice with ice cold PBS and prepared for detergent extraction to enrich for membrane rafts (see section 2.9 Detergent Extraction Procedures) followed by immunoblot analysis (see section 2.8 Immunoblot Analysis).

2.3.3 EGFR Inhibition with AG1478

The EGFR inhibitor Tyrphostin (tyrosine phosphorylation inhibitor) AG1478 (Sigma) was reconstituted in a 1:1 mixture of methanol and DMSO at a working concentration of 10 mM. For EGFR inhibition, cells were plated and allowed to grow for 24-48 h and then treated with varying concentrations of AG1478 at various time points (see figure legends). Control cultures were treated with a 1:1000 dilution of vehicle only. For 48 h treatments a second bolus of AG1478 was given to the cells after 24 h. Following treatments, cells and supernatants were collected and subsequent experiments performed.

2.4 Methylation Analyses

Bisulfite modification of genomic DNA. Sodium bisulfite modification was performed based on a protocol by Grunau et al. (53) with additional modifications to accommodate a 96-well format (54). Briefly, 1 μg of genomic DNA was denatured with 3

M NaOH for 20 min at 42°C followed by deamination in saturated sodium bisulfite/10mM hydroquinone (Sigma; St. Louis, MO) solution for 4 h at 55°C. Nuclease-free water was added to the samples in bisulfite solution and transferred to a Montage PCR96 96-well filtration plate (Millipore; Billerica, MA). All remaining steps of the protocol were performed in the Montage PCR96 96-well filtration plate using a vacuum manifold (Millipore Multiscreen Vacuum Manifold) and an in-house vacuum source. The DNA was desalted with nuclease-free water three times followed by desulfonation with 0.1 M NaOH and a final wash step with water. The DNA was recovered in 50 μL of 10 mM Tris/HCl (pH 8.0) by using a plate shaker to release the DNA from the filtration matrix for 10 min (Vortex Genie 2) followed by transfer to individual tubes and storage at 4°C.

Bisulfite sequencing. Bisulfite-treated genomic DNA was PCR-amplified with primers specific for bisulfite-converted sequences. Primer sequences include: (5'-3') **F1** GGG AGT AAT TTT TTA TTT TTA GGT AGA (forward), **F3** GTT AGA TTT ATA GTT TTT AGT TTT GG (forward), **R2** ACC AAA AAC CAC TCA CAA ACT C (reverse), **R3** AAA CCA CTA AAC AAA ATA CTA CCC (reverse), **R4** CCA AAA CTA AAA ACT ATA AAT CTA AC (reverse), and **R5** CAA AAC AAA ACC ACT TTA ATC AAA (reverse). The PCR products were resolved on agarose gels, purified using Sigma GenElute spin columns (Sigma; St. Louis, MO) followed by cycle sequencing (Thermo Sequenase Radiolabeled Terminator Cycle Sequencing Kit; Amersham Biosciences,

Piscataway, NJ). Following resolution of the sequencing reactions on denaturing polyacrylamide gels, dried gels were exposed to radiographic film (Kodak X-OMAT MR; New Haven, CT) and/or a phosphorimager screen followed by a quantitative determination of relative band intensity using the Storm PhosphorImager System and ImageQuant Software (GE Healthcare Life Sciences; Piscataway, NJ). Specimens with average methylation ranging from 40-100% were classified as heavily methylated, those exhibiting methylation levels between 5 and 40% partially methylated, and specimens with methylation levels <5% were designated as unmethylated. Methylation of DCIS samples was analyzed by fluorescence-based cycle sequencing using Big Dye Terminator Cycle Sequencing Reagents (Applied Biosystems; Foster City, CA).

Methylation-specific PCR (MSP). For analysis of the MAL promoter region, two independent primer sets were used that are designed to specifically amplify methylated and unmethylated DNA. The methylated primer set is as follows (5'-3'): forward primer GGT CGC GTA TAT TAA CGT ATT TAG C and reverse primer ACT TTA ATC AAA CGC TCC TCG TA. The unmethylated primer set is as follows (5'-3'): forward primer GGT TGT GTA TAT TAA TGT ATT TAG TGG and reverse primer CCA CTT TAA TCA AAC ACT CCT CAT A. Reactions were assembled with 40 ng template DNA, 1X PCR buffer, 3 mM MgCl2, 0.2 mM each dNTP, and 2 U Platinum Taq DNA Polymerase (Invitrogen; Carlsbad, CA) and then divided in half prior to adding 0.4 μM each primer in order to ensure even distribution of the template between the two reactions with

different primer sets. PCR conditions were as follows: 94°C for 3 min, then 35 cycles of 30 s at 94°C, 30 s at 58°C and 30 s at 72°C, followed by a 5 min extension at 72°C. PCR amplicons were resolved on 2% agarose gels and visualized by ethidium bromide staining. Universally methylated and unmethylated bisulfite modified human genomic DNA controls were used to establish reaction conditions for MS-PCR and controls in which water replaced template DNA were run for each primer set (methylated and unmethylated) alongside the specimens analyzed in each reaction.

2.5 Quantitative RT-PCR

Total RNA (1 μg) was reverse transcribed using Transcriptor RT (Roche; Basel, Switzerland). Subsequent real-time PCRs (Taqman Assays-on-Demand; Applied Biosystems, MAL-Hs00242748_m1, CD2-Hs00233515_m1, CD27-Hs00386811_m1) were done using a 1:15 dilution of the cDNA according to the manufacturer's recommendation on an ABI Prism 7900HT Sequence Detection System (Applied Biosystems) with the exception that a 25 μL reaction volume was used with 50 total cycles. The relative expression level of the target genes was obtained for each sample by normalization to the expression level of the human β-2 microglobulin (B2M) gene (Applied Biosystems, 4326319E). All target gene and B2M expression analyses were done in parallel. Results are from two separate experiments performed in triplicate. For comparison of average gene expression levels between samples, two-tailed t-tests were used to calculate significance.

2.6 Laser Capture Microdissection

The Veritas LCM system (Arcturus Engineering, Mountain View, CA) was used to obtain pure populations of ductal carcinoma in situ (DCIS), normal or malignant breast epithelial cells. Pure DCIS samples, with no invasive component, were obtained under an IRB-approved protocol from patients undergoing mastectomy's at Duke University Medical Center between 1990 and 1995. The normal breast tissue specimens were obtained from women undergoing reduction mammoplasty with no evidence of cancer. Seven-micron sections were stained with hematoxylin and areas to be captured were selected based upon cytologic morphology. DNA was extracted using the Puregene DNA extraction kit (Gentra Systems; Minneapolis, MN), followed by sodium bisulfite modification and sequence analysis as described above with the exception that the DNA was recovered in 25 μL of 10 mM Tris/HCl (pH 8.0).

2.7 Immunohistochemical Analysis

2.7.1 Breast Tissue

Tissue specimens were obtained under an IRB-approved protocol from patients undergoing breast surgery at Duke University Medical Center between 1990 and 1998. Data for the survival analysis and clinico-pathologic features listed in Table 2 were obtained from 122 invasive breast cancer patients. Interval of disease free survival was measured from the date of initial diagnosis to the date of first recurrence or the date of last follow-up. Non-cancerous tissue samples were obtained from reduction

mammoplasties. These specimens were flash frozen and maintained at -135°C. Sections of 5 μm thickness were cut, air dried, and fixed in acetone for 5 min. Immunologic detection using the anti-MAL 6D9 mouse monoclonal antibody, a kind gift from Dr. Miguel Alonso (10, 11) or mouse IgG (Vector Laboratories; Burlingame, CA) was performed on all specimens. The primary MAL antibody was received from Dr. Alonso as a mouse ascites stock and was initially titered up to a 1:5000 dilution. We utilized a 1:300 working dilution of the anti-MAL 6D9 antibody and slides were incubated at room temperature for 1 h. Human kidney was used as a positive control in all staining runs and lymphocytes, which express MAL, were used as internal positive control cells. Binding of the antibody was visualized using the ABC (Vector Laboratories) immunoperoxidase system according to the manufacturer's recommendations. An arbitrary cutoff point of >20% positively staining malignant epithelial cells was utilized to classify MAL expressing tumors. Survival curves were generated for primary breast cancer patients with the Kaplan-Meier estimate and log-rank test using the Prism statistical software (GraphPad; San Diego, CA). Significant differences between clinico-pathologic features of patient sub-groups (methylated vs. unmethylated; MAL+ vs. MAL-; Chemo+ vs. Chemo-) were calculated using chi squared analysis or Fisher's exact test when groups contained an $n<5$.

2.7.2 Ovarian Tissue

Immnohistochemical analysis was done on 144 late-stage serous cancers specimens with known outcome, obtained under an IRB-approved protocol from patients treated at both Duke University Medical Center and H. Lee Moffitt Cancer Center in Tampa, FL. Formalin-fixed, paraffin-embedded tissues were serially sectioned in 5 μm-thick sections, deparaffinized in three changes of xylene, and then rehydrated in graded alcohols. The slides were quenched for endogenous peroxidase with an aqueous solution of 3% hydrogen peroxide for 10 min. The sections were rinsed in three washes of PBS, preincubated in Background Terminator (Biocare Medical) for 5 min, then incubated in a humidity chamber with a 1:300 dilution of the anti-MAL 6D9 antibody at room temperature for 1 h. Detection was accomplished with the two-step Heuristic Pattern Reduction (HPR) method of detection, using the Universal 4plusHPR horseradish peroxidase kit and the chromogen diaminobenzidine (Biocare Medical). Slides were counterstained with hematoxylin, and dehydrated and coverslipped. A gynecologic pathologist evaluated an adjacent tissue section stained with H&E to confirm correct histology and that viable cancer was present. Staining results were expressed on a scale of 0 to 4 based on the sum of the products of the fraction (0-1.0) of cells stained at different intensities (0-4). Survival was evaluated using Kaplan-Meier [Log-rank (Mantel-Cox) Test]. Lower MAL expression was associated with improved survival no matter what staining cutoff was used. Multivariate analysis of MAL

immunostaining with clinical and demographic parameters was done using the Cox proportional hazards model on the 122 advanced-stage cases for which complete data were available.

2.8 Immunoblot Analysis

Protein sample concentrations were determined using a Bradford dye (Biorad) assay with a standard curve. For immunoblot analysis, 100-200 μg of protein was run on a Tris HCl Criterion gradient SDS-polyacrylamide gel (Biorad) under reducing conditions and transferred to Whatman nitrocellulose membranes. After blocking with 10 or 5% (w/v) nonfat dry milk, 0.1% (v/v) Tween-20 in PBS for 1 h, membranes were incubated with the primary antibody according to the manufacturer's instructions. After several washings, membranes were probed with the appropriate secondary antibody for 1 h, washed extensively, and developed using the Western Lightning Chemiluminescence Kit (PerkinElmer; Boston, MA).

2.9 Detergent Extraction Procedures

Glycolipid-enriched membranes (GEMs) were isolated by standard procedures (55). Cells were grown to confluence in 100-mm dishes, rinsed with phosphate-buffered saline and lysed for 20 min in 1 mL of 25 mM Tris-HCl, pH 7.5, 150 mM NaCl, 5 mM EDTA, 1% Triton X-100 at 4°C. The lysate was scraped from the dishes with a rubber cell scraper, the dishes were rinsed with 1 mL of the same buffer at 4°C, and the lysate was homogenized by passing the sample through a 22-gauge needle. The extract was finally

brought to 40% sucrose in a final volume of 4 mL and sequentially overlaid with 6 ml of 30% sucrose and 2 mL of 5% sucrose. Gradients were centrifuged for 18 h at 39,000 rpm at 4°C in a Beckman SW40 rotor. The opalescent band at the 5-30% sucrose interface, containing rafts, was collected as the Triton X-100 insoluble fraction whereas the 40% sucrose layer containing the load was harvested as the Triton-X soluble fraction. In experiments that show fractions 1-12, 1 mL gradient fractions were collected from the bottom gradient. Aliquots were then subjected to immunoblot analysis (see section 2.8).

2.10 In Vitro Wound-Healing Assay

Cell motility was measured using an *in vitro* wound-healing assay. Cells were seeded on six-well tissue culture plates and grown to 100% confluence. Wounds were created by scraping the monolayer with a sterile pipette tip (1mm O.D.). The wounded monolayers were washed twice with PBS to remove cell debris then incubated in fresh medium, imaged through a Nikon Diaphot inverted microscope and photographed with a Nikon D50 digital camera at 0, 12, 24, 36 and 48 hours. Replicate areas were wounded and measurements of the wound closure were made on the digital images.

2.11 Soft Agar Assay

Log-growing cells were trypsinized, counted, and diluted to $1x10^5$ cells/mL. A bottom layer of 1.5 mL of agar-media mix [0.60% agar (Difco), 50% 2X media, 10% FCS and 15% water] was placed in 2 mm grid plates (Costar) and allowed to cool. Next, 2 mL of cell suspension was mixed with 2 mL of top agar-media mix [0.60% agar, 50% 2X

media, 10% FCS, and 15% water); and 1 mL of the cell/agar mix placed on top of plates containing the bottom agar layer. This resulted in $5x10^4$ cells/plate. Soft agar plates were grown in a standard cell incubator under standard conditions (See section 2.1) for 21 days and fed gently once per week with the following: 50% 2X Media, 10% FCS. After 21 days colonies were counted and the average of 4 plates was calculated. At least two separate experiments were conducted.

2.12 Cell Cycle Analysis

Approximately 10,000 cells were resuspended in 70% ethanol prepared with 1X phosphate buffered saline (PBS) (Sigma). The cells were washed in 1X PBS (Sigma) and then resuspended in 0.5 mL of 50 μg/mL propidium iodide/0.5 mg/mL RNase/PBS (Sigma). The cells were incubated at 4°C for 30 minutes prior to being analyzed by flow cytometry at the Duke University Medical Center Flow Cytometry Facility.

2.13 Proliferation Assay

A total of 500-4,000 cells per well in 150 μL were plated in 96-well plates and allowed to grow for 1, 3, 5 and 7 days. At the indicated time points the plates were wrapped in parafilm and stored at -80°C until being processed. At the time of processing, the plates were thawed on the benchtop for 15 min and then incubated at 50°C for 45 min. Next, 50 μL of propidium iodide solution (200 μg/mL) was added to each well and the plates allowed to incubate at room temperature in the dark for 1-1.5 h.

Finally, fluorescence was measured at the appropriate wavelength using a microplate reader.

2.14 Growth Response in AG1478

Cells were seeded in full medium in 12-well plates at a density of $3x10^4$ cells/well in triplicate; AG1478 was added the next day. Medium and inhibitor were replenished 24 h later. After growing in the inhibitor for a total of 48 h, the remaining adherent cells were harvested by trypsinization and counted using a hemacytometer.

2.15 3-D Culturing of MCF10A Cells

MCF10A stably transfected cells were grown in a three-dimensional laminin-rich extracellular matrix (Matrigel, BD Biosciences; San Jose, CA) as described (56). Briefly, a layer of Matrigel was added to each well of an eight-well glass chamber slide and spread evenly using a P200 tip. Once the layer of Matrigel had solidified, a cell suspension containing $5x10^4$ cells in medium containing 2% Matrigel and 5 ng/mL EGF was added to the wells. The cells were grown at standard cell culture conditions for 20 days. Every 4 days the cells were fed with assay medium containing 2% Matrigel and 5 ng/mL of EGF. Acinar structures were then fixed and analyzed by immunofluorescence, described below.

2.16 Immunofluorescence

Cells were prepared as described in section 2.1 cell culture and deposited onto cleaned microscope slides using a Shandon cytocentrifuge at 600 rpm. These cytospins

were allowed to dry overnight at room temperature before staining. After drying, the cells were fixed in 100% methanol and washed in 0.1% Triton X-100. The cells were then blocked with normal goat serum for 1 h. The primary antibody was placed on the cells for approximately 1 h at room temperature or overnight at 4°C. The appropriate secondary antibody was placed on the cells for 1 h following washes in 1X phosphate buffered saline (PBS) (Sigma). The cells were fixed using 4% paraformaldehyde and then probed with a Hoechst DNA stain (Molecular Probes). After placement of the coverslip using Vectashield (Vector Laboratories; Burlingame, CA), the cells were imaged using a Zeiss LSM 510 inverted confocal microscope (Carl Zeiss MicroImaging; Jena, Germany).

For 3-D cultured cells, immunofluorescent staining was done as previously described (56). Briefly, media was removed from chamber slides and the cells were fixed with 2% paraformaldehyde for 20 min at room temperature. The cells were then permeabilized in PBS with 0.5% Triton X-100 for 10 min at 4°C. After being carefully rinsed three times with PBS/100 mM glycine for 10 min per wash, a primary block was added for 1-1.5 h followed by a secondary block for 30-40 min. The primary antibody was placed on the cells overnight at 4°C. The appropriate fluorescent secondary antibody was added for 50 min at room temperature following washes in Immunofluorescent Buffer. The cells were then counterstained with Hoechst DNA stain (Molecular Probes) and mounted with Vectashield (Vector Laboratories). After drying overnight, acini were imaged using a Zeiss LSM 510 inverted confocal microscope (Carl

Zeiss MicroImaging; Jena, Germany). Analysis by confocal microscopy was performed as previously described (56).

2.17 Caspase 3/7 Luminescence Assay

Cells were plated in white-walled 96-well plates (Costar) at a density of 1000 cells per well and allowed to grow for 24 h. Cells were then treated with varying concentrations of the EGFR inhibitor AG1478 for various lengths of time (see Figure Legends). Following treatment, plates were removed from the incubator and allowed to equilibrate to room temperature. Next, 100 μL of the Caspase-Glo 3/7 Reagent (Promega) was added to each well containing either 100 μL of blank, negative control cells, or treated cells in culture medium. The contents of the plate were then mixed gently on a plate shaker at 300-500 rpm for 30 s and incubated at room temperature for 1 h. Subsequently, luminescence was measured on a BioTek Synergy2 Microplate reader (BioTek; Winooski, VT).

2.18 Matrigel Invasion Assay

For this assay the BD BioCoat Tumor Invasion System (BD Biosciences, San Jose, CA) FluoroBlok 24-well plate was used. The FluoroBlok plate was rehydrated according to the manufacturer's instructions. Near confluent 100 mm dishes of MCF10A and MCF7 stably transfected cells were labeled with 10 μg/mL of DiI (Molecular Probes, Carlsbad, CA) for 1 h at 37°C. DiI (1,1'-dioctadecyl-3,3,3',3'-tetramethylindocarbocyanine perchlorate) is a nontoxic, lipophilic, carbocyanine dye that binds to cellular

phospholipid bilayer membranes and is suitable for long-term labeling and trafficking of cells. Following labeling, a cell suspension was prepared by trypsinizing the cell monolayers and resuspending the cells in media without serum. A total of 0.5 mL of the labeled cells was added to the top chambers at the following densities: MCF-10A ($5x10^4$ cells/chamber) and MCF7 ($2x10^5$ cells/chamber). Immediately, 750 μL of culture media containing 5% FCS was added to the bottom chambers as a chemoattractant. The plate was then incubated at 37°C under standard cell culture conditions and the fluorescence of invaded cells measured on a microplate reader at 1, 2, 3, and 6 days. Only those cells that had invaded the BD Matrigel matrix and passed through the pores of the BD FluoroBlok membrane were detected.

2.19 Antibodies Utilized

- anti-MAL 6D9 monoclonal antibody obtained from Miguel Alonso, Universidad Autónoma de Madrid (10, 11) at 1:300-500 for WB and IHC.
- anti-V5 from Invitrogen at 1:1300 for WB and 1:200 for IF.
- anti-flotillin-1 from Transduction Laboratories at 1:500 for WB.
- anti-actin Ab from Sigma at 1:5000 for WB.
- anti-phospho Akt (Ser473) from Cell Signaling at 1:1000 for WB.
- anti-Akt from Cell Signaling at 1:1000 for WB.
- anti-phospho-p44/42 MAP Kinase (Thr202/Tyr204) from Cell Signaling at 1:1000 for WB.
- anti-p44/42 MAP Kinase from Cell Signaling at 1:1000 for WB.
- anti-phospho EGFR from Cell Signaling at 1:1000 for WB.
- anti-total EGFR from Abcam at 1:200 for WB.
- anti-M30 from Roche at 1:10 for IF.
- Alexa Fluor 488 goat anti-mouse IgG from Molecular Probes at 1:500 for IF.

3. MAL is a Novel Epigenetically Regulated Gene in Breast Cancer

3.1 Introduction

Cancer can be characterized by the accumulation of both genetic and epigenetic changes leading to downstream changes in gene expression patterns. Unlike permanent genetic modifications, epigenetic changes do not involve an alteration in the actual DNA sequence but occur on the DNA and can be reversible events. Due to their reversible nature, cancer-related epigenetic changes are attractive therapeutic targets. The most common epigenetic modifications known to be involved in gene silencing and cancer progression are DNA hypermethylation and histone deacetylation. Methylation occurs at cytosine residues when arranged 5′ to guanine in a CpG dinucleotide pair and is catalyzed by a family of enzymes called DNA methyltransferases (DNMT). CpG methylation facilitates the binding of DNA methyl-CpG binding domain (MBD) proteins, which in turn recruit histone deacetylases (HDACs) resulting in chromosomal condensation and a transcriptionally repressed chromatin state (57). It is traditionally thought that DNA hypermethylation and histone deacetylation work synergistically to silence gene expression.

Promoter hypermethylation has been shown to play a role in the inactivation of genes involved in all stages of tumor progression and metastasis. Many of these genes are documented tumor suppressors while others are cell cycle regulatory genes, genes involved in the maintenance of genomic integrity, and metastasis suppressor genes that

encode cell adhesion molecules and motility factors (58, 59). Loss of function of these critical genes results in subsequent cellular changes that facilitate tumor development.

DNA hypermethylation usually occurs in the promoter of involved genes, in areas enriched for CG dinucleotides termed CpG islands. Although 70-80% of the CpGs in human cells are normally methylated, cytosines in CpG islands are protected from methylation (57). Studies have shown that while CpG islands are unmethylated, the areas flanking the islands are methylated and act as barriers against aberrant promoter methylation (60, 61). In neoplasia, the barriers protecting the promoter CpG island are somehow overridden and de novo methylation begins at the outskirts of the island and progressively spreads into the core resulting in gene silencing (60). The pattern and amount of promoter hypermethylation can be very heterogeneous, with levels of methylation varying not only within a given cell population but also between alleles of a given gene and from one CpG site to another in a single CpG island (62). Given the dynamics of promoter methylation, it is important not only to investigate the presence or absence of methylation in a given CpG island but the pattern and density as well.

The studies in this chapter describe the identification of the myelin and lymphocyte (MAL) gene as a novel epigenetically regulated gene in breast cancer. Using bisulfite genomic sequencing we examined the methylation profile of the MAL promoter region in both benign and breast cancer specimens. Our results show that hypermethylation of the MAL promoter is common in primary breast cancer and that in

some cases methylation appears to impair gene transcription. Further, we describe a cancer-specific methylation pattern that should guide future epigenetic studies at this locus.

3.2 Results

3.2.1 The MAL promoter is commonly methylated in breast cancer cell lines.

The MAL gene has a promoter CpG island of approximately 1500 bp that contains 116 CpG dinucleotides and extends into the first intron. Our initial bisulfite sequence analysis covered 22 CpG dinucleotides spanning the region from −48 to +82 relative to the start of MAL transcription (Fig. 3-1A). Comparing a series of cultured mammary epithelial cells ranging from benign primary cells derived from breast reductions (HMEC), immortalized cell lines from breast reductions, and cancer cell lines, we found that the methylation status in this region was highly variable (Fig. 3-1B). HMEC cultures from four different reduction specimens (ages ranging from 15-43) showed no evidence of methylation in this region. Four immortalized cell lines each had detectable methylation with the MCF10A line showing the highest and the telomerase-immortalized DU99 line the lowest level of methylation. Of the six cancer lines analyzed, the ER-positive MCF7 and T47D cells had the highest levels of methylation (Fig. 3-1C). It is notable that even in these long-cultured cell lines, methylation at any given CpG was not necessarily uniform over the 22 dinucleotide pairs assayed. These data indicate that the MAL promoter region may be a common target for hypermethylation in breast cancer.

Fig. 3-1.

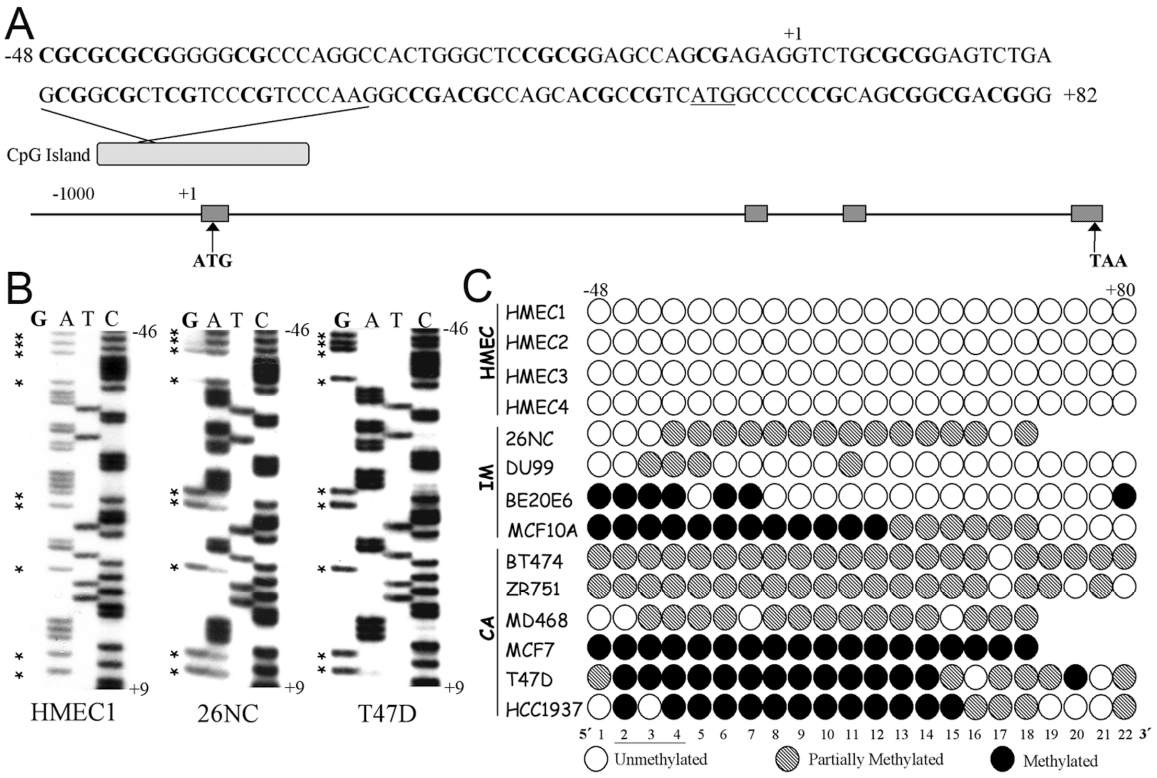

Figure 3-1. Methylation of the MAL promoter region in breast cancer and reactivation of expression by DAC. A. Diagram of the MAL gene indicating the four alternatively spliced exons by shaded boxes and the promoter CpG island with a solid bar above the sequence. The complete sequence of the region analyzed by bisulfite sequencing is shown on top with the CpG dinucleotides in bold, the transcription start site indicated with +1, and the ATG translation initiation codon underlined. **B.** Representative bisulfite sequencing gels for primary human mammary epithelial cells (HMEC1), immortalized (26NC), and breast cancer cell lines (T47D). The region was sequenced using the reverse primer R3, the complement of the methylated C is evident in the G lane. Positions of the

top and bottom nucleotide relative to the start of transcription are indicated to the right of the sequencing gel. Asterisks to the left of the gel indicate cytosines arranged in CpG dinucleotide pairs. **C.** A schematic of bisulfite sequencing of the MAL promoter region in the complete panel of benign and cancer cells showing unmethylated CpGs in human mammary epithelial cells (HMEC), partial methylation in immortalized cell lines (IM), and hypermethylation in the breast cancer cells (CA). The position of the first and last CpG dinucleotide relative to the start of transcription is indicated above the diagram.

3.2.2 Methylation of the MAL promoter in primary breast tumors

To determine if the pattern of methylation seen in the cancer cell lines was also present in breast tumors, we analyzed a series of 36 primary breast cancer specimens and matched constitutive DNA (from peripheral blood lymphocytes) by bisulfite sequencing. We observed varying degrees of methylation and classified the cancers into three categories based upon the average percent methylation quantified by phosphorimaging of the sequencing gels; heavily methylated (defined as an average methylation level >40%), partially methylated (5-40%), and unmethylated (<5%) (Fig. 3-2A). Of 36 primary cancers analyzed, 7 of 36 (19%) were heavily methylated, 18 of 36 (50%) exhibited partial methylation and the remaining 11 (31%) had no evidence of methylation. In summary, we detected MAL promoter methylation in 25 of 36 (69%) of the primary tumors analyzed. All but one of the matched lymphocyte DNA samples was completely unmethylated in this region.

Using available patient data, we determined the association of hormone receptor status with methylation status. We observed a strong correlation of MAL hypermethylation with estrogen-(P= 0.003) and progesterone receptor-(P= 0.006) positive cancers (Table 1). This finding was consistent with the cell line data in that the ER-positive breast cancer cell lines tended to be hypermethylated in the MAL promoter.

The breast cancer specimens used in this study are typical of the disease and contained a heterogeneous admixture of cells. To confirm that hypermethylation of

MAL was derived from the cancer epithelium, we analyzed DNA extracted from laser capture microdissected (LCM) cancer and normal breast epithelia (from reduction mammoplasty specimens with no evidence of cancer). DNA suitable for bisulfite sequencing analysis was obtained from 10 cancers and 4 normal specimens. Comparing DNA extracted from bulk tumor versus the same tumor subjected to LCM indicates that the methylation signal was derived from the malignant epithelial cells (Fig. 3-2B). In the example shown, the cancer scored initially as partially methylated (28% as measured by phosphorimaging) appears to be completely methylated in this region after microdissection of the tumor epithelia. Importantly, DNA from microdissected normal breast epithelia exhibited no methylation in this region (Fig. 3-2B). While only primary cancers that contained at least 50% cancer cells were used in the analysis of bulk tumor DNA, it is likely that our scoring of partial methylation underestimates the degree of methylation in these cases. Absence of methylation in normal breast epithelium suggests that hypermethylation in cancer is associated with the oncogenic process.

Since promoter methylation is thought to occur early in cancer progression, we wanted to analyze the state of promoter methylation in non-invasive breast cancer. Methylation analysis of pure ductal carcinoma in situ (DCIS) samples (with no co-existing invasive component) demonstrated hypermethylation in 3 out of 5 specimens indicating that this epigenetic event can occur early during neoplastic progression (Fig. 3-3).

Fig. 3-2.

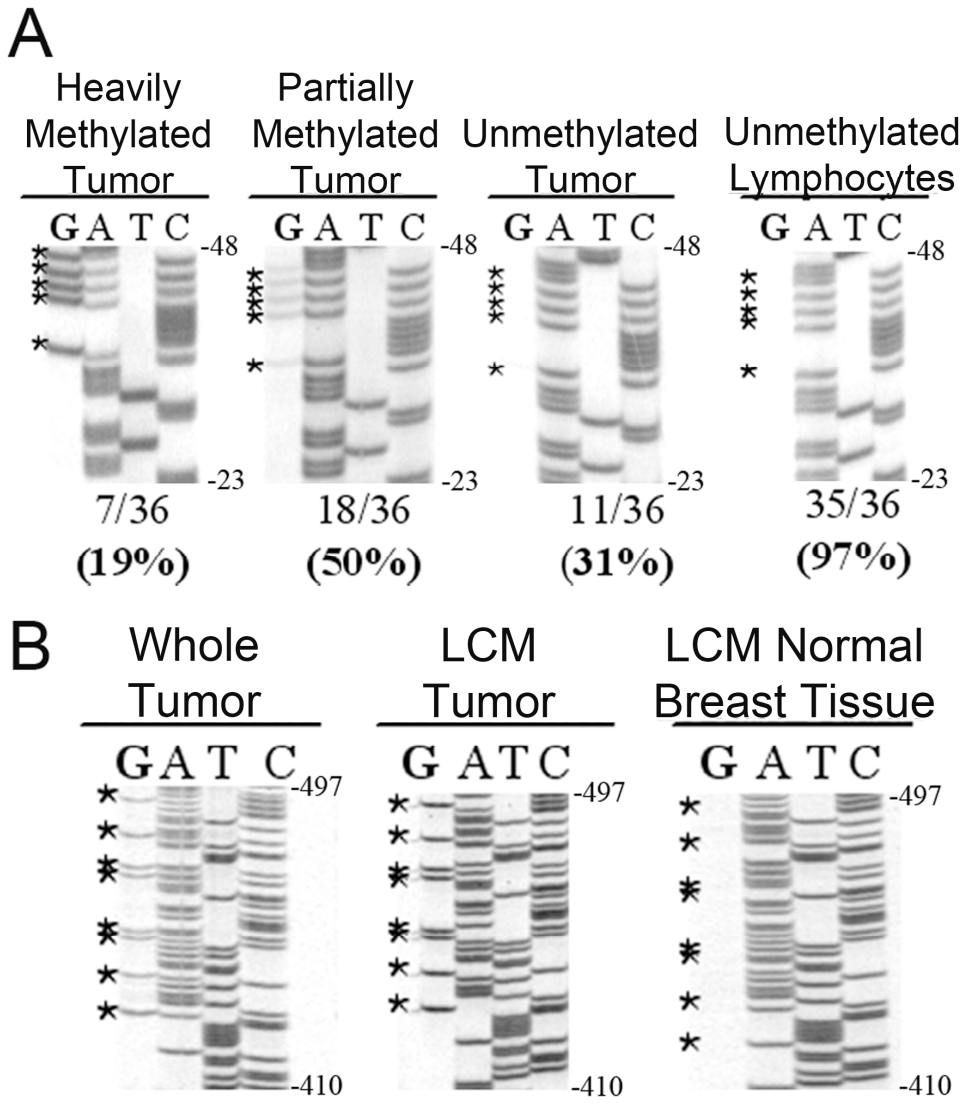

Figure 3-2. Methylation of the MAL promoter region in primary breast tumors. Methylation analysis of the MAL promoter region by bisulfite sequencing in a total of 36 primary breast tumors and matched lymphocytes revealed three distinct patterns of methylation in the tumors including: **A.** 7/36 tumor samples exhibited heavily

methylated cytosine residues, 18/36 tumor samples showed partial methylation of their cytosine residues, and 11/36 tumor samples were unmethylated while matched lymphocyte DNA revealed the absence of methylation in all but one of the samples analyzed. The region was sequenced using the reverse primer R3, the complement of the methylated C is evident in the G lane. Positions of the top and bottom nucleotide relative to the start of transcription are indicated to the right of the sequencing gel. **B.** The methylation status obtained from the whole tumor samples was confirmed by bisulfite sequencing of DNA from laser capture microdissected (LCM) cells. Bisulfite sequencing of LCM normal breast epithelial cells revealed the absence of methylation. The region was sequenced using the reverse primer R5, the complement of the methylated C is evident in the G lane. Positions of the top and bottom nucleotide relative to the start of transcription are indicated to the right of the sequencing gel. Asterisks to the left of the gel indicate cytosines arranged in CpG dinucleotide pairs.

Table 1. Clinico-pathologic features of patients by methylation status

	Tumor Status		
	Methylated	**Unmethylated**	
	n (%)	**n (%)**	***P***
Mean Age	53.5	50.2	NS
Mean tumor size (cm)	3.2	3.0	NS
Estrogen receptor status	**(n=23)**	**(n=9)**	
Positive	15 (65)	0 (0)	
Negative	8 (35)	9 (100)	0.003
Progesterone receptor status			
Positive	14 (61)	0 (0)	
Negative	9 (39)	9 (100)	0.006

*Statistical significance calculated using chi squared analysis

Fig. 3-3.

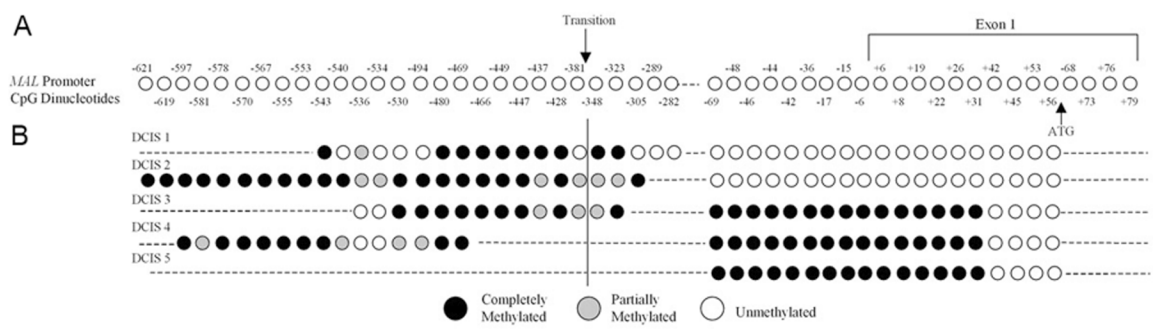

Figure 3-3. Profile of MAL promoter methylation in ductal carcinoma in situ (DCIS) samples. A. Schematic of a portion of the MAL promoter encompassing the transition point and region of differential methylation. Each circle represents a CpG dinucleotide pair with its location relative to the start of transcription indicated by the number either above or below the circle. The point at which the methylation profile transitions is indicated by the arrow. Exon 1 and the position of the translation start codon are indicated as well. **B.** A schematic of bisulfite sequencing of the MAL promoter in a panel of laser capture microdissected (LCM) DCIS samples showing the presence of differential methylation in 3 of 5 samples. The dashed lines throughout the sequence represent areas of the sequence that were unreadable.

3.2.3 Methylation-specific PCR confirms methylation in both breast cancer cell lines and primary tumor samples

In addition to sodium bisulfite sequencing, we also assessed MAL promoter methylation in HMEC, immortalized, and breast cancer cell lines using methylation-specific PCR (Fig. 3-4). The HMEC and normal immortalized cells were more likely to produce amplicons using primers specific for unmethylated DNA while the majority of the breast cancer cells lines were more likely to produce amplicons using primers specific for methylated DNA. Furthermore, MSP analysis of 37 matched tumor and lymphocyte DNAs showed a range of methylation levels in the primary tumors while the lymphocyte DNAs consistently showed amplicons using the unmethylated primer set (Fig. 3-5A). Moreover, 30 out of 37 (81%) tumor DNAs showed greater or equal amplification with methylated primers versus unmethylated primers while only 7 out of 37 (19%) showed greater amplification using unmethylated primer sets (Fig. 3-5B). These data confirm the bisulfite sequencing results and provide further evidence that the MAL promoter region is preferentially methylated in breast cancer.

Fig. 3-4.

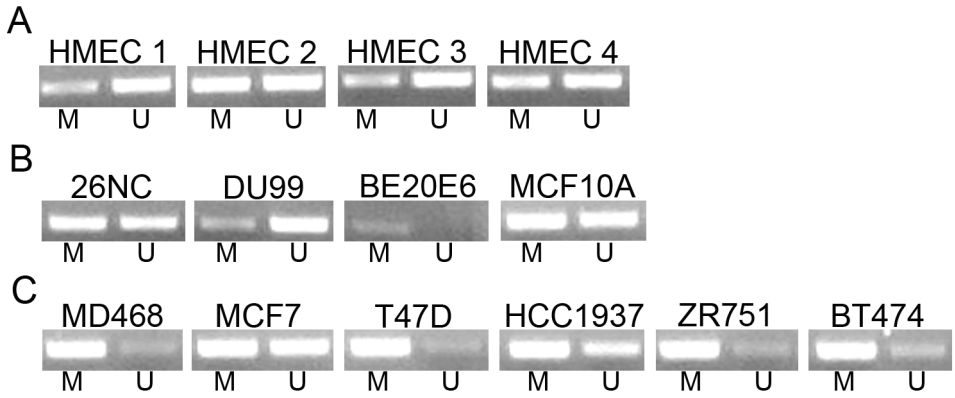

Figure 3-4. Methylation-specific PCR confirms bisulfite sequencing analysis in breast cell lines. Results from methylation-specific PCR using primers specific for either methylated (M) or unmethylated (U) bisulfite-modified DNA. **A.** Normal human mammary epithelial cells (HMEC) showing strong amplification using the unmethylated primer set. **B.** Immortalized cell lines showing amplicons with both primer sets but strongly unmethylated in the DU99 cell line. **C.** Breast cancer cell lines displayed amplification primarily with the methylated primer set.

Fig. 3-5.

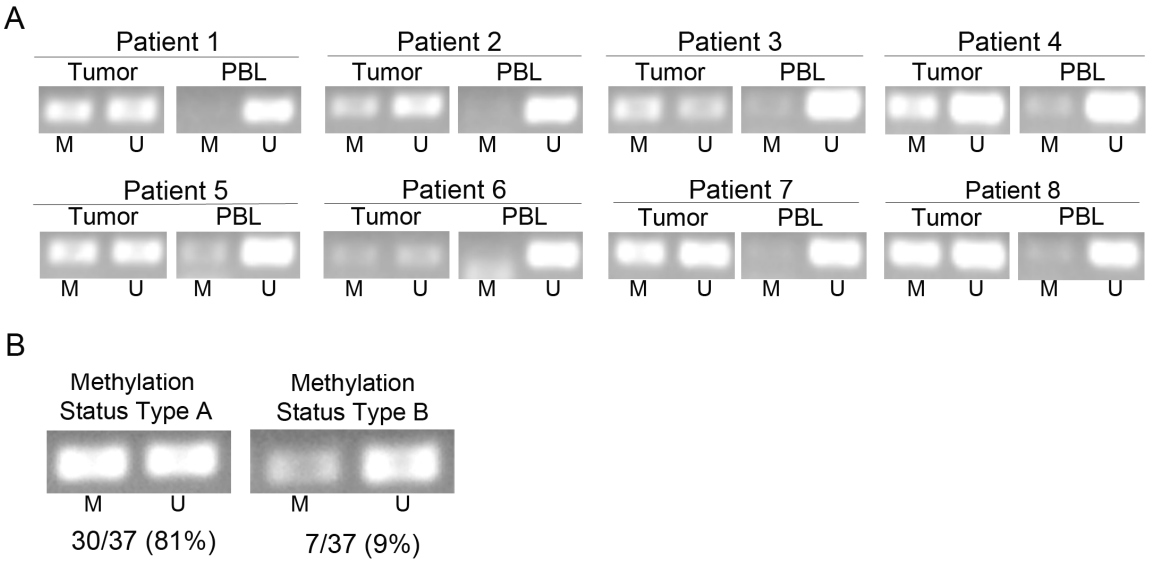

Figure 3-5. Methylation-specific PCR analysis of the MAL promoter region. A. Examples of the methylation status found in primary breast tumor samples and matched peripheral blood lymphocytes (PBL) using primers specific for the methylated sequence (M) and the unmethylated sequence (U). **B.** The methylation status of the tumors could be divided into two types; Type A showing equal or greater amplification using the methylated primer set or Type B showing greater amplification using the unmethylated primer set. The numbers below each panel indicate the number and percent of tumors exhibiting each type of methylation profile.

3.2.4 Differential methylation in the MAL promoter is confined to the proximal promoter region

In designing a methylation-specific PCR assay for this region, we noticed that placement of the upstream primer was critical in obtaining results consistent with the sequence analysis described above. This led to additional sequencing of the promoter region from a series of specimens that revealed an abrupt transition in the methylation profile approximately 350 bp upstream of the transcription start site.

We analyzed four microdissected normal breast epithelial specimens, four benign immortalized mammary epithelial cell lines, and 36 normal lymphocyte samples (from breast cancer patients) to determine the position and frequency of constitutive methylation in this region (Fig. 3-6). Upstream of this transition zone, the majority of normal breast epithelia, normal lymphocytes, and tumors were partially or fully methylated. Figure 3-7A shows the position of the transition point in both a normal breast and breast cancer sample taken from two separate patients, demonstrating the appearance of partial methylation upstream of the transition point in the normal specimen. This non-disease associated methylation extends to at least −621 by our sequence analysis (Fig. 3-7B). Therefore, the region of differential or disease-associated methylation is confined to a relatively small region of the proximal promoter.

Fig. 3-6.

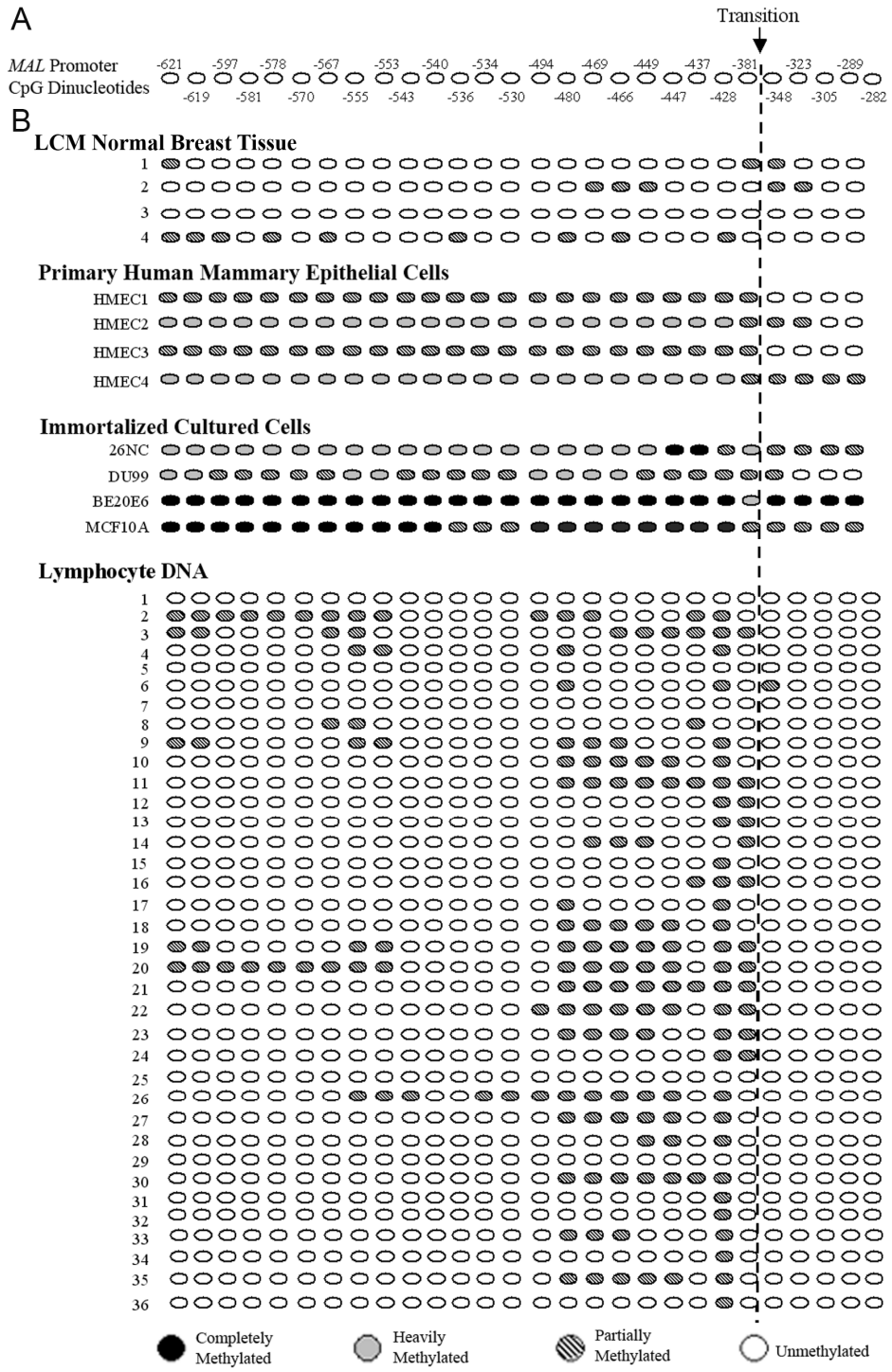
A
Transition
MAL Promoter
CpG Dinucleotides
-621 -597 -578 -567 -553 -540 -534 -494 -469 -449 -437 -381 -323 -289
-619 -581 -570 -555 -543 -536 -530 -480 -466 -447 -428 -348 -305 -282
B
LCM Normal Breast Tissue
1
2
3
4
Primary Human Mammary Epithelial Cells
HMEC1
HMEC2
HMEC3
HMEC4
Immortalized Cultured Cells
26NC
DU99
BE20E6
MCF10A
Lymphocyte DNA
1 2 3 4 5 6 7 8 9 10 11 12 13 14 15 16 17 18 19 20 21 22 23 24 25 26 27 28 29 30 31 32 33 34 35 36
Completely Methylated
Heavily Methylated
Partially Methylated
Unmethylated

Figure 3-6. Profile of MAL promoter methylation at the transition point. A. Schematic of a portion of the MAL promoter encompassing the transition point. Each circle represents a CpG dinucleotide pair with its location relative to the start of transcription indicated by the number either above or below the circle. The point at which the methylation profile transitions is indicated by the arrow. **B.** A schematic of bisulfite sequencing of the MAL promoter at the transition point in a panel of laser capture microdissected (LCM) benign breast tissue, primary human mammary epithelial cells, immortalized cell lines, and lymphocyte DNAs matched to the 36 primary tumor specimens analyzed in this study.

Fig. 3-7.

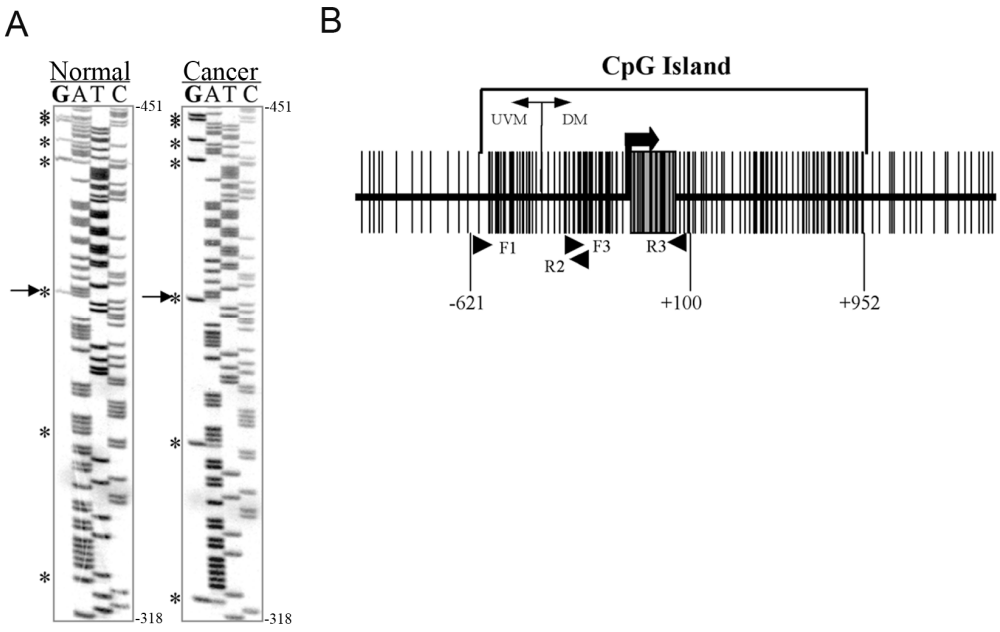

Figure 3-7. Cancer-related methylation confined to the proximal MAL promoter region. A. Examples of bisulfite sequencing of normal and breast cancer DNA indicating CpG dinucleotides by asterisks. The arrow indicates the point where the methylation profile transitions, located at −356 relative to the start of transcription. Positions of the top and bottom nucleotide relative to the start of transcription are indicated to the right of the sequencing gel. Asterisks to the left of the gel indicate cytosines arranged in CpG dinucleotide pairs. **B.** Diagram showing the MAL promoter CpG Island and flanking regions with arrowheads indicating the positions of the sequencing primers and the area where the methylation profile transitions from differential methylation (DM) to universal methylation (UVM). Vertical lines indicate CpG dinucleotides and the start of transcription is designated by the thick black arrow.

3.2.5 MAL promoter methylation is associated with gene silencing

To assess the effects of promoter methylation on MAL mRNA expression we treated a series of cultured benign and breast cancer cells with the methylation inhibitor 5-aza-2'-deoxycytidine (DAC) and then measured mRNA expression by quantitative RT-PCR. We initially took two of the most methylated cell lines, MCF7 and T47D, and performed a dose response with DAC to monitor reactivation of MAL mRNA expression. With increasing concentrations of the methylation inhibitor, MAL mRNA expression increased in a dose-dependent manner (Fig. 3-8). Next, we conducted a similar experiment using a single concentration (5 μM) of DAC over a range of benign and cancer breast cells. We observed induction (10-40 fold) of MAL mRNA transcription in the cancer cell lines T47D, MCF7, and ZR751 but either very little or no increase in the benign DU99 line and primary mammary epithelial cells (Fig. 3-9). MAL expression was also strongly induced by DAC in the immortalized cell line MCF10A. Comparing methylation status to reactivation by DAC (Fig. 3-9B), we found that only the cell lines with the highest degree of promoter methylation induced MAL expression after treatment with the methylation inhibitor. The status of three of the most differentially methylated residues located at −46, −44, and −42 relative to the start of transcription correlate most closely with reactivation by DAC.

Basal expression of MAL in these cells was also highly variable. The three primary HMEC cultures had nearly identical MAL mRNA levels whereas each of the

four cell lines with DAC -inducible expression had very low basal levels (MCF10A, T47D, MCF7 and ZR75-1) as detected by both qRT-PCR (Fig. 3-9) and RT-PCR (Fig. 3-10). Two of the cancer lines (BT474 and HCC1937) expressed particularly high levels of MAL, approximately 15 and 150 fold higher than the HMEC cultures, respectively. The partial methylation observed in these two lines indicates that epigenetic control is only one factor regulating expression of this gene in breast cells.

Fig. 3-8.

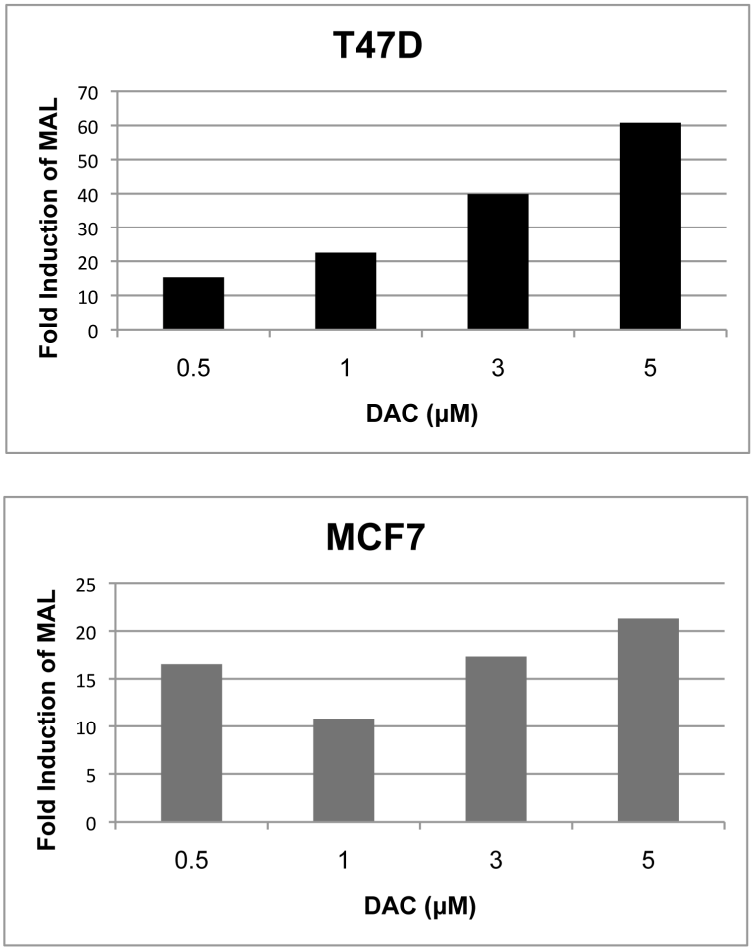

Figure 3-8. Dose-dependent reactivation of MAL expression with DAC. Graphs show reactivation of MAL mRNA expression in the breast cancer cell lines T47D and MCF7 with increasing concentrations of the methylation inhibitor DAC. Expression was measured by TaqMan qRT-PCR.

Fig. 3-9.

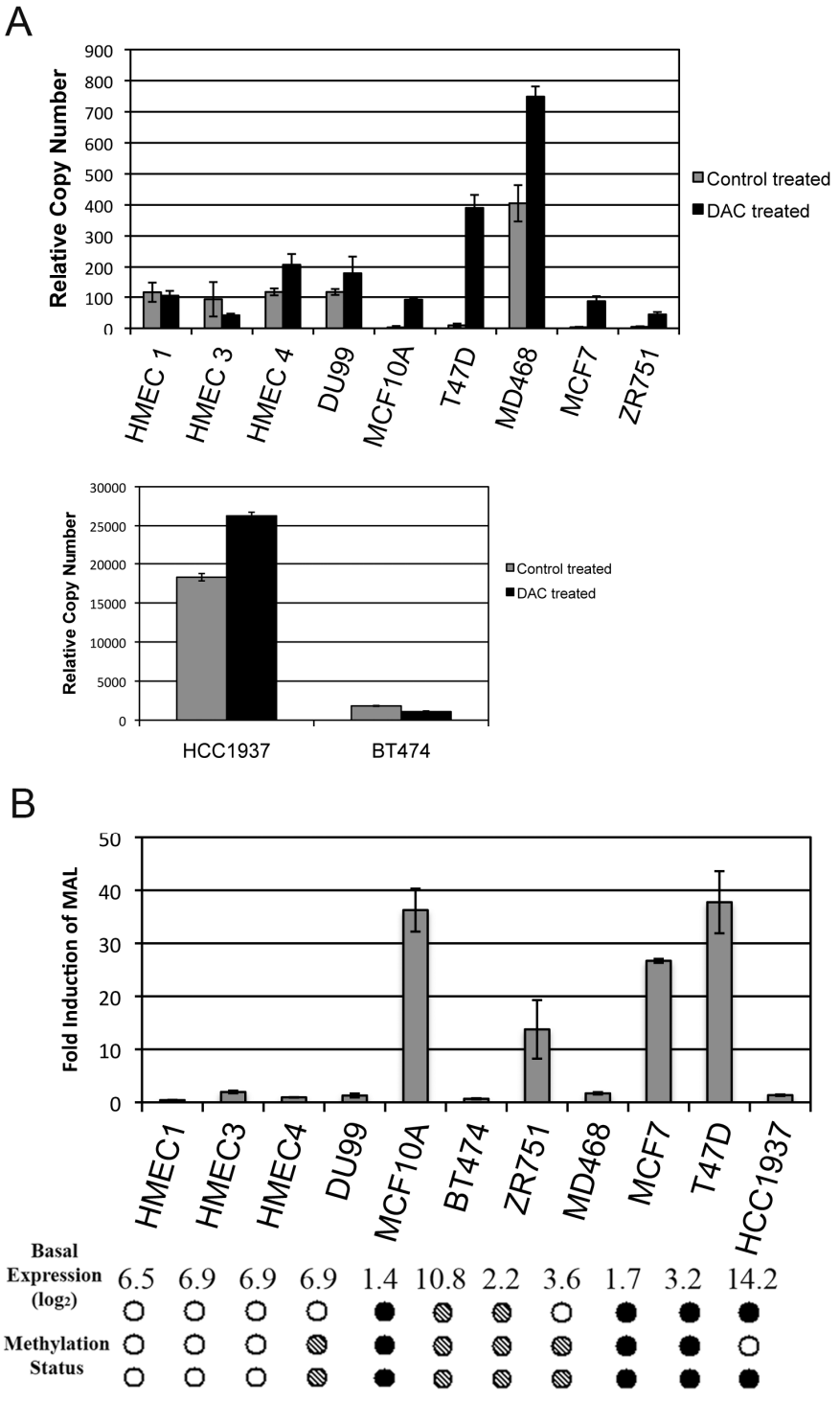
A
Relative Copy Number
900
800
700
600
500
400
300
200
100
0
Control treated
DAC treated
HMEC 1
HMEC 3
HMEC 4
DU99
MCF10A
T47D
MD468
MCF7
ZR751
Relative Copy Number
30000
25000
20000
15000
10000
5000
0
Control treated
DAC treated
HCC1937
BT474
B
Fold Induction of MAL
50
40
30
20
10
0
HMEC1
HMEC3
HMEC4
DU99
MCF10A
BT474
ZR751
MD468
MCF7
T47D
HCC1937
Basal Expression (log2)
6.5 6.9 6.9 6.9 1.4 10.8 2.2 3.6 1.7 3.2 14.2
Methylation Status

Figure 3-9. Reactivation of MAL expression with DAC in a panel of breast cell lines. **A.** Graph shows reactivation of MAL expression in cell lines treated with vehicle or 5 μM DAC. mRNA expression was measured by TaqMan real-time PCR. **B.** Graph shows fold induction of MAL mRNA in DAC-treated cells over control cells. Induction of MAL expression was seen specifically in methylated cancer cell lines and the immortalized cell line MCF10A. Two-tailed t-tests were used to calculate significance. The numbers below the graph indicate the basal level (log_2) of expression measured by qRT-PCR and the status of three of the most differentially methylated residues in the MAL promoter is also shown, corresponding to cytosines 2, 3, and 4 underlined in panel C of Figure 3-1.

Fig. 3-10.

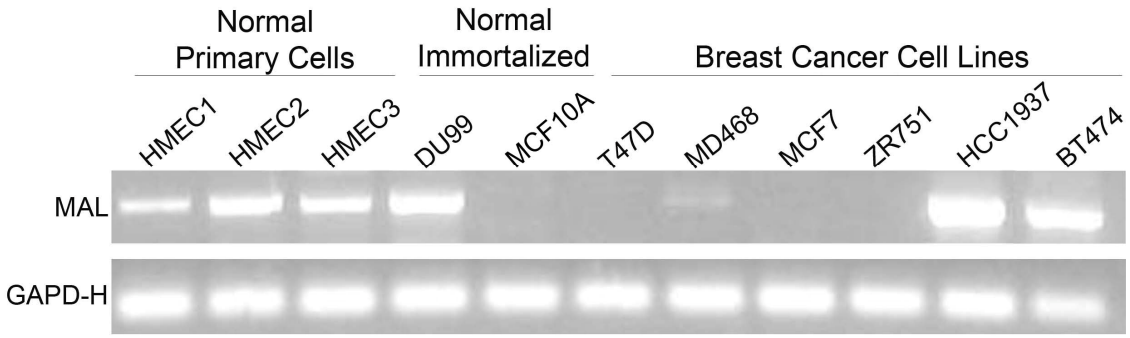

Figure 3-10. Expression analysis of the basal levels of MAL mRNA. Reverse transcription-polymerase chain reaction (RT-PCR) was used to measure MAL mRNA expression in a panel of human mammary epithelial cells (HMEC), normal immortalized and breast cancer cell lines. All of the normal primary cells and the DU99 cell line showed strong bands. The majority of the breast cancer cell lines with the exception of HCC1937 and BT474 showed absent or significantly reduced MAL expression.

3.2.6 MAL mRNA expression in primary breast tumors is variable and does not directly correlate with promoter methylation status

Since promoter methylation has a direct effect on gene transcription levels, we initially looked for a relationship between MAL promoter methylation and mRNA expression. Analyzing thirty-six primary tumors by quantitative RT-PCR we observed varying levels of mRNA expression with the average MAL expression in the methylated tumors (288 ± 62, expression normalized to β2M) being lower than that observed in those lacking methylation (468 ± 171), however this difference did not reach statistical significance (P= 0.23) (Fig. 3-11). This finding suggests that MAL promoter methylation, although common in breast cancer, cannot exclusively account for the observed differences in MAL expression.

From available gene expression array data (63), we found that MAL is contained within a group of coordinately regulated genes (metagene) that are immune cell-related. MAL was first discovered as a T cell-specific protein. Therefore it was formally possible that the bulk of MAL transcription in breast cancer could be attributed to infiltrating inflammatory cells. To address this, we compared levels of MAL expression to the expression of T cell-restricted genes (CD2 and CD27) by qRT-PCR and array analysis (Fig. 3-12). While some cancers with very high levels of MAL also co-expressed T cell markers, this association was not invariant. Together with microdissection data, immunohistochemistry, immunoblotting, and cell culture results, we are confident that breast epithelial cells can and do express MAL mRNA and protein. However, elevated

expression of MAL mRNA seen in some cancers that are bulk extracted may be more indicative of the presence of immune cells in these tissues than an upregulation of the gene in malignant epithelia.

Fig. 3-11.

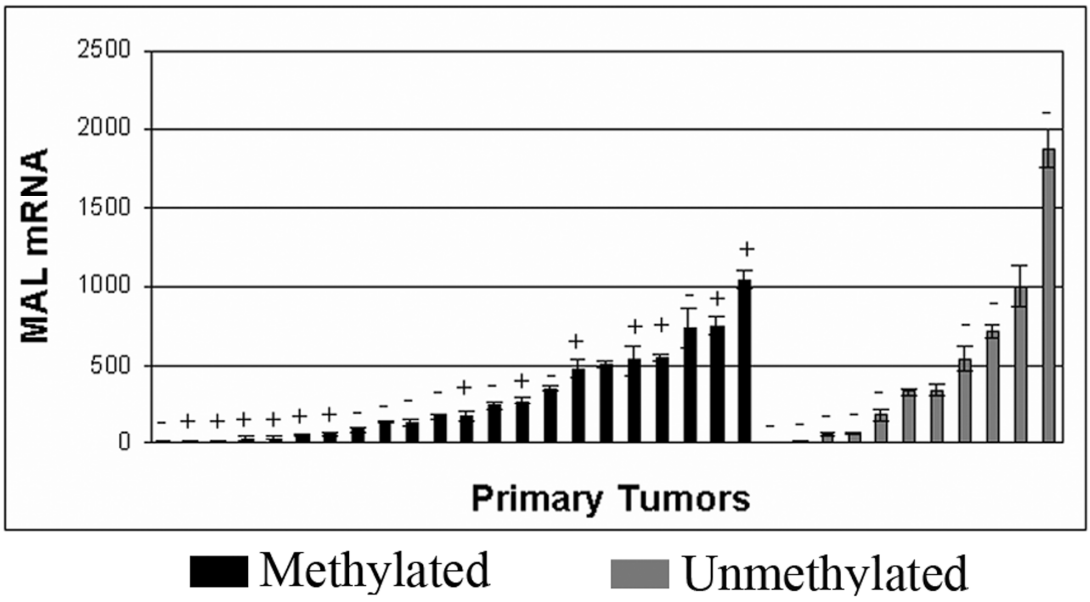

Figure 3-11. MAL mRNA expression in primary tumors. Detection of MAL mRNA in methylated and unmethylated primary breast tumors. The mRNA was detected by quantitative RT-PCR and normalized to β2M. Two-tailed t-tests were used to calculate significance (P= 0.23). A positive or negative symbol above the bars represents ER status for patients with available data.

Fig. 3-12.

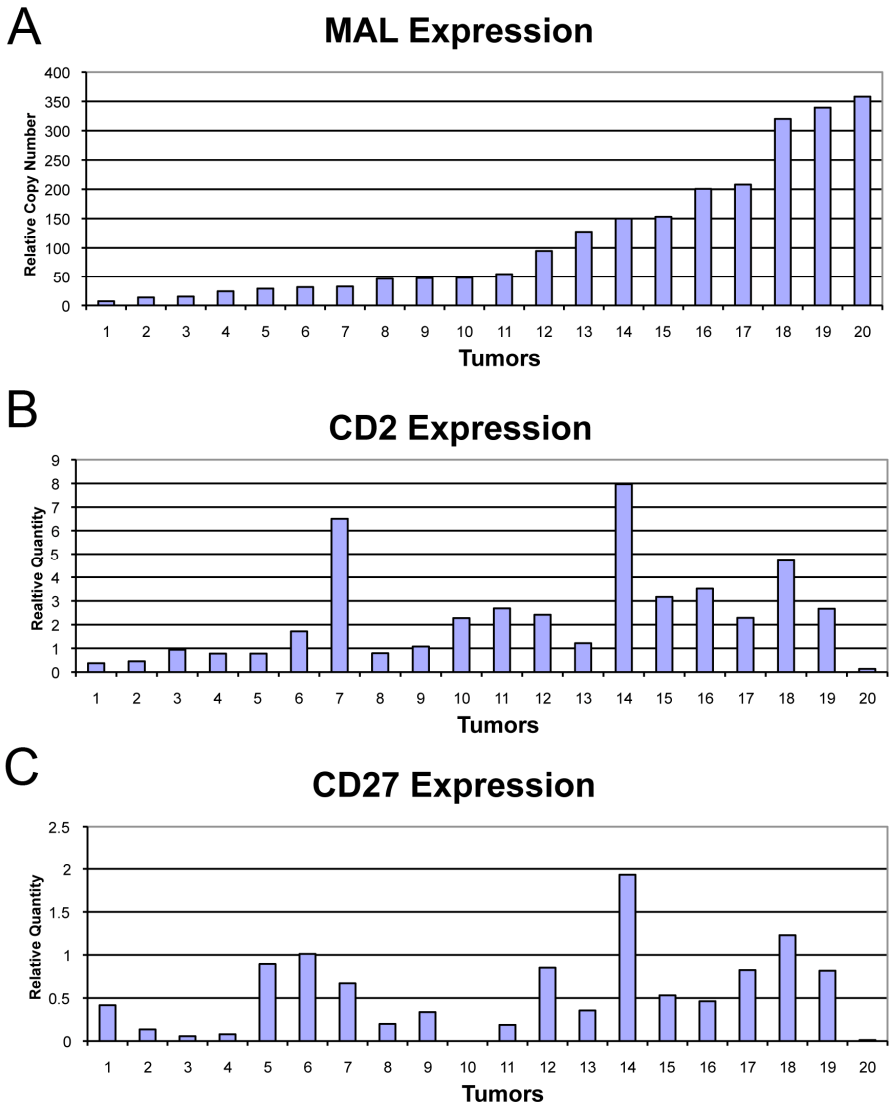

Figure 3-12. Comparing MAL mRNA levels to the levels of T cell-specific genes. Messenger RNA expression levels of **A.** MAL, **B.** CD2 and **C.** CD27 measured by Taq-Man qRT-PCR. MAL mRNA expression did not directly correlate with the expression of CD2 (correlation coefficient 0.23) or CD27 (correlation coefficient 0.27).

3.3 Discussion

Hypermethylation of gene promoters leading to transcriptional silencing is associated with the onset and progression of cancer. Identification of genes that are epigenetically regulated in cancer can provide targets for early detection and therapeutics. We have identified MAL as a novel epigenetically regulated gene in breast cancer. Loss or reduced MAL expression through promoter methylation may prove to be an important early event in the transformation process.

Hypermethylation of the MAL promoter was seen in all of the breast cancer cell lines (6/6) and 69% of primary tumors analyzed relative to cultured primary breast epithelial cells, patient-matched lymphocytes, and normal breast tissue from healthy donors. The high frequency of promoter methylation in the cancer samples and its absence in benign samples confirms that MAL methylation is a cancer-specific phenomenon. Moreover, recent studies published by other labs in parallel with my own have replicated my findings demonstrating that the MAL promoter is methylated in breast cancer affirming the importance of this gene in breast carcinogenesis (27, 64, 65).

The identification of novel genes that are preferentially methylated in cancer epithelial cells holds great importance with regards to early detection. In particular, the potential for using cancer-specific gene methylation as a marker for detecting malignant cells in bodily fluids. Research has shown that tumor DNA is released into plasma and serum of cancer patients providing a readily accessible source of detecting tumor

specific gene changes (66, 67). Esteller *et al.* reported a strong correlation between the detection of methylated cancer-related genes in serum and the methylation of the identical genes in the primary tumor using MSP (68). In addition, tumor cell-specific promoter hypermethylation was successfully detected in serum from pre-invasive and early stage breast cancer patients suggesting that hypermethylation-based screening of serum, a readily accessible bodily fluid, may enhance early detection of breast cancer (69). Our detection of MAL promoter hypermethylation in DCIS samples strongly supports the possibility that aberrant MAL methylation is an early event in the transformation process. Moreover, recent studies have detected MAL promoter methylation in head and neck (24) and cervical carcinomas (22) suggesting that MAL methylation has the potential to serve as a marker for the early detection of multiple epithelial cancers.

We have yet to determine the mechanism by which MAL promoter hypermethylation mediates gene silencing in breast cancer. Among several possibilities, two likely scenarios include the direct interference of transcription factor binding and the recruitment of DNA methyl-CpG binding domain (MBD) proteins. In colorectal cancer the expression of adenomatous polyposis coli gene, a gene involved in apoptosis and cell cycle arrest, is silenced by promoter methylation that interferes with the binding of the transcription factor CCAAT-binding factor (70). In lung cancer, epigenetic silencing of CCAAT/Enhancer binding protein α, a candidate tumor suppressor gene is

associated with the inhibition of upstream stimulatory factor binding (71). These studies highlight the fact that methylation can impede transcription factor binding resulting in the loss of key proteins leading to neoplastic changes.

To determine which transcription factors could possibly bind to the MAL promoter region, we entered the promoter sequence into the online Transcription Element Search System (TESS) (72). TESS is a web-based software tool for predicting possible transcription factor binding sites in DNA sequences. TESS revealed several transcription factors with probable binding sites in the MAL promoter region including activator protein-2 (AP2), upstream stimulatory factor (USF), early growth response protein (EGR), and Wilms-tumor protein-1 (WT1). Of these transcription factors, hypermethylation has been shown to inhibit the binding of both AP2 and USF leading to the loss of target gene expression (71, 73). Bisulfite sequencing analysis of the MAL promoter revealed preferential hypermethylation of the putative EGR and WT1 binding sites in breast cancer cell lines suggesting that interference with transcription factor binding may be a method by which methylation silences MAL gene expression.

Alternatively, gene silencing via promoter methylation can be mediated through the binding of MBD proteins. Following CpG methylation, MBD proteins are recruited and bind to the gene promoters where they then recruit histone deacetylases (HDACs) resulting in histone modifications and chromatin condensation (74). Results from Ballestar *et al.* support the idea that the presence of MBD proteins is an essential and

general feature in the methylation-mediated silencing of tumor suppressor and DNA repair genes (75). The study further asserts that MBD binding sites could potentially identify sites of epigenetic inactivation in human cancer through genome wide screening (75). Moreover, MBD proteins have been shown to function as transcriptional repressors in association with CpG island hypermethylation through their interactions with HDAC complexes in colon carcinoma and breast cancer cells (76, 77). The combination of CpG methylation, MBD binding and histone deacetylation leads to a compact, transcriptionally repressive chromatin structure that is inaccessible to gene regulatory proteins. Epigenetic-mediated gene silencing provides a selective advantage to neoplastic cells resulting in progressive cell damage and cancer progression. We have shown that areas of the MAL promoter CpG island are selectively methylated in breast cancer leading to gene silencing. Future studies will provide further insight into the manner by which promoter methylation causes MAL transcriptional silencing.

The pattern and amount of promoter hypermethylation can be very heterogeneous leading to varying degrees of gene silencing in tumor cells. Given the heterogeneous nature of promoter methylation we thought it necessary to not only consider the presence or absence of methylation in a few CpG dinucleotides within the MAL promoter, but the pattern of methylation over a relatively large portion of the promoter region. We surveyed over 800 bp of sequence, which included the methylation status of 71 CpG dinucleotides. From this sequence analysis we observed a transition

point in the methylation profile. Differential methylation between normal and cancer cells was confined to a region within 356 bp upstream of the start of transcription. We are confident that we have identified a region of the MAL promoter that is critical for methylation-based gene silencing. Interestingly, two recent papers examining the role of MAL promoter hypermethylation in gastric and colon cancer revealed that methylation in the proximal promoter region was the most critical. Buffart *et al.* showed that methylation of the proximal MAL promoter (-92 to -7 bp relative to the first ATG) correlated with better disease-free survival in gastric cancer patients, while methylation of the promoter farther upstream (-680 to -573 bp relative to the first ATG) did not (28). In colon cancer, Lind *et al.* found hypermethylation of the MAL promoter close to the transcription start site while CpGs located farther upstream relative to the transcription start point were frequently unmethylated and/or partially methylated (27). These published data are corroborative evidence supporting my finding that methylation within the area close to the start of transcription is critical for cancer-related MAL gene silencing.

The phenomenon of methylation-related gene silencing confined to the proximal promoter region is not exclusive to the MAL gene. Interestingly, methylation at CpG sites in a proximal region of hMLH1 promoter was detected in colorectal tumors that showed no hMLH1 expression, while no methylation was shown in normal mucosa and tumors which express hMLH1. However methylation in the distal region was observed

in all tissues including normal mucosa and hMLH1 expressing tumors (78). Furthermore, sharp transitions in methylation have been observed in other CpG islands including those associated with the beta-glucuronidase (61), E-cadherin, and von Hippel-Lindau genes (60). A distinct definition of boundaries between methylated and unmethylated regions was correlated with the presence of SP1 binding sites and multiple Alu repeats of both the E-cadherin and von Hippel-Lindau genes in benign breast and kidney cells, respectively. Analysis of this region in the MAL promoter did not reveal any Alu repeats; however, MAL contains several SP1 binding sites in the 5'-flanking proximal promoter region (~110 bp upstream of the transcriptional start site) (79). The transition point we have defined may represent the 5'-boundary of the functional MAL promoter CpG island.

When attempting to correlate the levels of MAL expression to promoter methylation we found that this association could be made for some but not all cell lines or primary tumors. The consequences of promoter methylation on MAL expression could be demonstrated in breast cell culture in that MAL mRNA expression was inducible by DAC only in hypermethylated cell lines. In a series of cell lines we observed a correlation between the degree of hypermethylation and induction of the MAL transcript, specifically in MCF7, T47D, ZR75-1 and MCF10A cells. MAL expression was not affected in primary mammary epithelial cells that have no detectable methylation. Further, methylated cell lines that responded to DAC had basal levels of

MAL transcripts that were 10-40 fold below that found in benign HMEC cultures. Inhibiting methylation in these cells induced MAL to a level comparable to primary breast epithelia.

Since cytosine methylation is reversible, utilizing demethylating agents such as DAC in cancer patients is an attractive therapeutic strategy that could potentially re-express aberrantly hypermethylated growth regulatory genes thus lessening the cancer phenotype. Clinical trials using DNA methylation inhibitors have shown evidence of some anti-tumor effects and accompanying changes in DNA methylation (80-82). In theory, breast cancer patients that exhibit MAL promoter methylation would exhibit a greater clinical response with the addition of demethylating agents to their chemotherapeutic regimen. Notably, the HCC1937 and BT474 were hypermethylated in the MAL promoter yet both lines exhibited high basal levels of expression that were not further induced by DAC treatment. The presence of completely unmethylated residues, for example in CpG sites 1 and 3 of HCC1937 (Fig. 3-1C), may indicate that the critical CpG residues for the transcriptional regulation of this gene are not sufficiently methylated in these lines or that the observed methylation is not biologically relevant. Alternatively, these cell lines may contain high levels of certain transcription factors allowing for the elevated expression of MAL. Ultimately, high basal expression in the presence of partial methylation in these two lines indicates that promoter methylation is not the only mechanism regulating MAL expression in breast cells. Other mechanisms

of MAL gene regulation in breast cancer could include loss of heterozygosity (LOH) or genetic mutations. Future experiments will be required to investigate these possibilities.

Hypermethylation of MAL was readily detectable in primary breast cancer specimens and, using microdissection, we confirmed that these events occur in the malignant epithelial cells within the tumor. Similar to what was seen in certain breast cancer cell lines (HCC1937 and BT474), promoter methylation may explain down-regulation of MAL gene expression in some but not all primary breast cancers. On average, lower MAL mRNA expression was seen in the methylated tumors compared to unmethylated tumors, however, this difference did not reach statistical significance (Fig. 11). Further, of the cancers that exhibited methylation (either partial or heavy), the majority were nuclear hormone receptor-positive while all of the unmethylated cancers for which data was available were ER/PR negative (Table 1). This was consistent with our cell line data showing that the hormone receptor positive MCF7, T47D, and ZR75-1 lines are all methylated and MAL expression could be reactivated by DAC. This is not the first finding that links ER/PR status with promoter methylation in breast cancer. A study published by Wei *et al.* (83) showed that methylation of the BRCA1 promoter was more frequently observed in women with high-grade ER- and PR-negative tumors. If reduced MAL expression is associated with loss of polarity, then it is possible that the higher percentage of ER+ cancers that exhibit MAL hypermethylation is indicative of a greater selection for this property during the neoplastic progression of luminal type

cancers compared to ER− cancers more likely to be of the basal subtype. Whether this reflects the varied etiology of these cancers or a cell lineage phenomenon remains to be determined.

4. Biological Consequences of Aberrant MAL Expression in Breast Cancer

4.1 Introduction

In the article "Hallmarks of Cancer", authors Hanahan and Weinberg suggest that cancer cells acquire six essential alterations in their physiology which dictate malignant growth: (1) self-sufficiency in growth signals, (2) insensitivity to growth-inhibitory signals, (3) evasion of programmed cell death (apoptosis), (4) limitless replicative potential, (5) sustained angiogenesis, and (6) tissue invasion and metastasis (84). Furthermore the authors assert that these capabilities are shared among most if not all types of human tumors. Consequently, identifying genes whose disruption leads to alterations in breast cell physiology and subsequent malignant growth could be relevant to multiple tumor types.

Promoter methylation leading to the silencing of key cancer-related genes is involved in the initiation and progression of various types of cancers including breast cancer. Using the classification established by Hanahan and Weinberg, DNA methylation was found to contribute to each of the six acquired characteristics in breast carcinogenesis, highlighting the importance of methylation in the transformation process (85). For example, the tumor suppressor gene RASSF1A is methylated and silenced in about 62% of primary breast cancers irrespective of grade (86). Re-expression of RASSF1A induced cell cycle arrest and inhibited cyclin D1 accumulation in breast cancer cells (87) and reduced colony formation and suppressed anchorage-independent

growth in lung cancer cells (88). Expression of the invasion/tumor suppressor gene E-cadherin is frequently lost in breast cancer due to promoter hypermethylation (89). Furthermore, loss of E-cadherin expression may be an independent negative prognostic factor for infiltrating ductal carcinoma (90). We are interested in understanding if loss of MAL expression via promoter methylation contributes to the breast cancer phenotype and moreover, what utility MAL has as a prognostic or predictive factor for breast cancer.

A characteristic feature of polarized cells is the division of their surface into functionally distinct membrane domains, which requires an intricate sorting machinery that delivers proteins and lipids to the correct membrane domains (91). Consequently, the protein sorting machinery is fundamental in the generation of epithelial cell polarity. Moreover, malignant transformation of epithelial cells requires the disruption of apical/basal polarity. Loss of polarity in tumors disrupts tissue structure, compromises the segregation of signaling effectors, and exacerbates the increased cell proliferation induced by other oncogenic signals (92, 93). One known function of the MAL protein is in GEM-mediated apical sorting of membrane and secretory proteins in polarized epithelial cells. Given the involvement of impaired cell polarity and aberrant protein sorting in carcinogenesis, it is plausible that the functional loss of the MAL protein in polarized epithelial cells could have implications in the development and progression of cancer.

After demonstrating that the myelin and lymphocyte (MAL) gene promoter is frequently hypermethylated in breast cancer, we next sought to determine if MAL induces a phenotypic effect related to cancer progression in breast cells. We therefore established stable breast cell lines that either exogenously expressed a V5-tagged MAL protein or shRNA directed to the MAL gene promoter and performed several functional studies to measure characteristics such as proliferation, cell migration and anchorage-independent growth. We also investigated the potential use of MAL as a prognostic or predictive factor for breast cancer. The data presented in this chapter demonstrate that MAL has a functional role in the transformation process and is an independent predictor of benefit from adjuvant chemotherapy.

4.2 Results

4.2.1 Stable breast cell lines utilized in MAL functional studies

To begin to investigate the functional implications of MAL expression in breast cancer, we established mammary epithelial cell lines either stably overexpressing MAL or with a stable knockdown of MAL expression. For exogenous expression of the MAL protein we transfected a C-terminal V5 tagged MAL or a vector control into the breast cancer cell lines MCF7, MDA-MB-468 and the normal immortalized cell line MCF10A. Additionally, we transfected shRNA directed to the MAL promoter (shMAL) or a non-silencing shRNA control vector (shCtrl) into the normal immortalized DU99 cells. This section will describe the cell lines used in our functional assays. For the majority of the assays we used two separate MAL expressing clones side by side in each experiment.

MCF7 is a cultured human breast cancer cell line exhibiting characteristics of luminal mammary epithelial cells. MCF7 cells are positive for both the estrogen and progesterone receptor. The MAL promoter is hypermethylated in these cells with non-detectable MAL expression measured by quantitative RT-PCR. In the MCF7 cells, we stably overexpressed the MAL-V5 protein or a vector control and used both a high and low MAL-expressing clone in our functional studies (Fig. 4-1A).

MCF10A is a spontaneously immortalized mammary epithelial cells derived from human fibrocystic mammary tissue. MCF10A cells were produced by long-term culture in serum-free medium with low CA^{2+} concentration. These cells are non-

tumorigenic in immunosuppressed mice but do form colonies in semisolid medium. MCF10A cells are ER- and PR-negative and exhibit characteristics of luminal ductal cells. The MAL promoter is hypermethylated in these cells with non-detectable MAL expression measured by quantitative RT-PCR. In the MCF10A cells, we stably overexpressed the MAL-V5 protein or a vector control and used both a high and low MAL-expressing clone in our functional studies (Fig. 4-1B). Interestingly, the MCF10A cells behave very similarly to the breast cancer cell lines in our functional studies.

MDA-MB-468 (MD468) is a cultured human breast cancer cell line exhibiting characteristics of basal mammary epithelial cells. MD468 cells were isolated from a patient with metastatic adenocarcinoma of the breast. These cells are ER-, PR-, and HER-2/neu-negative. Additionally, MD468 cells harbor an inactivating mutation in the phosphatase and tensin homolog deleted on chromosome ten (PTEN) gene, an important negative regulator of the PI3K/AKT signaling pathway. The MAL promoter is hypermethylated in these cells with low MAL expression measured by quantitative RT-PCR. In the MD468 cells, we stably overexpressed the MAL-V5 protein or a vector control and used both a high and low MAL-expressing clone in our functional studies (Fig. 4-1C).

DU99 cells began as primary human mammary epithelial cells (HMEC) cultured from a reduction mammoplasty. Primary HMEC isolated and grown in this manner exhibit the characteristics of basal mammary epithelial cells (94). After retroviral transfer

of the gene encoding the enzymatic subunit of telomerase, an immortalized clone was derived and has been in continuous culture in our lab for over 8 years. Additionally, DU99 cells are non-tumorigenic in immunocompromised mice. DU99 cells have an unmethylated MAL promoter and express MAL mRNA measured by quantitative RT-PCR. Using shRNA directed at the MAL gene we stably knocked down MAL expression as indicated by both qualitative and quantitative RT-PCR (Fig. 4-2).

Fig. 4-1.

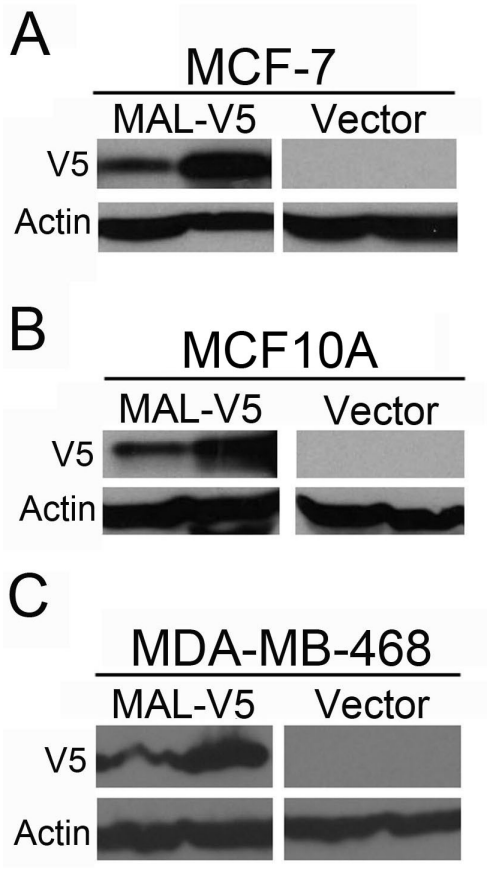

Figure 4-1. Overexpression of MAL-V5 in breast epithelial cells. Western blots detecting the stable expression of the V5-tagged MAL protein or a vector control in the **A.** MCF7 and **B.** MCF10A, and **C.** MDA-MB-468 cell lines using an anti-V5 monoclonal mouse antibody.

Fig. 4-2.

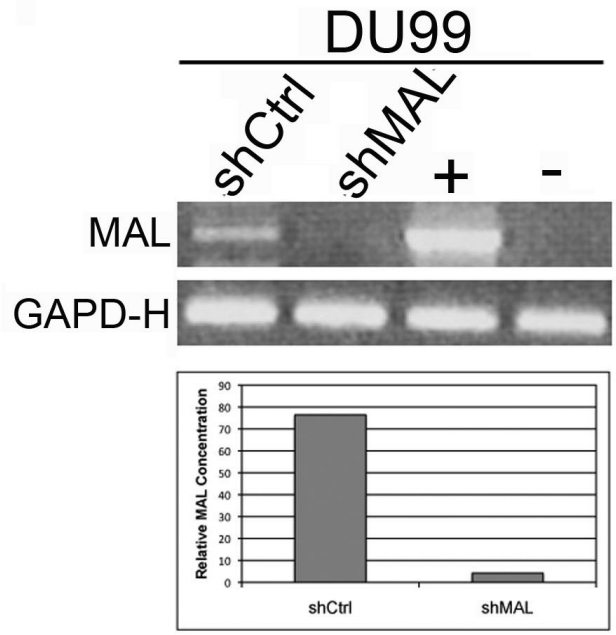

Figure 4-2. Knockdown of MAL expression in DU99 cells. shRNA directed at the MAL gene was used to stably knockdown MAL expression (shMAL). We verified the level of MAL expression using both qualitative and quantitative RT-PCR. By quantitative RT-PCR we were able to knockdown 95% of MAL mRNA expression. As a control, DU99 cells were also transfected with a non-silencing control (shCtrl) plasmid. HCC1937 and T47D cell lines were used as positive and negative controls respectively.

4.2.2 Sub-cellular localization of the MAL-V5 protein

After stably transfecting mammary epithelial cells with the MAL-V5 construct we sought to determine if the exogenously expressed V5-tagged MAL localizes to the same area of the cell as the endogenous MAL protein. Cytospins of MCF7 cells stably expressing MAL-V5 were subjected to immunofluorescence analysis with an anti-V5 primary antibody and a fluorescently-conjugated secondary antibody. The MAL-V5 expression pattern corresponded to what has been published regarding the sub-cellular localization of endogenous MAL (13), specifically perinuclear staining consistent with the trans-golgi network (Fig. 4-3, left panel). While the greater majority of the cells exhibited perinuclear staining, MAL-V5 expression was also present on the cell membrane of some cells consistent with an itinerant protein cycling between the trans-golgi network and the plasma membrane (Fig. 4-3, right panel).

Furthermore, the MAL protein is known to localize to detergent-insoluble membrane microdomain fractions within epithelial cells. Fractionation of detergent-extracted cells by sucrose gradient velocity sedimentation followed by immunoblot analysis showed the MAL-V5 protein enriched in the detergent-insoluble fractions, which is indicative of its association with membrane rafts (Fig. 4-4). Detection of the membrane raft resident protein flotillin-1 (95) and endogenous MAL in HCC1937 cells confirmed the biochemical location of MAL-V5.

Fig. 4-3.

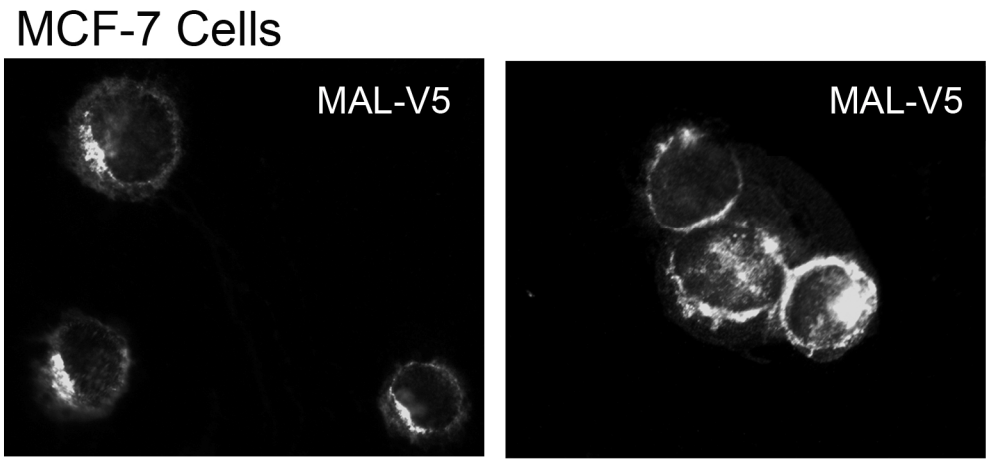

Figure 4-3. MAL-V5 subcellular localization in MCF7 cells. Cytospins of MCF7 cells stably expressing MAL-V5 were subjected to immunofluorescence analysis with an anti-V5 primary antibody and a fluorescently-conjugated secondary antibody. The pattern of MAL expression showed both perinuclear staining consistent with the trans-golgi network (*left panel)* and membrane staining *(right panel).*

Fig. 4-4.

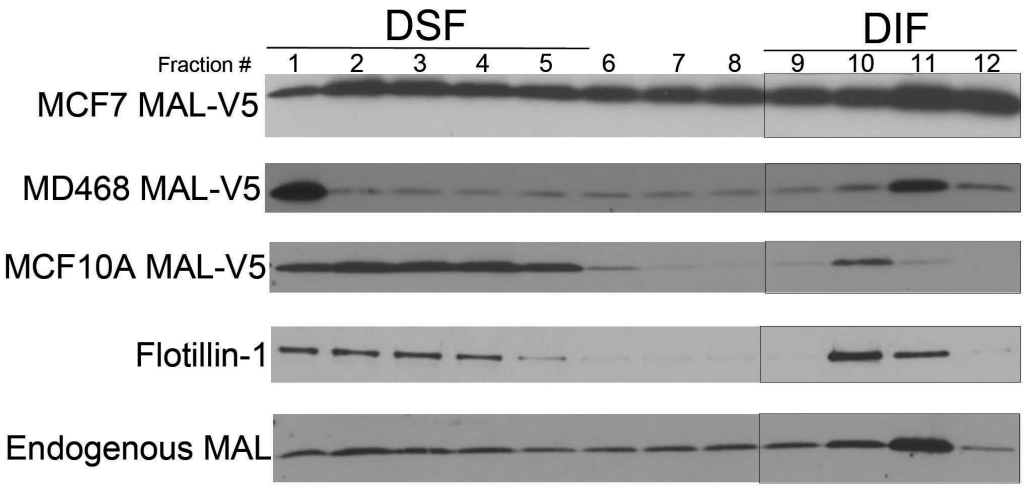

Figure 4-4. MAL-V5 localizes to membrane rafts. Detection of V-5 tagged MAL in stable transfectants after extraction with 1% Triton-X and centrifugation to equilibrium. The MAL-V5 protein was detected predominantly in the detergent-insoluble fraction (DIF) containing membrane rafts and to a lesser extent in the detergent-soluble fraction (DSF) containing other cellular proteins. Flotillin-1 was used to confirm membrane raft location. Also endogenous MAL expression was enriched in the detergent-insoluble fraction of HCC1937 cells. Fractions are labeled from the bottom to the top of the sucrose gradient.

4.2.3 Effect of MAL expression on cell growth and cell cycle progression

To study the effects of MAL on the cell cycle, stable cell lines were incubated in serum-free medium for 48 hours and subsequently stimulated to progress through the cell cycle with the addition of serum-containing medium for 18 hours followed by cell cycle analysis. MCF10A cells showed no difference in cell cycle progression between the MAL-expressing or vector control cells (Fig. 4-5A). However, both the MCF7 and MD468 MAL-V5 expressing cells showed a slight increase (7%) in G1 paired with a decrease in G2M (7% and 9% respectively) compared to their respective vector controls (Fig. 4-5B and C). Interestingly, in the MD468 MAL-expressing cells there was also a slight increase (3%) in the percentage of cells in the sub-diploid (SD) fraction suggesting that MAL expression might be increasing the baseline level of apoptosis in these cells (Fig. 4-5C). Knockdown of MAL expression in DU99 cells resulted in both a decrease in G1 (5%) and increase in S phase (7%), demonstrating that loss of MAL expression increases the rate at which DU99 cells progressed through the cell cycle.

In addition to cell cycle progression, we also assessed the effect of MAL overexpression on the rate of cell growth. Briefly, cells were plated in 96-well plates at varying concentrations, allowed to grow for 1 week and collected at days 1, 3, 5, and 7. The DNA content of the cells was measured by staining with propidium iodide and subsequent fluorescent analysis. MCF10A and MCF7 cells showed no difference in the growth rate between MAL-expressing or vector control cells (Fig. 4-6A and B). However,

in the MCF7 cells, the higher MAL-V5 #10 expressing clone grew at a slightly faster rate than the lower MAL-V5 #4 expressing clone (Fig 4-6B). In the MD468 cells, MAL overexpressing cells exhibited a slower rate of growth than the vector control cells (Fig 4-6C). Taken together, these data suggest a role for MAL in regulating mammary epithelial cell growth and proliferation.

Fig. 4-5.

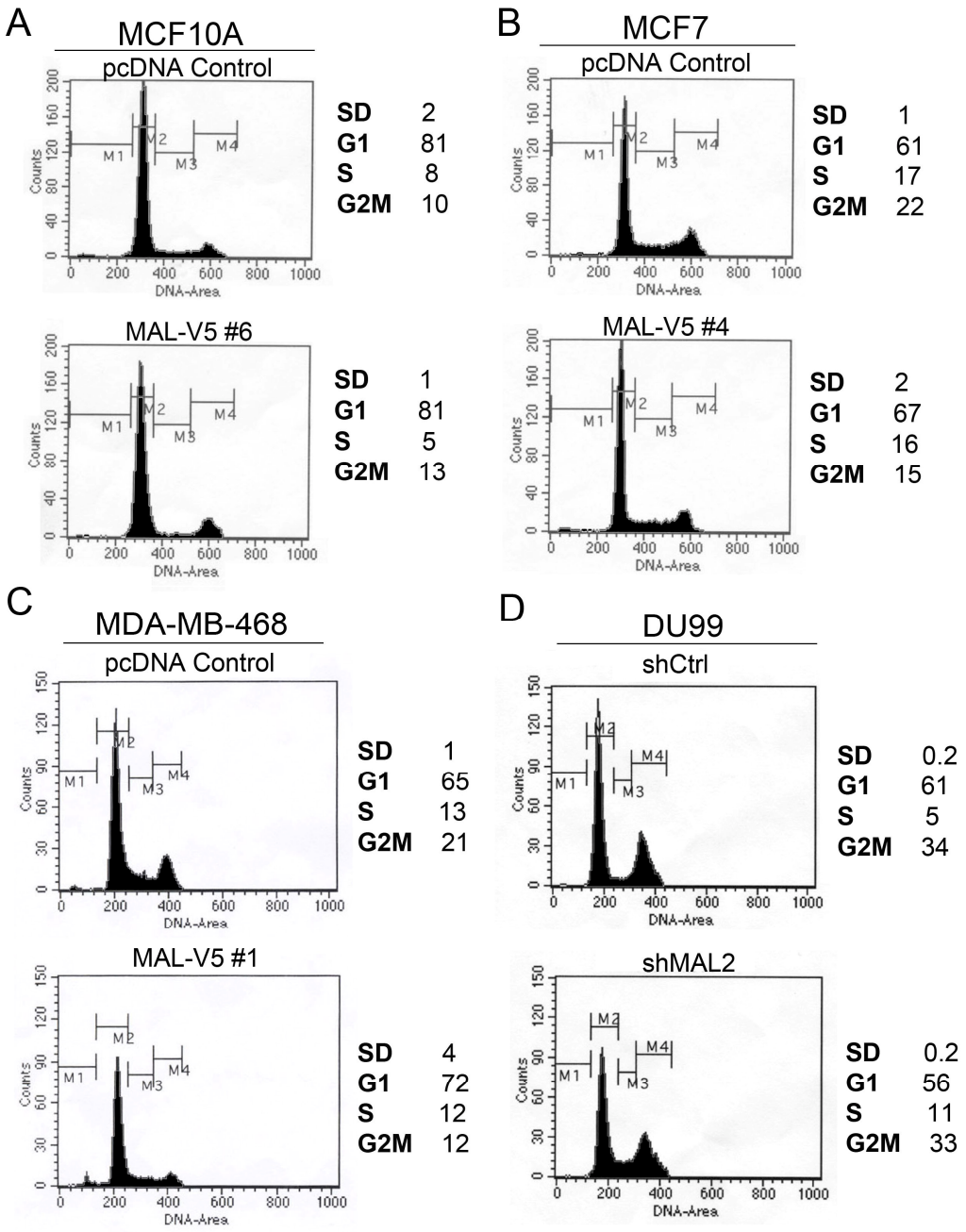
A
MCF10A
pcDNA Control
SD 2
G1 81
S 8
G2M 10
MAL-V5 #6
SD 1
G1 81
S 5
G2M 13
B
MCF7
pcDNA Control
SD 1
G1 61
S 17
G2M 22
MAL-V5 #4
SD 2
G1 67
S 16
G2M 15
C
MDA-MB-468
pcDNA Control
SD 1
G1 65
S 13
G2M 21
MAL-V5 #1
SD 4
G1 72
S 12
G2M 12
D
DU99
shCtrl
SD 0.2
G1 61
S 5
G2M 34
shMAL2
SD 0.2
G1 56
S 11
G2M 33
Counts
DNA-Area
M1
M2
M3
M4

Figure 4-5. Effect of MAL expression on cell cycle progression. Cell cycle profiles of breast epithelial cells either overexpressing or with knockdown of MAL expression. Flow cytometry with use of propidum iodide staining shows the percentage of cells in the sub-diploid (SD) fraction, G1, S, and G2-M phases of the cell cycle. MAL overexpression had no effect on the cell cycle in **(A)** MCF10A cells but caused a delay in cell cycle progression in both **(B)** MCF7 and **(C)** MDA-MB-468 cells. Knockdown of MAL expression in **(D)** DU99 cells accelerated cell cycle progression.

Fig. 4-6.

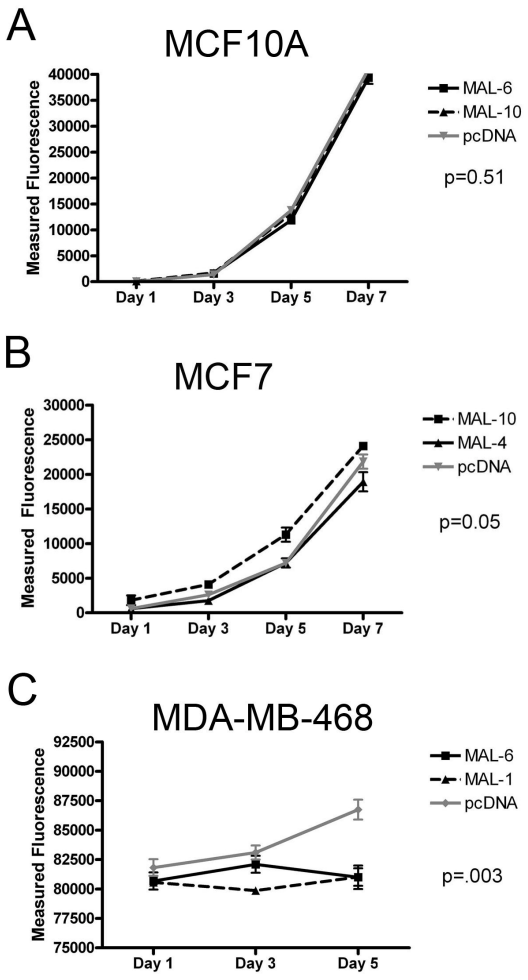

Figure 4-6. Effect of MAL overexpression on the rate of cell growth. Graphs showing the rate of growth in **A.** MCF10A, **B.** MCF7, and **C.** MDA-MB-468 cells stably transfected with either a vector control plasmid (pcDNA) or the MAL-V5 plasmid (MAL). At the indicate time points DNA content was measured by propidum iodide staining followed by fluorescence analysis. Statistical significance was calculated using a two-factor ANOVA test.

4.2.4 Exogenous expression of MAL decreases anchorage independent growth in soft agar

To assess the ability of MAL to inhibit colony formation *in vitro*, we utilized a soft-agar assay to monitor anchorage-independent growth of our stable breast cell lines. The overexpression of MAL substantially decreased the soft agar colony-forming ability of MCF7, MD468 and MCF10A cells resulting in both fewer and smaller colonies (Fig. 4-7A and B). As reported with immortal non-tumorigenic lines, MCF10A cells formed few colonies when grown in soft agar. However, in cells overexpressing the MAL protein, the presence of colonies was barely detectable (Fig 4.7B). The telomerase-immortalized DU99 cells did not grow any detectable colonies regardless of MAL expression.

Fig. 4-7.

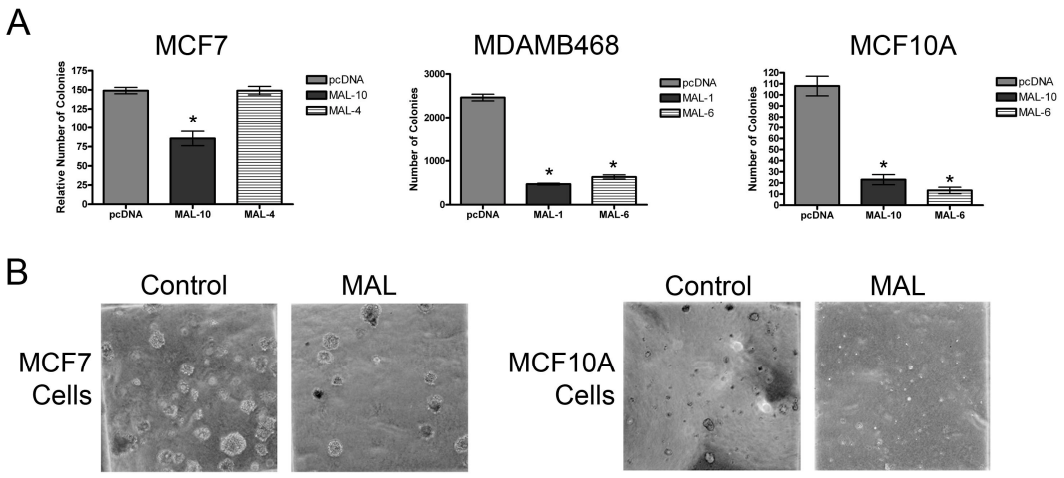

Figure 4-7. MAL expression reduces anchorage-independent growth. Soft agar assay of stable cell lines either expressing MAL-V5 or a vector control. **A.** MAL expression reduced the number of colonies that were able to grow in soft agar. Data are means ± SEM of three separate plates. Asterisks indicate statistical significance compared to the respective vector control (Student's *t*-test **P*<0.003). **B.** Examples of the size and number of soft-agar colonies grown in MCF7 and MCF10A cells.

4.2.5 Expression of MAL reduces cell migration and invasion through Matrigel

The ability of MAL to affect cell migration was measured by a wound-healing assay in which a scratch is made in a cell monolayer and the ability of the cells to completely close the wound is measured over time. MAL-expressing MCF10A cells demonstrated a significant decrease in cell migration compared to the vector control cells (Fig. 4-8A). In the transformed MCF7 and MD468 cells, a similar trend was observed in which MAL expression caused a reduction in motility, however this difference was not statistically significant (Fig. 4-8B and C). Reduced cell motility was not attributable to changes in proliferation as measured by propidium iodide in MCF10A or MCF7 cells, however the same cannot be said for MD468 cells. DU99 cells showed no difference in cell migration, as measured by the wound-healing assay, between the MAL knockdown and shCtrl clone (Fig. 4-8D).

In view of the observed MAL-induced reduction in cell migration, we examined if overexpression of MAL could reduce the invasiveness of MCF10A and MCF7 cell lines by analyzing cell invasion through Matrigel. As predicted, MAL-expressing MCF10A cells exhibited a lower level of invasion through the Matrigel basement membrane matrix compared with the vector controls (P=0.01) while the difference in MCF7 cells did not reach statistical significance (P=0.14) (Fig. 4-9).

Fig. 4-8.

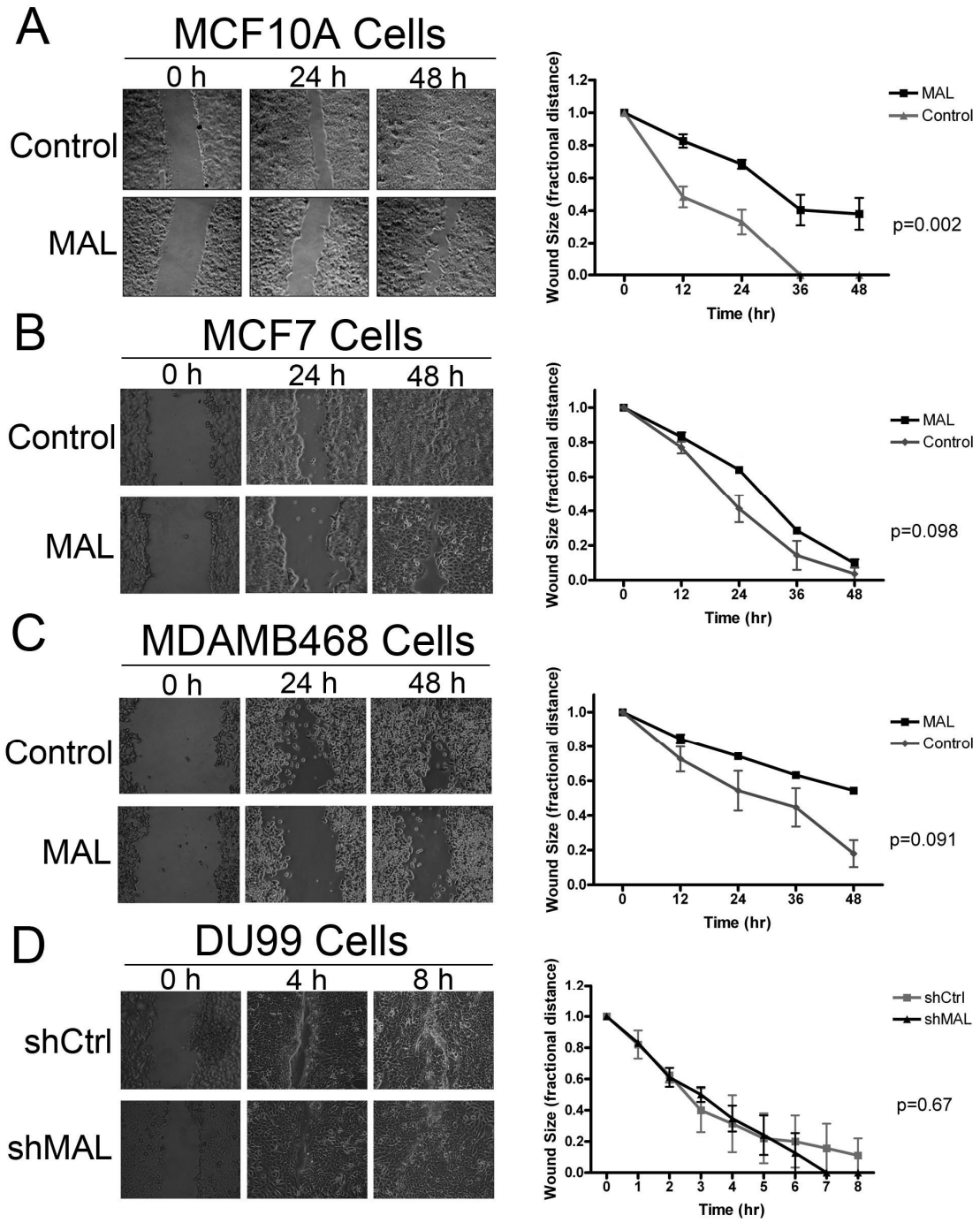
A
MCF10A Cells
0 h
24 h
48 h
Control
MAL
Wound Size (fractional distance)
Time (hr)
MAL
Control
p=0.002
B
MCF7 Cells
0 h
24 h
48 h
Control
MAL
Wound Size (fractional distance)
Time (hr)
MAL
Control
p=0.098
C
MDAMB468 Cells
0 h
24 h
48 h
Control
MAL
Wound Size (fractional distance)
Time (hr)
MAL
Control
p=0.091
D
DU99 Cells
0 h
4 h
8 h
shCtrl
shMAL
Wound Size (fractional distance)
Time (hr)
shCtrl
shMAL
p=0.67

Figure 4-8. MAL overexpression reduces cell migration. Representative images from an *in vitro* wound-healing assay performed on **A.** MCF10A, **B.** MCF7, **C.** MDA-MB-468 breast epithelial cells stably transfected with either vector control (top panels) or V5-tagged MAL (bottom panels) or **D.** DU99 cells stably transfected with shCtrl or shMAL plasmids. Original magnification X10. The graphs on the right panels show quantitation of the rate of closure for the wound-healing assay in both control and MAL-expressing cell lines. Statistical significance was calculated using a two-factor ANOVA test.

Fig. 4-9.

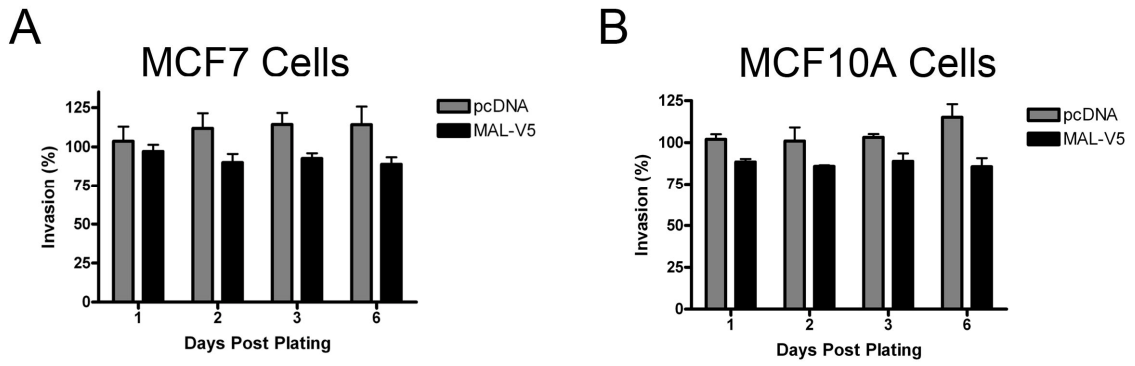

Figure 4-9. MAL expression reduced cell invasion through Matrigel. Monolayers of both **A.** MCF7 and **B.** MCF10A cells were labeled with the fluorescent label DiI, trypsinized and plated in a BD BioCoat Matrigel Invasion System with 5% FCS in the bottom chamber. The fluorescence of invaded cells on the lower side of the membrane was measured using a microplate reader. Representative results are shown as percent invasion, calculated as: (measured fluorescence at indicated Day X/measured fluorescence at Day 0) X 100. Statistical significance was calculated using a two-factor ANOVA test, MCF7 P=0.14 and MCF10A P=0.01.

4.2.6 MAL overexpression disrupts acinar structure in MCF10A cells grown in three-dimensional Matrigel culture

Culturing MCF10A mammary epithelial cells on a reconstituted basement membrane results in the formation of polarized, hollow, acinar-like spheroids that recapitulate several aspects of glandular architecture in vivo (56). Considering MAL's function in protein sorting in polarized epithelial cells we thought it relevant to assess how modulating MAL expression would affect acinar formation in three-dimensional culture. Evaluating the formation of these structures will provide an assessment of how MAL expression affects proliferation and apoptosis, two processes that contribute to acinar formation.

Growing MCF10A vector control cells in three-dimensional culture resulted in the formation of polarized hollow acinar structures while MAL-overexpressing cells exhibited incomplete luminal clearance (Fig 4-10). Further, when staining the acini structures for M30, an apoptotic marker, we saw greater M30 staining in vector control cells compared to MAL-expressing cells which could account for the difference in luminal clearance. Given that we observed no differences in the growth rate of stably transfected MCF10A cells (Fig. 4-6), it is highly unlikely that the differences in acini structure between MAL+ and MAL- cells is due to changes in cell proliferation.

Fig. 4-10.

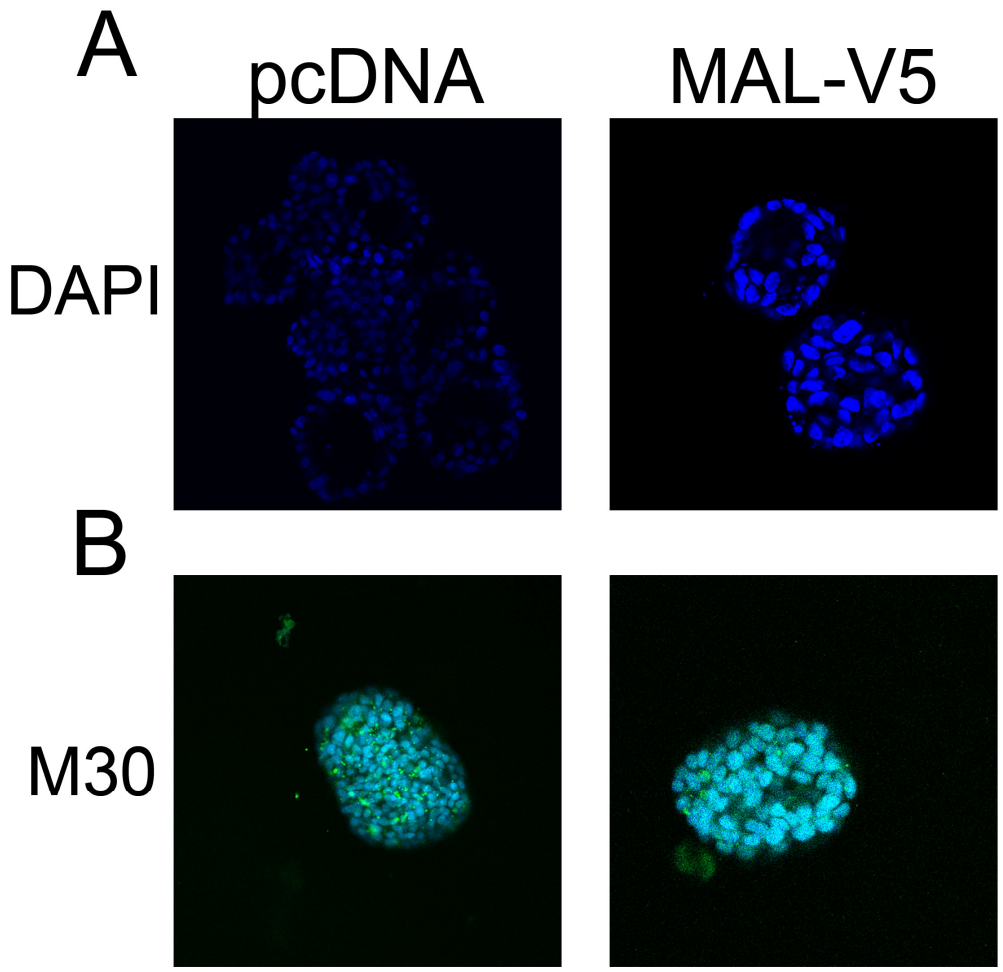

Figure 4-10. Effect of MAL on acini formation in MCF10A cells. 3-D culturing of MCF10A cells stably expressing vector control plasmid *(left panels)* or MAL-V5 *(right panels)*. **A.** Cells were stained with either DAPI showing proper lumen formation in vector control cells and incomplete lumen clearance in MAL-expressing cells. **B.** Apoptotic cells were stained with M30 (green) showing more apoptotic cells in the vector control cells. Nuclei are stained with DAPI and shown in blue.

4.2.7 The MAL protein is expressed in normal breast tissue

Since its identification in T cells, MAL protein expression has been detected in a wide range of epithelia (16). Also, a separate immunohistochemical study reviewed the range of MAL expression in several normal human tissues compared with that of neoplastic tissue (96); however, mammary tissue sections were not included in either study. To our knowledge, expression of the MAL protein in breast epithelial cells has yet to be demonstrated. Consequently, we wanted to confirm that the MAL protein is expressed in normal breast tissue.

By immunohistochemistry using a well-characterized monoclonal antibody (10, 11, 16), we were able to detect MAL in normal breast epithelium from reduction mammoplasty specimens (Fig. 4-11B). In each assay we used kidney sections as both a positive and negative control. Distal and collecting tubules express high levels of the MAL protein while glomeruli and proximal tubules are negative (Fig. 4-11A). Furthermore, when looking at normal epithelium adjacent to malignant tissue, we observed positive MAL staining in the normal cells while the cancerous tissue was negative for MAL expression (Fig. 4-11C).

Fig. 4-11

A

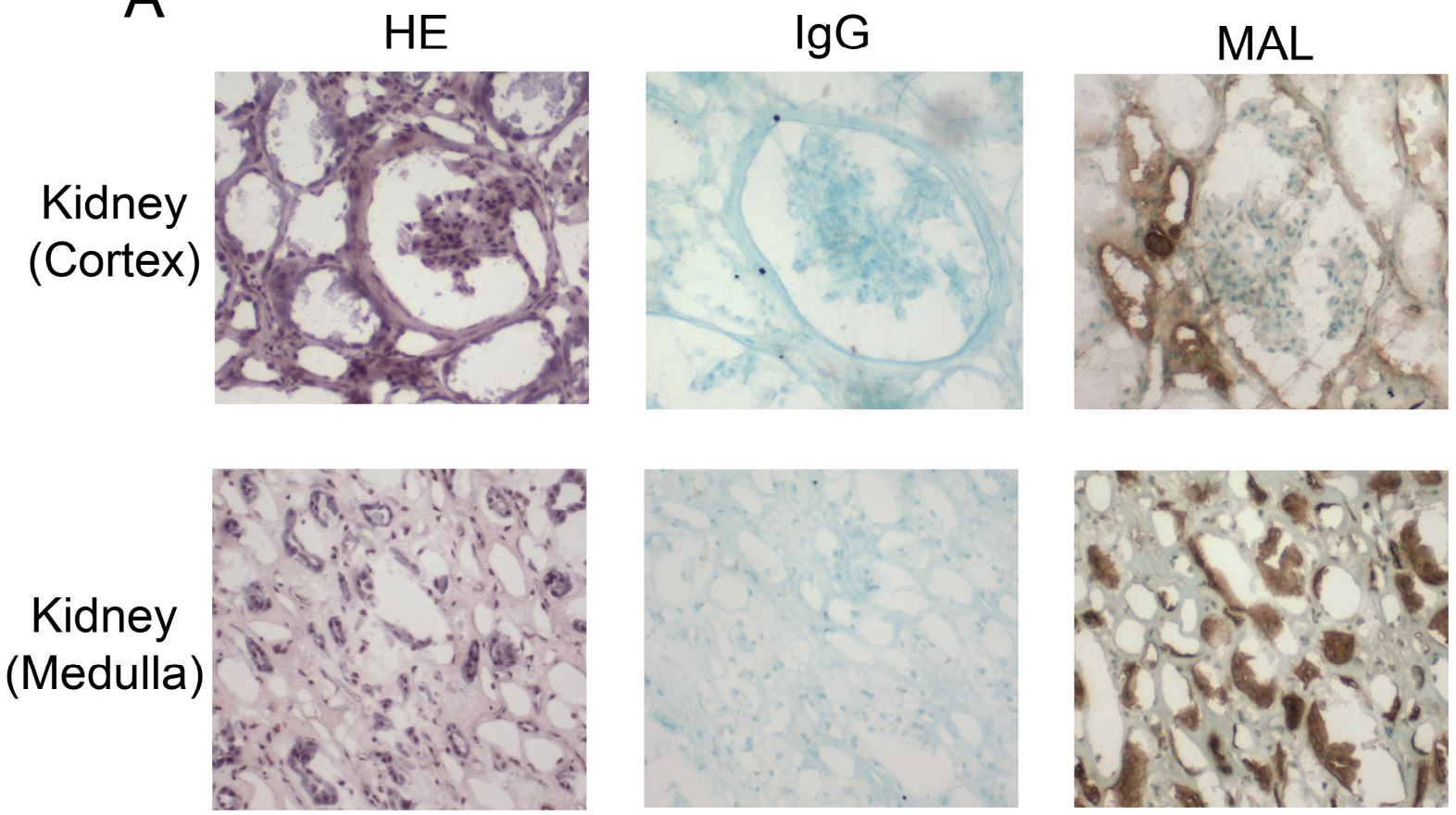

B

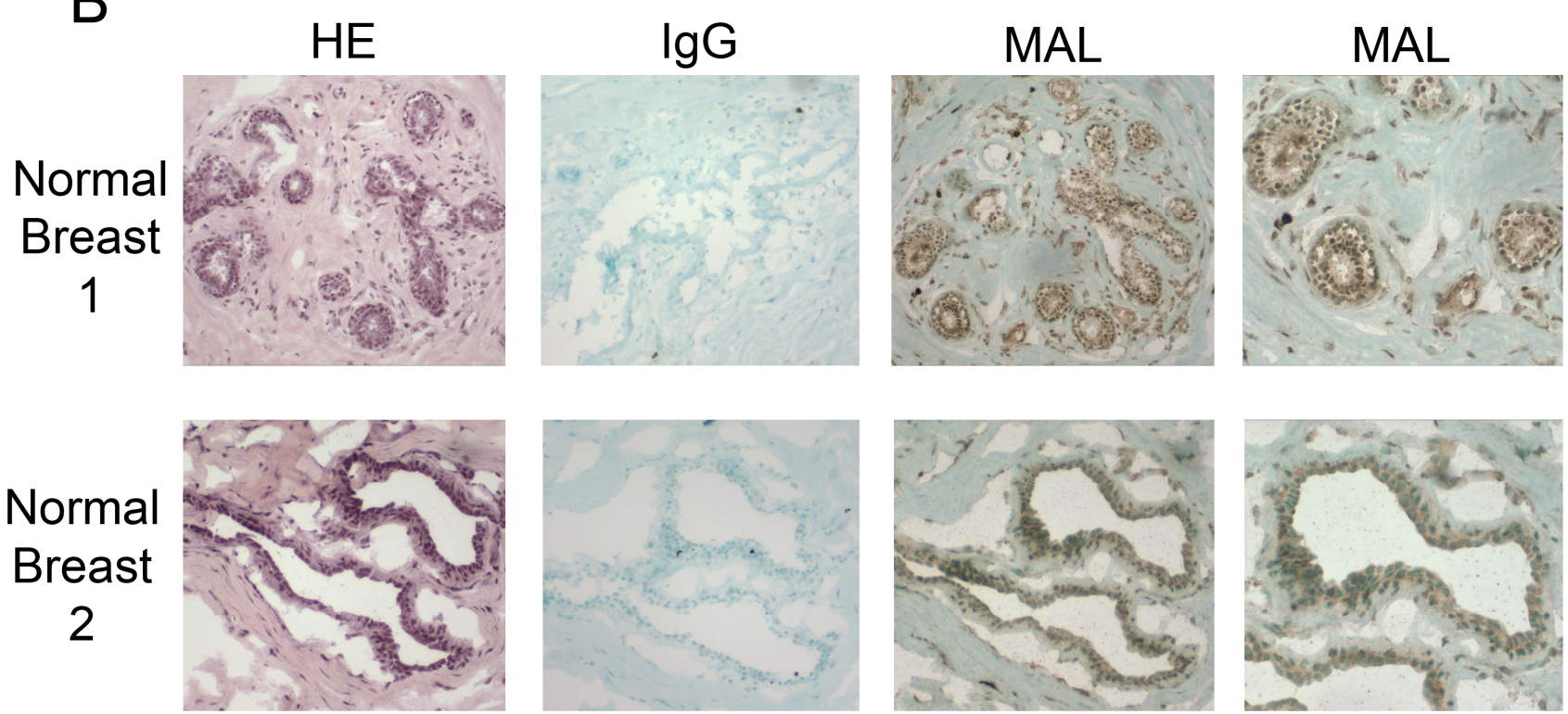

C

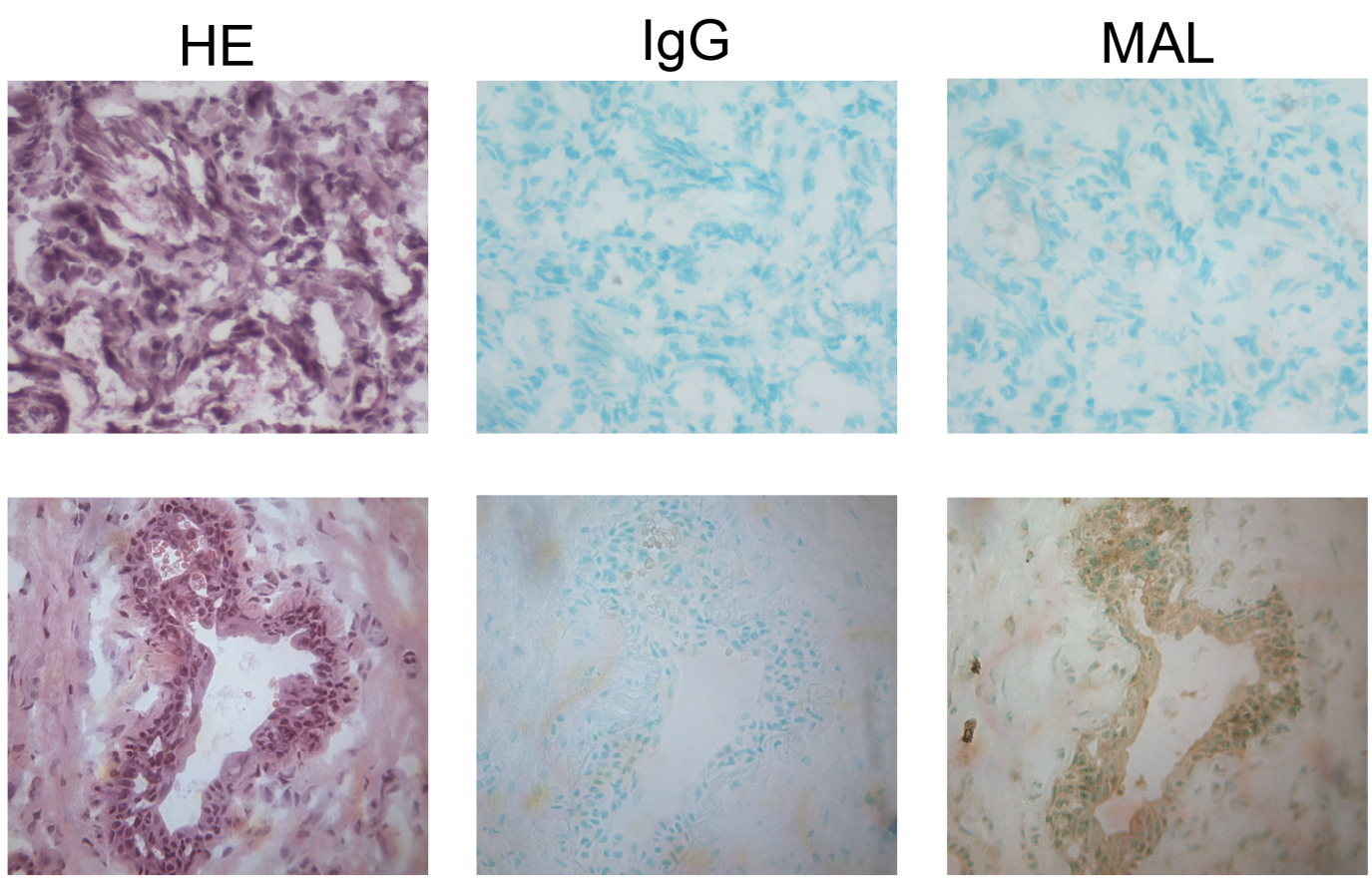

Figure 4-11. The MAL protein is expressed in normal breast tissue. Frozen tissue sections were subjected to immunohistochemical analysis with either rabbit IgG, anti-MAL 6D9 monoclonal antibody, or stained with hematoxylin and eosin (HE). **A**. As a control human kidney sections were stained showing positive staining in the distal and collecting tubules and negative staining in the glomeruli. Original magnification X10. **B.** Sections of benign breast tissue, from patients with no evidence of cancer showing positive MAL staining. Original magnification X10 and X20 (right panels only). **C.** In breast cancer sections that were negative for MAL expression, adjacent normal epithelium exhibited positive MAL staining. Original magnification X20.

4.2.8 MAL protein expression has predictive value in primary breast cancer

Data from our functional studies suggests that MAL has a role in regulating cell properties such as proliferation and invasion, which can contribute to tumor development. Moreover, we found that MAL promoter methylation correlated with estrogen and progesterone receptor positivity in a subset of 36 breast cancer patients. Since promoter methylation does not always directly correlate with MAL expression, we wanted to determine if MAL protein expression correlated with any common clinico-pathologic features in a larger cohort of breast cancer patients.

We evaluated MAL expression by immunohistochemical (IHC) staining in a representative sample of 122 banked frozen breast cancers resected at Duke University Medical Center between 1990 and 1998. In all staining runs, controls included a normal breast specimen and a normal kidney as positive and negative controls and to normalize for inter-assay variability in intensity. In addition, 20 cancers were included (in a blinded fashion) in more than one staining run to assure reproducibility. Within the invasive cancer samples, we observed highly variable MAL protein levels, from undetectable to abundant similar to the kidney distal tubule epithelium (Fig. 4-12). Tissues were categorized as negative or positive for MAL staining in the malignant breast epithelium (Fig. 4-12). Many of the cancers contained infiltrating inflammatory cells that reacted with the antibody serving as an internal control. We observed no significant relationship between MAL protein expression and common clinico-

pathologic parameters (Table 2). Disease-free survival, with an average follow-up of 96 months, trended towards better outcome in patients with MAL-expressing cancers but did not reach statistical significance (Fig. 4-12C).

While MAL expression does not have strong prognostic value, predictive value is of equal or greater importance as a determinant of who will derive benefit from adjuvant chemotherapy. Overall, we observed no difference in disease-free survival based on the delivery of chemotherapy alone (Fig. 4-13A). MAL staining did not identify a difference in the subpopulation of patients that received adjuvant cytotoxic therapy (Fig. 4-13B). However, in the group of patients who were not treated, absence of MAL staining was a significant predictor of disease progression (Fig. 4-13C). Although a multivariate analysis was not conducted on this data set, MAL-positive and -negative tumors from patients who did not receive adjuvant chemotherapy were not significantly different based on age, nodal status, tumor size, or hormone receptor status (Table 3) indicating that the MAL protein may be an independent predictor of benefit from chemotherapy.

Fig. 4-12.

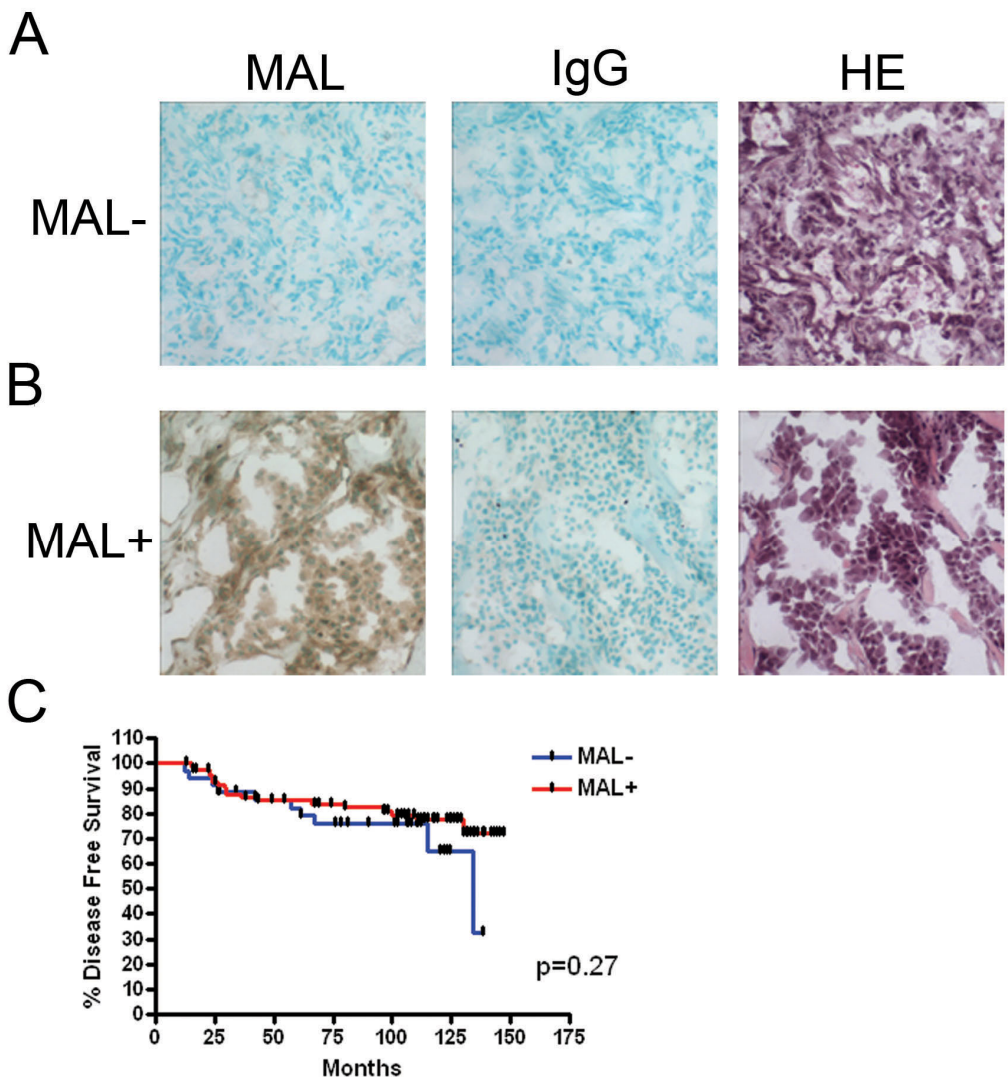

Figure 4-12. MAL protein expression and survival analysis in breast cancer patients. **A.** Representative IHC of a breast tumor negative for MAL expression stained with either MAL6D9 monoclonal antibody, mouse IgG, or H&E. **B.** Representative IHC of a breast tumor positive for MAL expression. Original magnification X20. **C.** Kaplan-Meier plot of percent disease survival for MAL- and MAL+ breast cancer patients.

Table 2. Clinico-pathologic features of patients by MAL IHC

	MAL- n (%)	MAL+ n (%)	*P*
Patients (n)	35 (29)	87 (71)	
Age			0.44
≤50	18 (51)	38 (44)	
>50	17 (49)	49 (56)	
Race			0.62
White	28 (80)	66 (76)	
Non-White	7 (20)	21 (24)	
Black	7	16	
Am Indian	0	2	
Asian	0	3	
Estrogen receptor status			0.47
Positive	18 (55)	50 (62)	
Negative	15 (45)	31 (38)	
Progesterone receptor status			0.70
Positive	17 (52)	45 (56)	
Negative	16 (48)	36 (44)	
Node involvement			0.14
Yes	16 (48)	28 (34)	
No	17 (52)	55 (66)	
Stage			0.19
I or IIA	22 (63)	60 (75)	
IIB and higher	13 (37)	20 (25)	
Tumor stage			0.49
T1 A, B, C	15 (45)	32 (39)	
T2 and higher	18 (55)	51 (61)	
Histologic Grade			0.17
1	1 (3)	3 (4)	
2	5 (17)	25 (34)	
3	24 (80)	45 (62)	
Adjuvant chemotherapy			0.37
Yes	22 (63)	47 (54)	
No	13 (37)	40 (46)	
Hormonal therapy			0.18
Yes	15 (43)	49 (56)	
No	20 (57)	38 (44)	
NOTE: Statistical significance calculated using chi squared analysis			

Fig. 4-13.

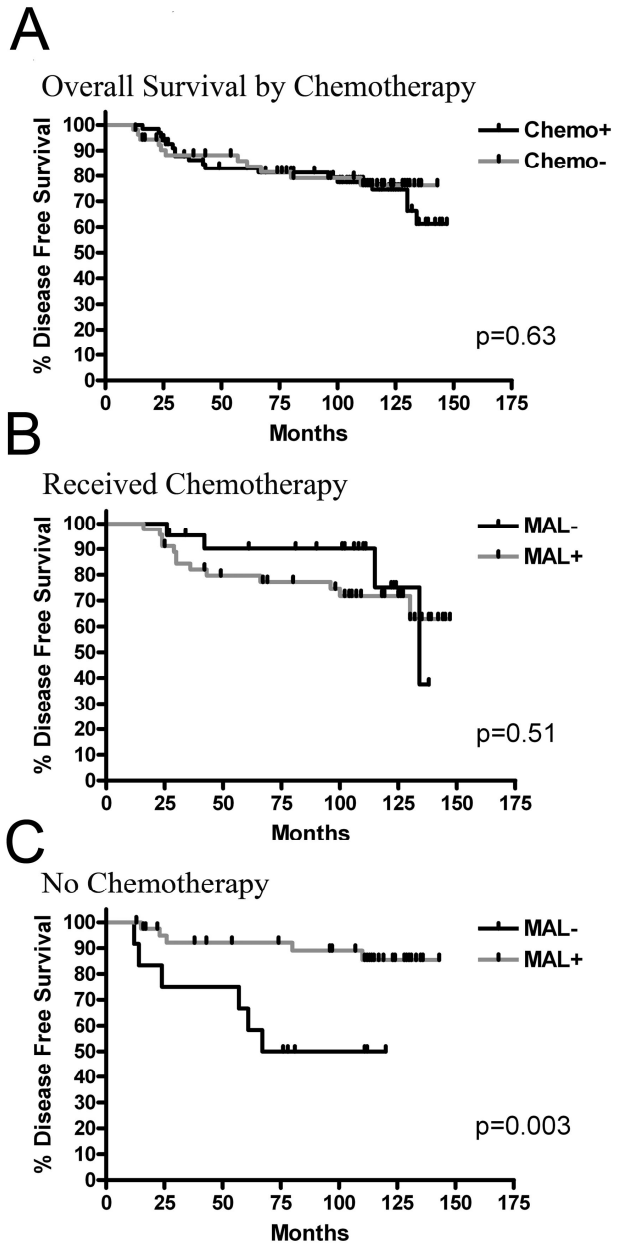

Figure 4-13. Survival analysis of breast cancer patients by adjuvant chemotherapy treatment. Kaplan-Meier plot of percent disease free survival for: **A.** all patients, **B.** those who received adjuvant chemotherapy, and **C.** those who did not receive chemotherapy.

Table 3. Clinico-pathologic features of patients stratified by chemotherapy received

	All Patients			Chemo– Only			Chemo+ Only		
	Chemo+ n (%)	Chemo– n (%)	*P*	MAL– n (%)	MAL + n (%)	*P*	MAL- n (%)	MAL+ n (%)	*P*
Patients	69 (57)	53 (43)		13 (25)	40 (75)		22 (32)	47 (68)	
Node –	31 (46)	41 (84)	<0.0001	9 (69)	33 (89)	0.11*	9 (45)	22 (48)	0.84
Node +	36 (54)	9 (16)		4 (31)	4 (11)		11 (55)	24 (52)	
T1	21 (32)	26 (51)	0.04	8 (62)	19 (49)	0.42	8 (38)	13 (30)	0.49
> T1	44 (68)	25 (59)		5 (38)	20 (51)		13 (62)	31 (70)	
ER+	34 (52)	34 (71)	0.03	9 (75)	25 (69)	0.51*	9 (43)	25 (56)	0.34
ER-	32 (48)	14 (29)		3 (25)	11 (31)		12 (57)	20 (44)	
>50	25 (36)	41 (77)	<0.0001	11 (85)	30 (75)	0.38*	6 (27)	19 (40)	0.29
≤50	44 (64)	12 (23)		2 (15)	10 (25)		16 (73)	28 (60)	

NOTE: Statistical significance calculated using chi squared analysis except where indicated by (*) Fisher's exact test used

4.3 Discussion

Protein sorting is involved in the maintenance of cell polarity and loss of polarity is a common characteristic of malignant epithelial cells. Disrupting MAL expression in polarized Madin-Darby canine kidney cells resulted in changes in protein sorting and cell morphology (16, 18). With the knowledge of the involvement of impaired cell polarity and aberrant protein sorting in carcinogenesis, it is plausible that loss of the MAL protein in polarized epithelial cells could lead to the development and progression of cancer. To begin to investigate the functional role of MAL in breast cancer, we conducted several *in vitro* studies with either knockdown or overexpression of the MAL protein and monitored subsequent phenotypic changes.

Recent data has suggested that the MAL gene might function as both a metastasis suppressor and tumor suppressor gene in several types of cancer. In esophageal cancer where MAL gene expression was found to be frequently reduced or absent, exogenous expression of MAL in carcinoma TE3 cell reduced cell motility, invasion, and enhanced apoptosis *in vitro* and reduced tumorigenicity *in vivo* (23). Recently, Overmeer *et al.* demonstrated that ectopic expression of MAL in cervical cancer SiHa cells reduced the proliferation rate and repressed tumor cell characteristics such as migration and anchorage-independent growth (22). We found that overexpression of MAL in the breast cancer cell lines MCF7 and MD468 resulted in slower progression through the cell cycle, decrease in anchorage-independent growth

and a decrease in cell migration. MAL expression was also able to reduce the rate of cell growth, but only in the MD468 cell line. The observed decrease in the growth rate of MAL-expressing MD468 cells compared to the vector control cells could be due in part to the increase in percent sub-diploid cells with MAL expression (Fig. 4-5C). The non-tumorigenic immortalized cell line MCF10A was also used in our functional studies. MCF10A cells are hypermethylated in the MAL promoter and have low MAL mRNA expression, similar to the breast cancer cell lines. Expressing the V5-tagged MAL protein in these cells had no effect on the rate of cell growth or progress through the cell cycle but caused a decrease in anchorage-independent growth and the rate of cell migration. Taken together, these data support the notion that loss of the MAL protein due to promoter hypermethylation in breast cells could potentially lead to phenotypic changes conducive to cancer progression. In order to strengthen this argument, *in vivo* studies need to be conducted to assess the tumorigenic potential of MAL +/- breast cancer cells. Based on our *in vitro* data, we would expect that MAL-expressing breast cancer cells would have a diminished ability to form tumors when transplanted into immunocompromised mice.

As mentioned previously, the MAL gene is thought to be a putative metastasis suppressor gene. Comparing matched primary and metastatic head and neck tumor-derived cell line pairs, researchers found selective down-regulation of MAL expression in metastatic cells (24). The observed down-regulation of MAL expression was

attributed to loss of heterozygosity and hypermethylation. From these data Beder *et al*. identified MAL as a new metastasis suppressor candidate for head and neck cancer. As a means to determine whether the MAL protein had any role in breast cancer invasion and metastasis, we examined the effect of MAL overexpression on both cell migration and invasion through Matrigel. Using a wound-healing assay to measure cell migration we found that overexpression of MAL in MCF10A cells significantly reduced their rate of wound closure. A similar trend was seen in both MCF7 and MD468 cells, however this difference did not reach statistical significance.

We next examined the invasion potential of our stable transfectants in an *in vitro* Matrigel invasion assay. Expression of MAL in both the MCF7 and MCF10A cell lines reduced their ability to invade through the artificial basement membrane. The MAL protein localizes to membrane rafts or lipid rafts in polarized epithelial cells where it functions in protein sorting. Moreover, these membrane rafts have been implicated in the process of tumor invasion and metastasis. In breast cancer cells, membrane raft integrity was found to be critical for EGF induced chemotaxis (48). Also, matrix metalloproteinases (MMPs), enzymes that degrade the extracellular matrix, and receptors for certain tissue serine proteases localize to membrane rafts (97). Thus, if MAL has a role in regulating membrane raft composition, disruption of MAL expression in mammary cells could contribute to cancer cell invasion and metastasis.

In addition to generating MAL-overexpressing cells we also stably knocked down MAL protein expression in the non-tumorigenic DU99 cell line. The shMAL clone progressed through the cell cycle slightly faster than the shCtrl clone evidenced by both a decrease in % G1 and increase in % S phase. As expected, the cell cycle changes seen in the DU99 MAL knockdown cells was converse to what was seen in MD468 and MCF7 MAL-overexpressing cell lines. When plated in soft agar, neither MAL expressing or knockdown cells formed any colonies. Also, using a wound-healing assay to measure cell migration, the rate of closure between the shMAL and shCtrl clones was not significantly different. Therefore we concluded that in DU99 cells loss of MAL alone was not sufficient to cause substantial tumorigenic changes. However, this does not undermine the role of MAL in breast carcinogenesis and progression. We propose that loss of MAL expression in breast cancer cells facilitates the interaction of signaling molecules and effectors contributing to the cancer phenotype. Thus loss of MAL alone may not be adequate to initiate the tumorigenic process but may aide in the progression of cancer. The non-transforming ability of knockdown of MAL expression on its own is apparent in MAL knockout mice which are viable and have a normal life span (15). Perhaps loss of MAL expression paired with an activating mutation in an oncogene would cause further transformation of the DU99 cells. What's more, MAL is a member of a family of transmembrane proteolipid proteins including MAL2 and BENE, either of which could be masking the effects of MAL loss in our functional assays as well as in the

MAL knockout mice. The existence of knockout mice for the MAL gene provides an excellent model system with which to examine more thoroughly how absence of MAL expression can affect properties such as tumor initiation, growth, and response to therapy.

Correct epithelial polarity regulates intracellular and extracellular proliferative signaling inputs through spatial organization and segregation of signaling effectors restraining cell proliferation (93). For example, in differentiated human airway epithelial cells heregulin α is present exclusively in the apical membrane physically separated from its receptors erbB3 and 4, which segregate to the basolateral membrane (98). This ligand-receptor system is activated whenever epithelial integrity is disrupted resulting in signal transduction cascades thereby stimulating proliferation. When grown in three-dimensional structure, MCF10A cells form acinar-like spheroid structures characterized by apicobasal polarization of the cells (56). Since they do lack MAL expression, we were interested in seeing what effect re-expression of MAL would have on MCF10A acinar formation. When MAL is overexpressed in MCF10A cells followed by three-dimensional culturing, the cells formed spheroids with incomplete lumen clearance (Fig. 4-10). The failure to completely clear the lumen was likely due to a decrease in luminal cell apoptosis evidenced by a lower amount of M30 staining in the MAL expressing cells compared to the vector controls.

Although MAL expression disrupted acini formation of MCF10A cells, this does not qualify MAL as an oncogene in this system. We must consider both the cell line we are using as well as the function of MAL in these cells. Although MCF10A cells are commonly considered a "normal" breast epithelial cell line, they harbor genetic abnormalities commonly associated with *in vitro* culture of mammary epithelial cells. Furthermore, they are hypermethylated in the MAL promoter, have low MAL expression, and behave similarly to the breast cancer cell lines in the functional assays after overexpression of MAL. Since MCF10A cells form polarized structures in the absence of MAL expression, it is clear that maintenance of cell polarity is not the primary function of MAL in these cells. Consequently, overexpressing MAL in this system could be disrupting the protein sorting machinery and thus acinar formation. Even with the caveats of using MCF10A cells in this particular assay, future three-dimensional culturing experiments could provide us with a greater understanding of the role MAL plays in establishing polarity in breast epithelial cells. Furthermore, given that MAL functions in polarized sorting in epithelial cells, studying its altered function and expression in breast cancer may provide a basis for understanding the loss of polarity phenotype that frequently accompanies neoplastic transformation.

Along with investigating the phenotypic effects of the MAL protein *in vitro* we were also interested in determining whether MAL expression had any predictive or prognostic value in our cohort of breast cancer patients. Given the complexity of the

methylation pattern at this locus and the availability of a high quality monoclonal antibody, we examined MAL expression at the protein level in a series of primary frozen breast specimens. Consistent with mRNA expression of cultured HMEC we found that benign breast epithelia expressed easily detectable MAL protein by immunohistochemical staining (Fig. 4-11). Categorizing 122 primary cancers based upon the absence or presence of staining in malignant epithelial cells, no significant correlations were found with standard clinico-pathologic parameters including age, stage, nodal status, tumor size, hormone receptor status, or disease-free survival. Over 40% of the patients in this study did not receive adjuvant cytotoxic chemotherapy. In this subgroup, absence of MAL protein expression was highly associated with shorter disease-free survival (P=0.003). In patients who were treated with chemotherapy, MAL staining was not predictive. As expected, patients who did not receive chemotherapy were older, had smaller tumors, and were more frequently node-negative and hormone receptor-positive (Table 3). One interpretation of these findings is that lack of MAL protein expression might identify a subgroup of breast cancer patients that would benefit from receiving adjuvant chemotherapy.

In gastric cancer, hypermethylation of the MAL proximal promoter correlated with significantly better disease-free survival and with down-regulation of expression (28). From these results the authors concluded that MAL has putative tumor-suppressor gene function in gastric cancer and detection of promoter hypermethylation may be

useful as a prognostic marker. In Hodgkin's lymphoma, MAL protein expression was shown to identify a subset of patients with an adverse outcome (26). Furthermore, MAL mRNA expression was most highly overexpressed in short-term ovarian cancer survivors compared with long-term survivors (30). Thus it appears that MAL promoter methylation, mRNA expression, and protein levels all have prognostic value with relation to cancer, dependent upon the tumor type.

5. Role of the MAL Protein in Cancer-Related Cell Signaling

5.1 Introduction

Membrane rafts, areas of the plasma membrane enriched in cholesterol and sphingolipids, contain a wide range of proteins including glycosylphosphatidylinositol (GPI)-anchored proteins, heterotrimeric G proteins and transmembrane proteins. One of the most important properties of membrane rafts is their ability to include or exclude proteins to variable extents (99). Rafts are thought to function in cellular signaling by concentrating or separating specific membrane and/or membrane-associated proteins in a unique lipid environment (37). Thus, the integrity and composition of lipid rafts is relevant to the maintenance of various signaling pathways.

Several lipids, proteins, and receptors that are relevant to cellular signaling are known to localize to membrane rafts including the Src-family tyrosine kinases, MAL, epidermal growth factor receptor (EGFR), and the lipid second-messenger PIP_2. The Src-family kinases (SFK) are involved in regulating numerous cellular functions through their interactions with membrane and cytosolic proteins. Membrane rafts are the site of SFK activation in breast cancer cells and raft-specific knockdown of SFK activity inhibited cell adhesion and cell cycle progression (100). The MAL protein is essential in raft-mediated signaling through the SFK in T cells where it physically interacts with SFK members Fyn and Lck (11), mediating Lck membrane recruitment and downstream signaling (49). Membrane rafts are also important regulators of EGFR activation, which

is associated with a number of cancers. Roepstorff *et al.* proposed that membrane rafts function as negative regulators of EGFR signaling by sequestering a fraction of the EGFR in a state inaccessible for ligand binding (46). This conclusion was based on studies conducted in HeLa cells showing that raft disruption via cholesterol depletion increases EGF binding to EGFR and causes an alteration in the amount of EGFR available for ligand binding. A similar result was seen in keratinocytes where raft destruction by cholesterol depletion released EGFR from the rafts where it became activated and further stimulated cell proliferation via extracellular signal-regulated kinase 2 (45). These data emphasize the importance of both membrane raft integrity and composition in regulating cellular signaling.

Phosphatidylinositol-4,5-bisphosphate (PIP_2), an important lipid second messenger in the PI3K/Akt pathway, has been identified in membrane raft fractions (101). In cancer, signaling through the phosphatidylinositol-3 kinase (PI3K) pathway begins with growth factor binding to receptor tyrosine kinases at the plasma membrane. PI3K is then recruited to the receptor, is activated and phosphorylates PIP_2 to generate PIP_3. PIP_3 accumulation in the membrane recruits the kinase Akt, through its pleckstrin homology (PH) domain where it binds to PIP_3 and is activated by two phosphorylation events. Akt activation triggers a complex cascade of signals that regulate growth, proliferation, survival and motility (102). The phosphatase PTEN (phosphatase and tensin homologue deleted on chromosome 10) dephosphorylates PIP_3 to PIP_2 thereby

acting as a negative regulator of this pathway. Membrane rafts play a key role in signaling via the PI3K/Akt pathway in several cancer types including lung, prostate and colon cancer (103, 104). In small cell lung cancer (SCLC) cells, membrane rafts are involved in the activation of PI3K signaling by facilitating the interaction of Src with specific PI3K isoforms (105). Using a novel fluorescent correlation spectroscopy strategy Lasserre *et al.* demonstrated that membrane rafts facilitate Akt recruitment and activation upon PIP_3 accumulation in the plasma membrane, thus playing a crucial role in triggering the PI3K/Akt pathway (42).

Considering the role membrane rafts play in regulating PI3K/Akt signaling and the fact that MAL localizes to membrane rafts and was shown to be critical in T cell signaling, we thought it relevant to investigate what role MAL plays in signaling via the PI3K/Akt pathway. Since our previous data identified MAL protein expression as a predictor of benefit from adjuvant chemotherapy in a cohort of breast cancer patients, we also examined whether MAL expression had any bearing on drug sensitivity. The data presented in this chapter demonstrate that MAL's effect on cell signaling is likely mediated through its ability to alter membrane raft composition. Furthermore, we show that MAL expression sensitizes the triple-negative breast cancer cell lines MD468 and BT20 to EGFR-targeted therapy by reducing Akt activation and inducing apoptosis.

5.2 Results

5.2.1 Expression of MAL results in altered membrane raft composition

In other epithelial cell types, the MAL protein localizes to cholesterol-enriched membrane rafts characterized by their resistance to detergent solubilization. As mentioned previously, sucrose gradient fractionation of the HCC1937 breast epithelial cells shows endogenous MAL predominantly located in the insoluble fraction (Fig. 5-1, left panels). Detection of the membrane raft resident protein flotillin-1 in this fraction confirmed the biochemical localization. Fractionating MCF10A stable cell lines indicated that the exogenous MAL-V5 protein localized to both the soluble and insoluble compartments. Interestingly, probing these same fractions for flotillin-1 indicated that MAL expression induces a compartmental change in this protein. Whereas flotillin-1 was found entirely in the soluble fraction in the vector control line (under G418 selection), introduction of MAL produced a dramatic redistribution of this protein into the insoluble fraction (Fig. 5-1, right panels). This suggests that decreased MAL expression in breast cancer cells may impact the protein composition of membrane rafts.

Fig. 5-1.

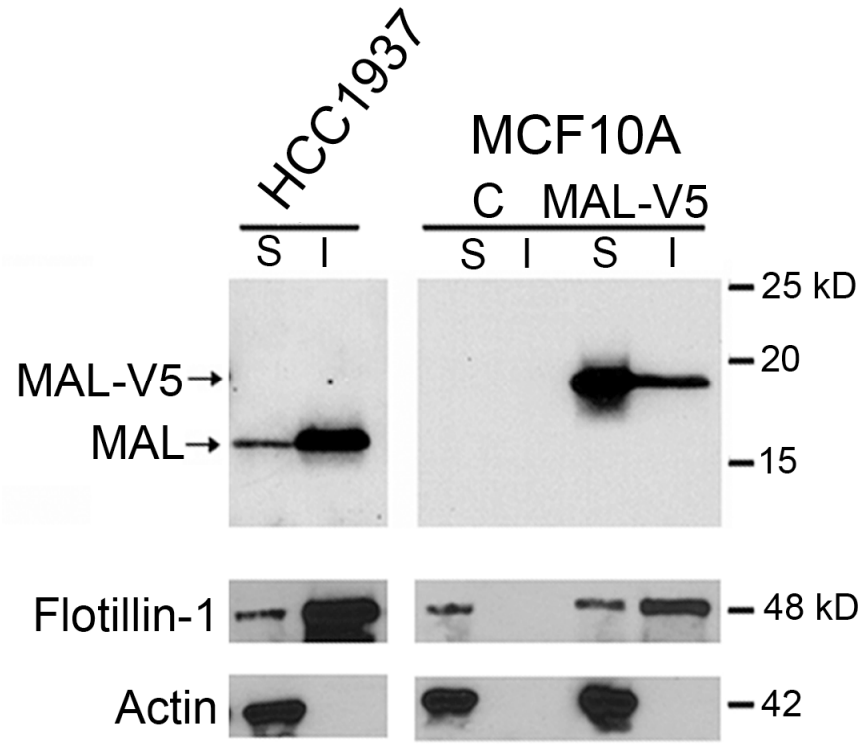

Figure 5-1. MAL expression alters membrane raft composition. Detection of either endogenous MAL in HCC1937 or exogenous C-terminal V5-tagged MAL in MCF10A cells after extraction with 1% Triton-X and centrifugation to equilibrium. Aliquots from either the detergent-soluble (S) or insoluble (I), lipid raft-containing fractions were analyzed with anti-MAL 6D9 mAb (top left blot), anti-V5 (top right blot), flotillin-1 or actin antibodies. No MAL protein was detected in the vector control (C)-containing cell lines and actin was only detected in the soluble fractions.

5.2.2 EGF drives migration of MAL-V5 both in and out of membrane rafts

Membrane rafts facilitate signaling events by concentrating or excluding signaling molecules within these specialized membrane microdomains. EGFR migration out of membrane rafts occurs in response to EGF stimulation (106). Apparently, entry or exit of signaling molecules in membrane rafts is an important control point for EGFR-mediated signal transduction. To investigate the migration of MAL in response to EGF stimulation, we monitored the movement of the MAL-V5 protein in sucrose gradients at various time points following the addition of EGF. MCF10A and MCF7 cells stably expressing MAL-V5 were serum-starved and stimulated with EGF for 2, 20 or 60 min or a vehicle control, followed by detergent extraction and sucrose gradient fractionation. Immunoblot analysis of MCF10A cells revealed a substantial migration of MAL-V5 out of the detergent insoluble fractions (DIF) upon EGF stimulation (Fig. 5-2A). This movement was transient as MAL-V5 was detected in the DIF after 60 min of EGF stimulation. Detection of flotillin-1 within these same fractions confirmed the membrane raft containing fractions (Fig. 5-2B). In MCF7 cells, EGF stimulation resulted in a significant accumulation of MAL-V5 within DIF (Fig. 5-3A). Again, movement of MAL-V5 into membrane raft fractions was transient. Detection of flotillin-1 within these same fractions confirmed the membrane raft-containing fractions (Fig. 5-3B). These data support the idea that the presence of MAL within membrane rafts has a bearing on EGF-mediated signaling, possibly via the EGF receptor. These experiments were also

conducted in vector control cells that showed no reaction with the V5 antibody as expected and no changes in flotillin-1 (data not shown).

Fig. 5-2.

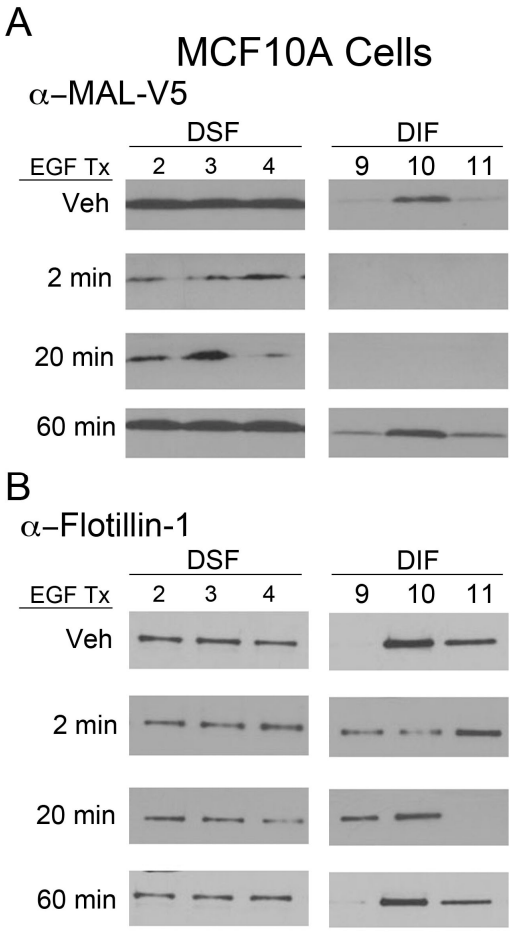

Figure 5-2. EGF induces MAL-V5 migration out of membrane raft fractions in MCF10A cells. A. EGF treatment (Tx) caused a transient migration of the MAL-V5 protein out of the detergent-insoluble fractions (DIF) containing membrane rafts, *top right panel*. There was also a slight decrease in MAL-V5 in the detergent-soluble fractions (DSF), *top left panel.* **B.** Flotillin-1 was detected to confirm membrane raft location, and showed a slight decrease in the DIF with EGF treatment. Fractions are labeled from the bottom to the top of the sucrose gradient.

Fig. 5-3.

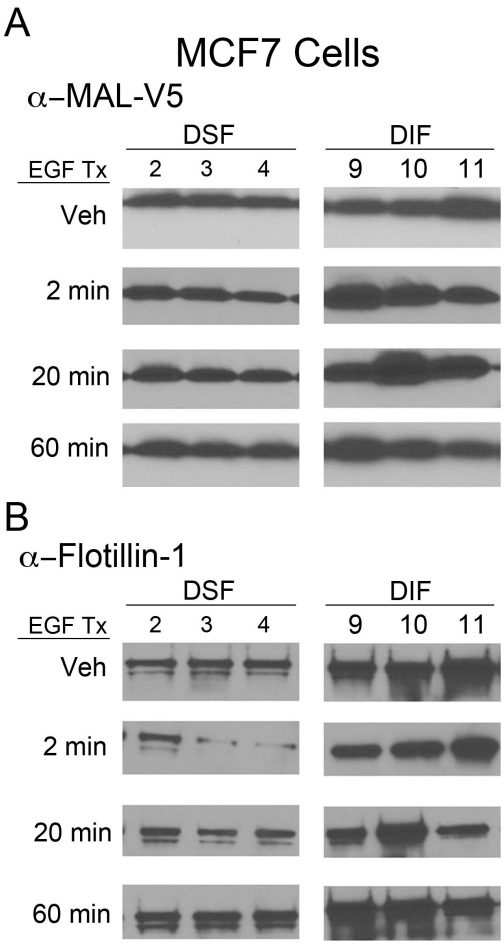

Figure 5-3. EGF induces MAL-V5 accumulation in membrane raft fractions in MCF7 cells. A. EGF treatment (Tx) caused a transient migration of the MAL-V5 protein out of the detergent insoluble fractions (DIF) containing membrane rafts, *top right panel*. There was not accompanied by any change in the detergent soluble fractions (DSF), *top left panel.* **B.** Flotillin-1 was detected to confirm membrane raft location, and showed no change with EGF treatment. Fractions are labeled from the bottom to the top of the sucrose gradient.

5.2.3 Expression of MAL sensitizes breast cancer cell lines to the EGFR inhibitor AG1478

Data from the previous experiment demonstrates that the MAL protein is responsive to EGF stimulation in breast epithelial cells, suggestive evidence that MAL might play a role in signaling via the epidermal growth factor receptor (EGFR). EGF is one of a few ligands that selectively binds to and activates the epidermal growth factor receptor. Binding of EGF to EGFR leads to homo- and hetero-dimerization with other erbB family members and subsequent receptor activation. Activation of EGFR in turn activates a variety of signaling cascades that regulate various biological processes such as cell proliferation, cell cycle progression, and cell survival.

Aberrant EGFR activation is correlated with the progression of multiple malignancies including lung, breast, and ovarian cancers (107). Thus, EGFR-targeted therapies such as tyrosine kinase inhibitors (gefitinib and erlotinib) or anti-EGFR monoclonal antibodies (cetuximab) are attractive anti-cancer agents. For our experiments we used the EGFR inhibitor AG1478. AG1478 is similar to gefitinib in that it is a small molecule inhibitor of EGFR that competitively binds to its ATP pocket inhibiting kinase activity. AG1478 has potent anti-proliferative effects both in culture and in vivo, however its clinical use is limited by its limited aqueous solubility (108-110). The antitumor effects of EGFR-targeting agents are mediated through the inhibition of downstream signaling effectors such as PI3K/Akt and MAPK. Interestingly, cells that

harbor mutations in the PI3K/Akt pathway have been shown to be less sensitive to the tyrosine kinase inhibitor gefitinib (111, 112).

To begin to examine the role of MAL in the response of breast cancer cells to EGFR-targeted therapy, we utilized the MD468 breast cancer cell line stably transfected with MAL-V5 or a pcDNA vector control. MD468 cells express high levels of EGFR and carry a deletion and frameshift mutation at codon 70 of the PTEN protein (113). Due to their lack of PTEN, MD468 cells maintain a high level of Akt kinase activity characterized by a high baseline level of phosphorylated Akt (114), and appear to be relatively resistant to EGFR-targeted therapy (112, 114). We were first interested in determining if expression of MAL had any effect on the baseline levels of phosphorylated Akt (P-Akt) in the MD468 cells (Fig. 5-4). Western blot analysis of log growing MD468 cells revealed a decrease in baseline P-Akt at S473 in MAL overexpressing cells suggesting that MAL is able to attenuate Akt activation.

We next asked if MAL overexpression could enhance the response of MD468 cells to the EGFR tyrosine kinase inhibitor AG1478. We first looked at the effect of AG1478 on the growth inhibition of MD468 stable cell lines. AG1478 effectively inhibited the growth of the MAL-expressing cell lines while the vector control cells appeared to be relatively resistant, up to a concentration of 10 μM (Fig. 5-5A). Since inhibition of EGFR via tyrosine kinase inhibitors is known to influence cell signaling events, specifically the PI3K/Akt pathway, we wanted to determine if MAL had an effect on AG1478-mediated

Akt inhibition. Treatment of MAL expressing clones with 10 μM AG1478 for 48 h almost eliminated P-Akt levels whereas it took at least 30 μM AG1478 to induce a similar reduction in P-Akt levels in the vector control cells (Fig. 5-5B). Moreover, cell cycle analysis of MD468 cells treated with 10 μM AG1478 revealed a substantial increase in the SD fraction of MAL expressing cells compared to the vector control (Fig. 5-5C). As a direct measurement of the effect of MAL on AG1478-induced apoptosis, we measured caspase 3/7 activation following 48 h of AG1478 treatment. AG1478 treatment resulted in a 3.5 fold increase in caspase 3/7 activation over the vehicle treated cells in the MAL-V5 clones whereas there was only a single-fold increase over the vehicle in vector control cells (Fig. 5-5D), confirming that MAL expression increases AG1478-mediated apoptosis.

To determine if MAL expression could sensitize MD468 cells to lower doses of AG1478, we exposed the stable cell lines to 1, 2.5, 5, and 10 μM concentrations of AG1478 for 48 h and measured Akt and MAPK activation, cell cycle progression, and caspase activation. Vector control cells showed no decrease in P-Akt levels with the lower concentrations of AG1478. However, in MAL-expressing clones we observed a significant decrease in P-Akt levels with an AG1478 concentration as low as 1 μM (Fig. 5-6A). We also examined P44/42MAPK (ERK1/2) levels following AG1478 treatment which showed an increase at 1 and 2.5 μM AG1478 and a decrease at 5 and 10 μM. Moreover, vector control cells appeared to have a lower baseline level of P44/42MAPK compared to MAL-expressing cells. As seen in earlier experiments, MAL expression in

MD468 cells resulted in an accumulation of cells in G1, treatment with AG1478 at the lower concentrations caused a modest increase over the baseline level of G1 arrest (Fig. 5-6B). There was not a significant change in the percent of cells in the SD fraction in either MAL-expressing or vector control cells. Consistent with cell cycle data, we observed no significant difference in caspase 3/7 activation between the stable cell lines following exposure to 1, 5, and 10 μM AG1478 for 4 hours (data not shown). However, analysis of P-Akt levels in MD468 cells following a short exposure to 5 μM AG1478 (5, 15, and 60 min) resulted in a decrease in P-Akt within 5 min of AG1478 exposure in the high MAL-expressing clone (MAL-1) but not in the vector control cells or the low MAL-expressing MD468 clone (MAL-6) (Fig. 5-6C). These data demonstrate that expression of the MAL protein in MD468 cells is sufficient to confer increased sensitivity to AG1478, possibly in alterations via membrane-associated signaling.

A constitutively active PI3K/Akt pathway due to a PTEN mutation is thought to contribute to the lack of sensitivity of MD468 cells to EGFR-targeted therapies (111, 112). Our data demonstrates that MAL expression enhances the response of MD468 cells to the EGFR tyrosine kinase inhibitor AG1478. To determine if MAL has a similar effect in another breast cancer cell line with constitutively active PI3K/Akt pathway, we utilized the BT20 breast cancer cell line. BT20 cells are similar to MD468 cells in that they are basal in origin and have high levels of EGFR and P-Akt. However, BT20 cells differ in that they have a PI3K activating mutation resulting in a constitutively active PI3K/Akt

pathway and high baseline levels of P-Akt (113, 115). After transiently transfecting BT20 cells with either MAL-V5 or the pcDNA vector as a control, we exposed the cells to 10 μM AG1478 for 48 hours and measured P-Akt and P-MAPK, cell cycle progression and caspase 3/7 activation. We observed no change in P-Akt levels in either of the BT20 transfectants following treatment with AG1478 for 48 h (Fig. 5-7A). Similar to what was seen in the MD468 cells, P-MAPK increased with increasing concentrations of AG1478. Interestingly, although we saw no decrease in P-Akt levels after a 48 h exposure to AG1478, cell cycle analysis revealed a significantly higher SD fraction in the MAL expressing BT20 cells compared to the vector control cells (Fig. 5-7B) suggesting that MAL expression is in fact sensitizing the BT20 cells to AG1478-induced apoptosis. Since the PI3K activating mutation in BT20 cells results in such a high level of Akt phosphorylation, we suspected that we were unable to detect the effect of MAL expression on P-Akt levels due to the high turnover rate in P-Akt production during the 48 h AG1478 treatment. Therefore, we measured P-Akt levels following 5, 15, 30, and 60 minutes of 5 μM AG1478 exposure in the BT20 transiently transfected cells. Immunoblot analysis revealed that MAL expression was able to delay the increase in P-Akt following AG1478 treatment in BT20 cells (Fig. 5-7C). Furthermore, analysis of caspase 3/7 activation following 4 hours of AG1478 treatment showed a significant dose-dependent increase in caspase activation in MAL-expressing cells while the vector control showed no significant increase (Fig. 5-7D). Taken together, these results indicate that MAL

expression is able to sensitize breast cancer cells with mutations in the PI3K/Akt pathway to AG1478-induced apoptosis accompanied by a reduction in Akt activation.

Fig. 5-4.

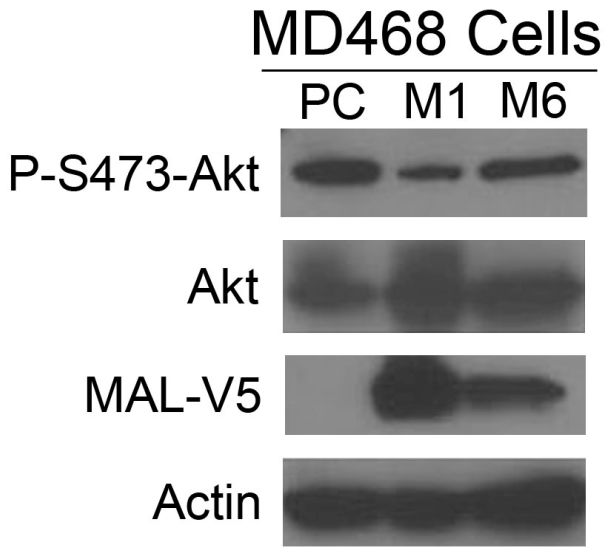

Figure 5-4. Exogenous MAL expression decreases the baseline levels of activated Akt. Comparison of the baseline levels of Ser473-phosphorylated Akt (P-S473-Akt) in MD468 cells stably transfected with either a pcDNA vector control (PC), or MAL-V5 (M1, *high*; M6, *low*). Expression of the MAL-V5 protein was able to reduce the baseline levels of phosphorylated Akt.

Fig. 5-5.

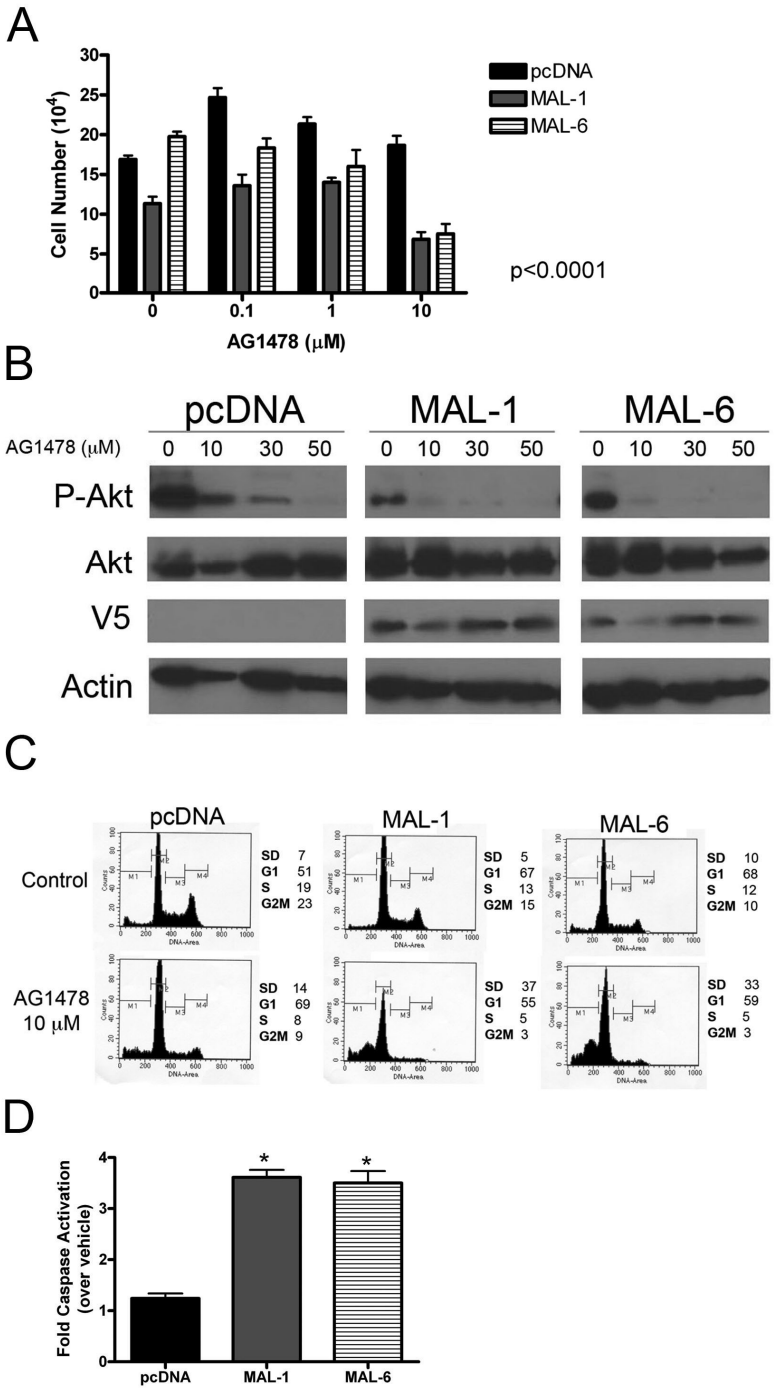
A
Cell Number (10^4)
30
25
20
15
10
5
0
0
0.1
1
10
AG1478 (μM)
pcDNA
MAL-1
MAL-6
p<0.0001
B
pcDNA
MAL-1
MAL-6
AG1478 (μM)
0 10 30 50
0 10 30 50
0 10 30 50
P-Akt
Akt
V5
Actin
C
pcDNA
MAL-1
MAL-6
Control
SD 7
G1 51
S 19
G2M 23
SD 5
G1 67
S 13
G2M 15
SD 10
G1 68
S 12
G2M 10
AG1478
10 μM
SD 14
G1 69
S 8
G2M 9
SD 37
G1 55
S 5
G2M 3
SD 33
G1 59
S 5
G2M 3
D
Fold Caspase Activation
(over vehicle)
4
3
2
1
0
*
*
pcDNA
MAL-1
MAL-6

Figure 5-5. MAL expression increases the sensitivity of MD468 breast cancer cells to AG1478. A. Stably transfected MD468 cells were seeded on 12-well plates at a density of $3x10^4$ cells/well. Following AG1478 treatment, adherent cells were trypsinized and counted. Each bar represents the mean ± SEM of four wells. ANOVA statistical analysis used to calculate *P* value. **B.** Stable cells were treated for 48 h with the indicated concentrations of AG1478 and subsequently harvested and processed for western blot analysis using the indicated antibodies. MAL-V5 expressing cells showed a marked decrease in P-Akt levels with 10 μM AG1478. **C.** After 48 h AG1478 treated cells were harvested and processed for flow cytometric analysis of cell cycle distribution. MAL expressing cells showed a substantial increase in the SD fraction with 10 μM AG1478. **D.** Following a 48 h treatment with 10 μM AG1478 caspase activity was measured using the Caspase-Glo 3/7 assay. Graph shows the fold change in caspase 3/7 activation over the vehicle treated cells. Each bar represents the mean ± SEM for 3 wells.

Fig. 5-6.

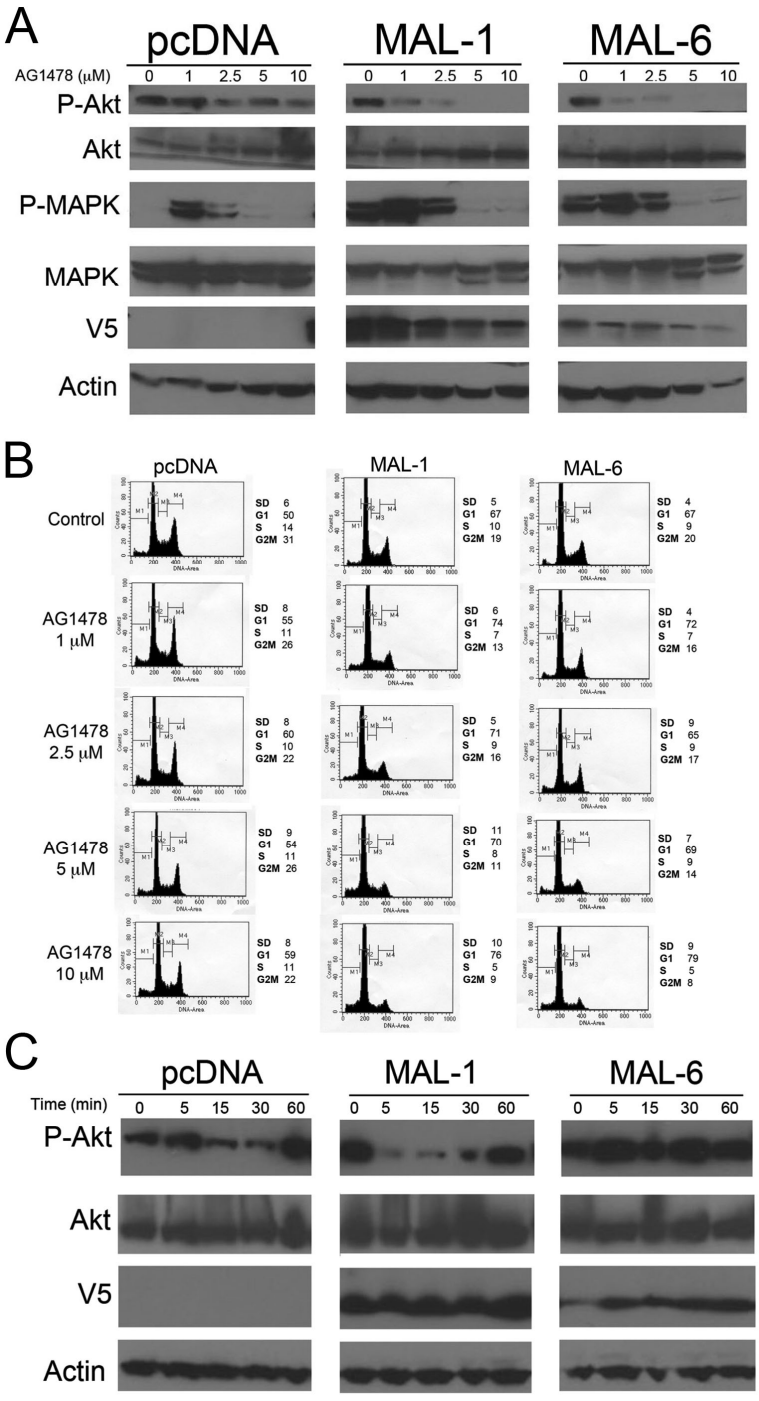
A
pcDNA
MAL-1
MAL-6
AG1478 (μM)
0 1 2.5 5 10
P-Akt
Akt
P-MAPK
MAPK
V5
Actin
B
pcDNA
MAL-1
MAL-6
Control
SD 6
G1 50
S 14
G2M 31
SD 5
G1 67
S 10
G2M 19
SD 4
G1 67
S 9
G2M 20
AG1478 1 μM
SD 8
G1 55
S 11
G2M 26
SD 6
G1 74
S 7
G2M 13
SD 4
G1 72
S 7
G2M 16
AG1478 2.5 μM
SD 8
G1 60
S 10
G2M 22
SD 5
G1 71
S 9
G2M 16
SD 9
G1 65
S 9
G2M 17
AG1478 5 μM
SD 9
G1 54
S 11
G2M 26
SD 11
G1 70
S 8
G2M 11
SD 7
G1 69
S 9
G2M 14
AG1478 10 μM
SD 8
G1 59
S 11
G2M 22
SD 10
G1 76
S 5
G2M 9
SD 9
G1 79
S 5
G2M 8
C
pcDNA
MAL-1
MAL-6
Time (min)
0 5 15 30 60
P-Akt
Akt
V5
Actin

Figure 5-6. MAL-dependent decrease in phosphorylated-Akt with low dose AG1478 treatment. A. Stable cells were treated for 48 h with the indicated concentrations of AG1478 and subsequently harvested and processed for western blot analysis using the indicated antibodies. MAL-V5 expressing cells showed a marked decrease in P-Akt levels with low concentrations of AG1478. **B.** After 48 h AG1478 treatment at the indicated concentrations, cells were harvested and processed for flow cytometric analysis of cell cycle distribution. **C.** Following treatment with 5 μM AG1478 at the indicated time points, cells were harvested and processed for western blot analysis using the indicated antibodies. The higher MAL-expressing clone (MAL-1) showed a decrease in P-Akt within 5 min of treatment while the vector control and low MAL-expressing clone (MAL-6) showed no change.

Fig. 5-7.

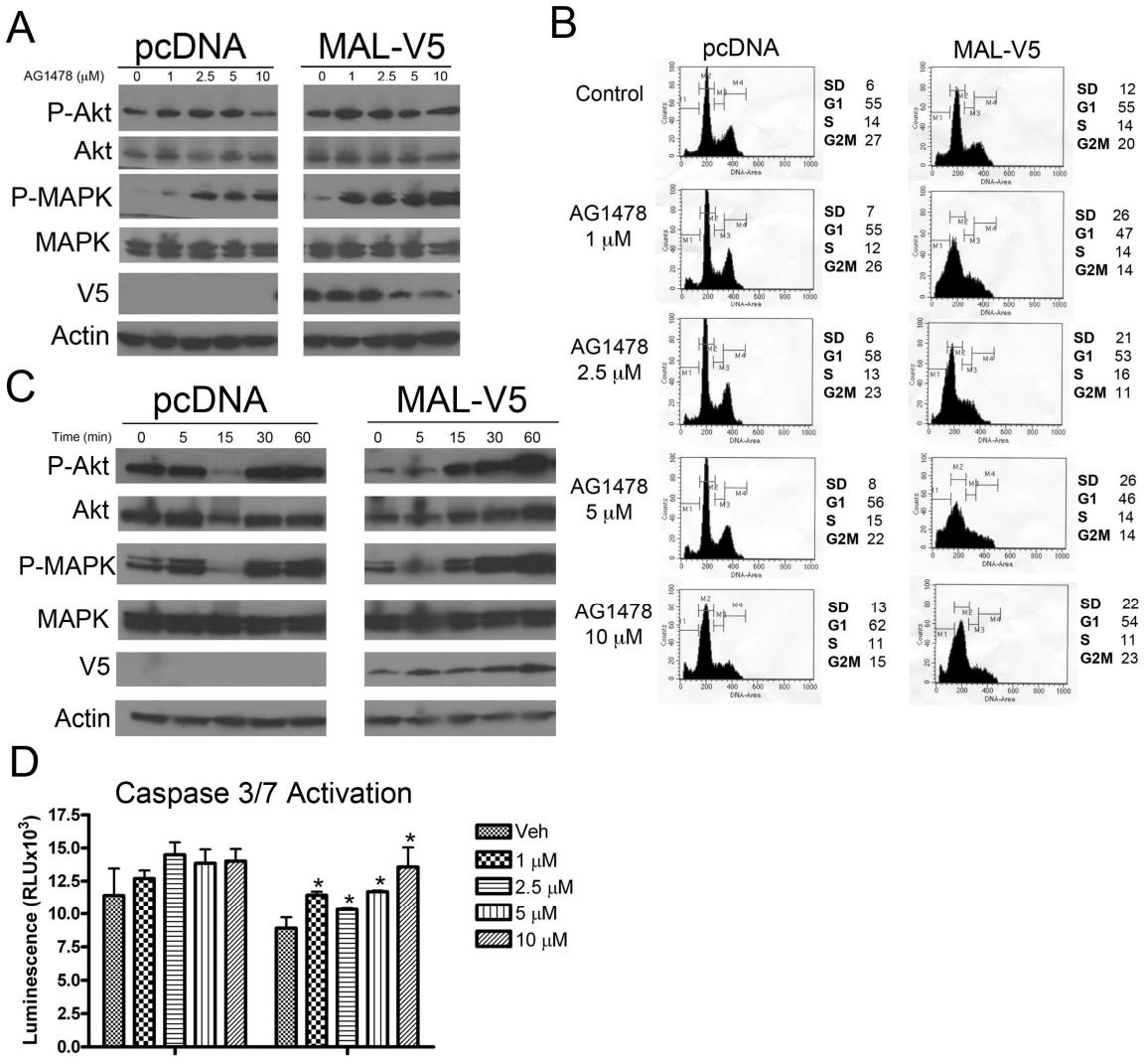
A
pcDNA
MAL-V5
AG1478 (μM)
0 1 2.5 5 10
P-Akt
Akt
P-MAPK
MAPK
V5
Actin
B
pcDNA
MAL-V5
Control
SD 6
G1 55
S 14
G2M 27
SD 12
G1 55
S 14
G2M 20
AG1478 1 μM
SD 7
G1 55
S 12
G2M 26
SD 26
G1 47
S 14
G2M 14
AG1478 2.5 μM
SD 6
G1 58
S 13
G2M 23
SD 21
G1 53
S 16
G2M 11
AG1478 5 μM
SD 8
G1 56
S 15
G2M 22
SD 26
G1 46
S 14
G2M 14
AG1478 10 μM
SD 13
G1 62
S 11
G2M 15
SD 22
G1 54
S 11
G2M 23
C
pcDNA
MAL-V5
Time (min)
0 5 15 30 60
P-Akt
Akt
P-MAPK
MAPK
V5
Actin
D
Caspase 3/7 Activation
Luminescence (RLUx10^3)
17.5
15.0
12.5
10.0
7.5
5.0
2.5
0.0
Veh
1 μM
2.5 μM
5 μM
10 μM

Figure 5-7. MAL expression increases the sensitivity of BT20 breast cancer cells to AG1478. A. Forty-eight hours after transfection with either a pcDNA vector control or the MAL-V5 plasmid, BT20 cells were treated for 48 h with the indicated concentrations of AG1478 and subsequently harvested and processed for western blot analysis using the indicated antibodies. **B.** After 48 h AG1478 treatment with the indicated concentrations, transiently transfected cells were harvested and processed for flow cytometric analysis of cell cycle distribution. MAL-expressing cells showed a substantial increase in the SD fraction with AG1478 treatment. **C.** Transiently transfected BT20 cells were treated with 5 μM AG1478 at the indicated time points, cells were harvested and processed for western blot analysis using the indicated antibodies. **D.** Following a 4 h treatment with increasing concentrations of AG1478, caspase activity was measured using the Caspase-Glo 3/7 assay. Each bar represents the mean ± SEM for 3 wells. Student's *t*-test was used to calculate statistical significance. **P*<0.05 comparing vehicle and AG1478 treated cells. There was no statistically significant difference between the vehicle- and AG1478-treated vector control cells.

5.2.4 MAL expression does not enhance AG1478 anti-tumor effects in MCF10A cells

As described above, MAL expression was able to sensitive breast cancer cell lines with constitutively high P-Akt levels to EGFR-targeted therapy. We next wanted to determine if MAL increased AG1478 sensitivity in the immortalized MCF10A cell line. MCF10A cells express EGFR and contain both a wild-type PTEN and PI3K gene. AG1478 exposure had similar effects on growth inhibition in both the MAL-expressing and vector control MCF10A cells (Fig. 5-8A). Whereas AG1478 treatment resulted in decreased P-Akt in MD468 and BT20 cells, MCF10A cells displayed a decrease in P44/42MAPK with increasing concentrations of AG1478 (Fig. 5-8B). However, there was no substantial difference seen when comparing the two stable clones. Similarly, cell cycle analysis following 48 h AG1478 exposure resulted in a comparable increase in %SD and %G1 fractions in the MAL-V5 and vector control cells (Fig. 5-8C). Therefore MAL expression is able to enhance AG1478 anti-tumor effects in breast cancer cell lines that are relatively resistant to the drug, associated with constitutively active Akt. The MCF10A cell line is responsive to the drug at low doses and this is not altered by the presence of MAL.

Fig. 5-8.

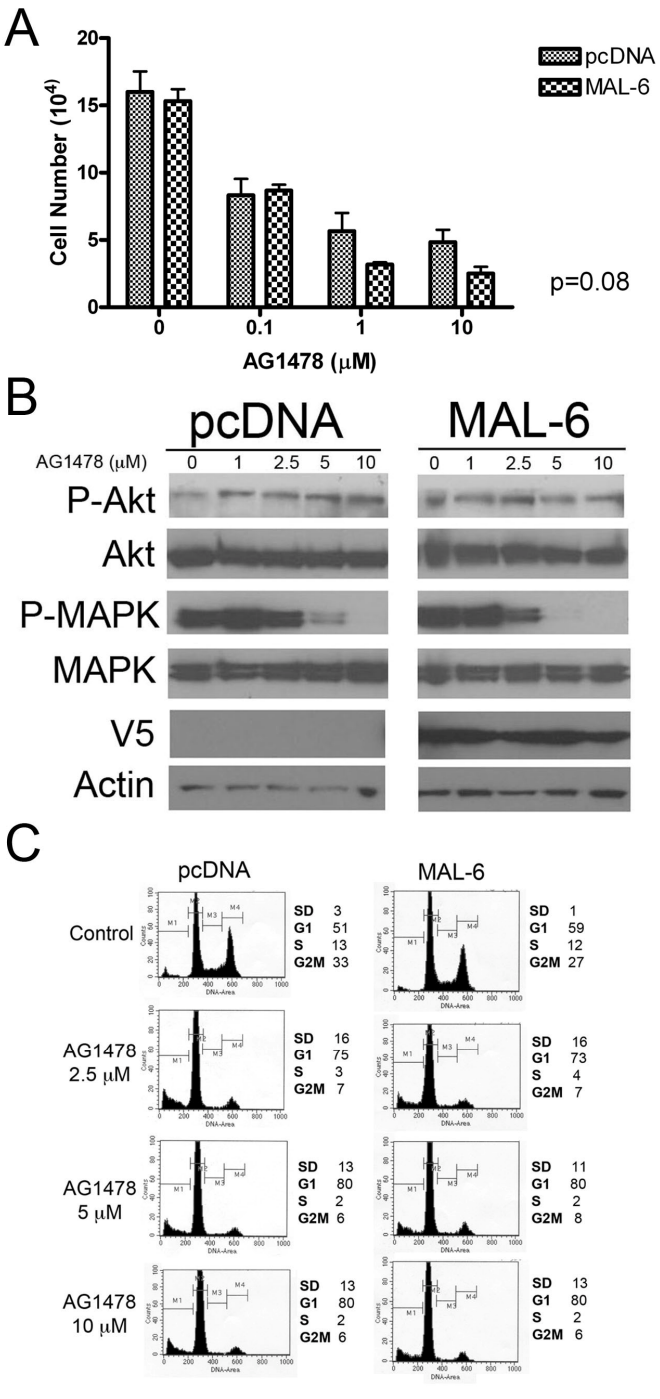
A
Cell Number (10^4)
20
15
10
5
0
0
0.1
1
10
AG1478 (μM)
pcDNA
MAL-6
p=0.08
B
pcDNA
MAL-6
AG1478 (μM)
0 1 2.5 5 10
0 1 2.5 5 10
P-Akt
Akt
P-MAPK
MAPK
V5
Actin
C
pcDNA
MAL-6
Control
SD 3
G1 51
S 13
G2M 33
SD 1
G1 59
S 12
G2M 27
AG1478 2.5 μM
SD 16
G1 75
S 3
G2M 7
SD 16
G1 73
S 4
G2M 7
AG1478 5 μM
SD 13
G1 80
S 2
G2M 6
SD 11
G1 80
S 2
G2M 8
AG1478 10 μM
SD 13
G1 80
S 2
G2M 6
SD 13
G1 80
S 2
G2M 6

Figure 5-8. No effect of MAL expression on MCF10A response to AG1478. A. Stably transfected MCF10A cells were seeded on 12-well plates at a density of $3x10^4$ cells/well. Following AG1478 treatment, adherent cells were trypsinized and counted. Each bar represents the mean ± SEM of four wells. ANOVA statistical analysis used to calculate *P* value. **B.** Stable cells were treated for 48 h with the indicated concentrations of AG1478 and subsequently harvested and processed for western blot analysis using the indicated antibodies. No difference seen in P-Akt or P-MAPK levels comparing pcDNA and MAL-V5 cells. **C.** After 48 h AG1478 treatment cells were harvested and processed for flow cytometric analysis of cell cycle distribution.

5.2.5 MAL expression in membrane rafts coincides with the exclusion of signaling molecules

Membrane rafts are thought to function in cellular signaling by concentrating or separating specific membrane and/or membrane-associated proteins in a unique lipid environment (37). We hypothesized that the MAL protein might mediate its effects on Akt activation by modifying the raft localization of PI3K/Akt pathway signaling molecules. To test this hypothesis, we subjected MD468 stable clones to sucrose gradient fractionation and immunoblot analysis to determine the cellular localization of P-Akt, P-44/42MAPK, and EGFR. Unfortunately, were not able to detect each of the aforementioned proteins in all three stable clones (MAL-1, MAL-6, and the pcDNA control) but were still able to make preliminary conclusions from the data obtained.

In the higher MAL-expressing clone (MAL-1) we observed an exclusion of P-Akt, P-MAPK and EGFR in the membrane raft fractions that contained the highest concentration of the MAL protein (Fig. 5-9A). In the lower MAL expressing clone (MAL-6) we noticed a similar trend where P-MAPK and EGFR levels were decreased in the fractions where MAL was highest (Fig. 5-9B). Of the proteins we were able to detect in the pcDNA control cells, P-MAPK and EGFR, each was detected mainly in the detergent-soluble fractions (Fig. 5-9C). This preliminary data suggests that MAL may directly or indirectly affect signaling mechanisms by its ability to modify membrane raft composition.

Fig. 5-9.

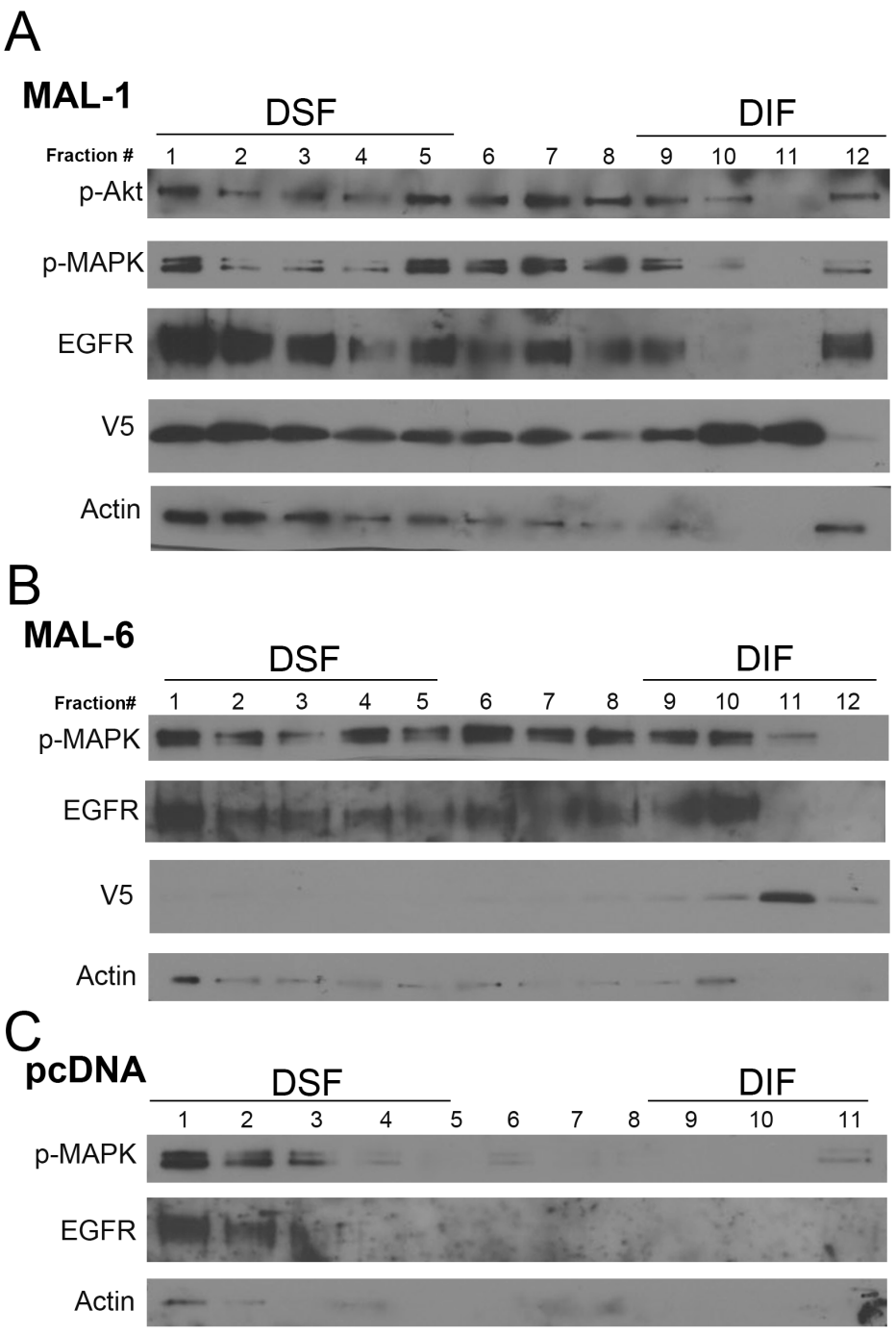
A
MAL-1
DSF
DIF
Fraction #
1 2 3 4 5 6 7 8 9 10 11 12
p-Akt
p-MAPK
EGFR
V5
Actin
B
MAL-6
DSF
DIF
Fraction#
1 2 3 4 5 6 7 8 9 10 11 12
p-MAPK
EGFR
V5
Actin
C
pcDNA
DSF
DIF
1 2 3 4 5 6 7 8 9 10 11
p-MAPK
EGFR
Actin

Figure 5-9. MAL expression in membrane raft fractions coincides with the exclusion of signaling molecules. Western blot analysis of MD468 stable cell lines following extraction with 1% Triton-X and centrifugation to equilibrium. **A.** The MAL-1 expressing clone showed high MAL expression in the detergent insoluble fractions (DIF), which correlated with low or absent P-Akt, P-MAPK and EGFR. **B.** The MAL-6 expressing clone exhibited high MAL in the DIF and absence of P-MAPK and EGFR in the same fractions. **C.** The pcDNA vector control cell showed accumulation of P-MAPK and EGFR in the detergent-soluble fractions (DSF).

5.3 Discussion

Mounting evidence in the literature supports the importance of membrane rafts in mediating signal transduction events. A common theme is that membrane rafts promote the compartmentalization of signaling components in specific areas of the membrane. Moreover, the clustering of separate rafts exposes proteins such as kinases and phosphatases to new membrane environments and even a small change of partitioning into a membrane raft can initiate signaling cascades (99). Herein we identify the raft resident protein MAL as an important mediator of signal transduction events in breast epithelial cells.

The MAL protein was first identified in T cells where it functions in membrane trafficking and intracellular protein transport (116). Since its initial discovery, the MAL protein has been shown to be a critical component of T cell signaling. Knockdown of MAL expression in T cells reduced the presence of the src kinase Lck at the membrane and its accumulation in the cytoplasm (49). Lck expression at the plasma membrane is crucial for T cell function since Lck mutants that are unable to reach the plasma membrane are defective in T cell signaling (117). Furthermore, Anton *et al.* demonstrated that MAL mediates the targeting of Lck to the plasma membrane by allowing recruitment of Lck to specialized intracellular membrane rafts and the formation of specific transport carriers for Lck targeting (49). This novel transport pathway involving the MAL protein is crucial for T cell receptor mediated signaling. Given the evidence for

MAL's involvement in T cell signaling and our observations that MAL expression reduces the tumorigenic properties of breast cancer cells, we thought it appropriate to investigate the role of MAL in signaling in breast epithelial cells.

The function of MAL in normal or neoplastic breast epithelial cells is unknown; however its location in the detergent-insoluble fraction in HCC1937 cells suggests that similar to other cell types, it plays an integral role in membrane microdomains. Exogenous expression of the MAL protein in MCF10A cells resulted in its accumulation in the detergent-insoluble fraction. Further, the lipid raft marker flotillin-1 was re-distributed from the soluble to the insoluble fraction when MAL was expressed in these cells, suggesting that MAL may be critical for organizing the composition and likely the function of these microdomains in breast epithelial cells.

The arrangement of signaling molecules such as EGFR and ER in membrane rafts may be important in regulating their signal transduction properties. Several studies have demonstrated that EGFR is activated by membrane raft disruption via cholesterol depletion (44, 118). Further, dependent upon the cell type, the EGFR has been shown to migrate both into (A431 epithelial carcinoma cells) and out of (fibroblasts) membrane rafts in response to EGF indicating that movement within membrane rafts is important for EGFR-mediated signaling (106, 119). In the immortalized MCF10A cells, EGF stimulation caused a dramatic migration of the MAL protein out of the membrane raft fractions. This movement was transient in that 60 min following EGF treatment MAL

was again found in the membrane raft fractions. Interestingly, the identical EGF stimulation in the MCF7 breast cancer cell line resulted in a transient aggregation of MAL into the membrane raft fractions. Furthermore, we did not see any substantial movement of the raft resident protein flotillin-1 within the membrane raft fractions upon EGF stimulation. Similar to what was seen with EGFR migration in fibroblasts and A431 cells, the differences in MAL movement between MCF10A and MCF7 cells might be due to cell type. MCF10A is a normal immortalized cell line while MCF7 is a breast cancer cell line. It is possible that MAL might be associated with one set of signaling events in MCF10A cells which requires it's location in the bulk plasma membrane while it is involved in another set of events in MCF7 cells requiring its location in membrane rafts. In colon carcinoma cells, the IGF-1 cell surface receptor (IGF-1R) was shown to mediate proapoptotic effects within membrane rafts and anti-apoptotic effects outside of membrane rafts (120). Thus, segregation of IGF-IR in and out of rafts appeared to contribute to contradictory regulatory effects in colon cancer cell death. We were unable to detect EGFR in the membrane raft fractions of MCF10A and MCF7 cells. However, if EGFR migrates in accordance with MAL in these cells, it would provide supportive evidence that MAL and possibly EGFR are involved in two separate signaling events in the two cell types. In either event, the data presented is suggestive evidence that MAL has a role in EGF-mediated signaling through the EGF receptor. Additionally, it highlights the importance of membrane rafts in mediating cell signaling events.

Our initial finding identifying MAL protein expression as a predictor of benefit from adjuvant chemotherapy in our cohort of breast cancer patients led us to investigate what role MAL might play in response to chemotherapy. As a means to examine this, we utilized the MD468 breast cancer cell line stably transfected with the MAL-V5 protein or a vector control and monitored the effect of MAL expression on response to the EGFR inhibitor AG1478. We chose this experimental model for two reasons: 1) MD468 cells are an example of the triple-negative breast cancers which are defined as tumors lacking the expression of ER, PR and HER2 and are associated with aggressive clinical behavior and poor prognosis (121). Also, since these triple-negative cancers are without targeted therapeutics, EGFR-targeted therapy alone or in combination with common chemotherapeutics are in testing for the treatment of triple-negative breast cancers (122), and 2) Evidence from She *et al.* and Bianco *et al.* demonstrated that due to their PTEN mutation, MD468 cells are unresponsive to the EGFR tyrosine kinase inhibitor gefitinib (111, 112). Moreover, targeting the membrane of MD468 cells with the alkylphospholipid perifosine in combination with the anti-EGFR monoclonal antibody cetuximab was shown to enhance anti-tumor activity.

Due to their PTEN mutation, MD468 cells have a constitutively active PI3K pathway resulting in high levels of phosphorylated Akt. When MAL is expressed in these cells, the baseline levels of P-Akt are decreased suggesting that the MAL protein is directly or indirectly affecting the activation of Akt. Of note, the vector control MD468

cells had lower baseline levels of P-44/42MAPK when compared to the MAL-transfected cells. MAPK activation mediated by EGFR has been shown to play a role in inducing peroxide-induced apoptosis (123). It is possible that the observed MAPK activation is a reflection of MAL-induced apoptosis in the MD468 cells since we have observed an increase in the baseline levels of apoptosis with MAL expression in previous experiments.

Overexpression of the MAL protein in MD468 cells was sufficient to restore AG1478 sensitivity measured by an inhibition in growth, induction of apoptosis and a modest delay in cell cycle progression in MAL-expressing cells. The observed increase in sensitivity was accompanied by a reduction in the levels of phosphorylated Akt. After activation, Akt mediates the activation and inhibition of various downstream targets such as Bad and GSK3, resulting in cell survival, growth, and proliferation (5). We would need to conduct future experiments looking at the phosphorylation levels of Akt targets to determine if the MAL-induced decrease in P-Akt levels correlates with a decrease in the kinase activity of the protein.

In addition to monitoring MD468 sensitivity to EGFR inhibition, we also looked at the ability of MAL to sensitize the PI3K mutant BT20 cells to AG1478. As with the MD468 cells, MAL overexpression was able to increase the anti-tumor activity of AG1478 in the BT20 cells. However, we did observe a more rapid turnover in Akt phosphorylation after AG1478 treatment in the BT20 cells compared to the MD468 cells,

which is likely a reflection of where their mutations occur within the PI3K/Akt pathway. We did not observe any enhancement of the anti-tumor effects of AG1478 with MAL expression in the immortalized MCF10A cell line. The implications for these results is two fold: 1) MAL expression might identify a population of triple-negative breast cancer patients that would benefit from EGFR-targeted therapy, and 2) inhibiting the PI3K/Akt pathway, with either a PI3K or Akt inhibitor, in combination with EGFR-targeted therapy might have a more substantial anti-proliferative and pro-apoptotic effect.

Treating MD468 cells with a combination of cetuximab and perifosine was able to restore sensitivity to EGFR-targeted therapy and was accompanied by a decrease in P-Akt levels (114). Perifosine is thought to reduce the level of Akt phosphorylation by disturbing the phosphatidylinositol-mediated recruitment of pleckstrin homology domain-containing molecules, including Akt, to the membrane proximity for phosphorylation (114). Since expression of MAL in AG1478-treated MD468 cells results in a similar phenotype as AG1478/Perifosine-treated MD468 cells, it is feasible that MAL is also interfering with Akt recruitment to the membrane.

To investigate a potential mechanism for MAL's ability to reduce Akt phosphorylation, we performed western blot analysis on sucrose gradient fractions of MD468 stable cells lines. Probing for common signal transduction molecules, P-Akt, P-MAPK, and EGFR revealed an exclusion of these molecules in membrane raft fractions that were enriched for the MAL protein. These preliminary results suggest that MAL

might mediate its effects on Akt by modifying is membrane localization. One possible explanation could be that MAL is sequestering either PIP_2 or PIP_3 within membrane rafts preventing Akt recruitment. Lasserre *et al.* demonstrated that membrane rafts play a crucial role in triggering the PI3K/Akt signaling pathway by facilitating Akt recruitment and activation upon PIP_3 accumulation in the plasma membrane (42). Thus, it is also probable that MAL plays a more direct role in PI3K/Akt signaling by affecting Akt membrane recruitment through its function in membrane rafts.

6. Examining the Consequences of Aberrant MAL Expression in Ovarian Cancer

6.1 Introduction

Despite advances in chemotherapy, ovarian cancer continues to be one of the most lethal gynecological cancers, largely due to late diagnosis (124). Since there are no reliable screening tests for ovarian cancer, it is often detected once the cancer has progressed to a more advanced stage. Therefore, novel early detection approaches combined with a greater understanding of the biology of advanced ovarian cancers could potentially lead to improved patient survival.

The median survival of women with advanced ovarian cancer is about three to four years and only a small minority are long-term survivors or are permanently cured. In a previous study published out of our lab, Affymetrix U133A microarrays were used to define gene expression patterns that distinguish between short-term (<3 years) and long-term (>7years) survival in advanced serous ovarian cancers (30). Data from this study identified the *MAL* gene as being the most highly expressed in short-term survivors (3-fold compared with long-term survivors, and 29-fold compared with early-stage cases). Paradoxical to the gene expression profile observed in breast cancer where loss of MAL is associated with malignancy, in ovarian cancers overexpression of MAL is indicative of a more malignant phenotype. As a result, we were interested in investigating the differences in MAL disruption between breast and ovarian cancer.

Multiple genetic and epigenetic aberrations have been identified in patients with ovarian cancer. Mutation of TP53 is a common genetic alteration seen in ovarian cancer (125), found in about 60-80% of cases. In the majority of ovarian cancers, mutations can also be found in common cancer-related signaling pathways that ultimately contribute to the inhibition of apoptosis, increased proliferation, motility, invasion, and metastasis. Overexpression of EGFR has been observed in ovarian cancer, and was shown to correlate with poor survival in women with advanced staged disease (126, 127). Also, the PI3K pathway is activated in approximately 70% of ovarian cancers, and activation of this pathway is associated with resistance to cytotoxic chemotherapy (124). Thus, exploring the kinetics of EGFR and PI3K signaling in ovarian cancer is relevant to understanding the biology of advanced disease.

The heterogeneous nature of ovarian cancer makes it difficult to treat. Generally, the standard treatment for ovarian cancer patients includes surgery, radiation, and platinum- and/or taxane-based chemotherapeutic regimens. The mechanism of platinum-induced cell death is through DNA binding and interference with the cell's repair mechanisms (carboplatin and cisplatin), while taxane-induced cell death involves the perturbation of microtubule function (Paclitaxel/Taxol). Since EGFR function is sometimes disrupted in ovarian cancer, targeting the EGFR pathway in combination with platinum and taxane therapies is an attractive therapeutic approach. Clinical trials are currently underway investigating the efficacy of Akt and PI3K inhibitors for the

treatment of ovarian cancer (124). The difficult task is identifying which patients would benefit from a particular therapeutic strategy.

Results presented in this chapter build on our initial findings, which described the differential expression of *MAL* in short-term and long-term ovarian cancer survivors. Moreover, we have developed two stable ovarian cancer cell lines that will be used in future *in vitro* studies to investigate the biological effects of modulating MAL expression in ovarian cancer.

6.2 Results

6.2.1 MAL protein expression is an independent predictor of poor survival in advance serous ovarian cancer

Because MAL was the most predictive transcript for distinguishing aggressive biology in ovarian cancer, we evaluated levels of the protein in a series of 144 late-stage serous cancers with known outcome. Immunohistochemical analysis of formalin-fixed paraffin-embedded samples, using the same MAL mouse monoclonal antibody used in breast cancer studies, revealed highly variable staining in the malignant epithelium (Fig. 6-1A). Tissues were categorically assigned a staining value from 0 to 4+ based upon the intensity multiplied by the percentage of positive cells. Of the 144 cases stained, microarray data was previously obtained on 52 and showed a high degree of concordance between RNA and protein levels of MAL (30). Using 1+ staining as a cutoff, we examined whether MAL protein levels had prognostic value in this cohort. Overall survival was significantly (P=0.0004) reduced in patients with tumors that showed high levels of the MAL protein (Fig. 6-1B). In multivariate analysis, MAL staining retained significance along with response to chemotherapy (Table 4). MAL was also highly expressed in the benign fallopian tube with accentuated staining at the apical surface of the serous epithelia consistent with its role in transport and signaling. Benign ovarian surface epithelial cells were negative for MAL expression using this MAL antibody (data not shown).

Fig. 6-1.

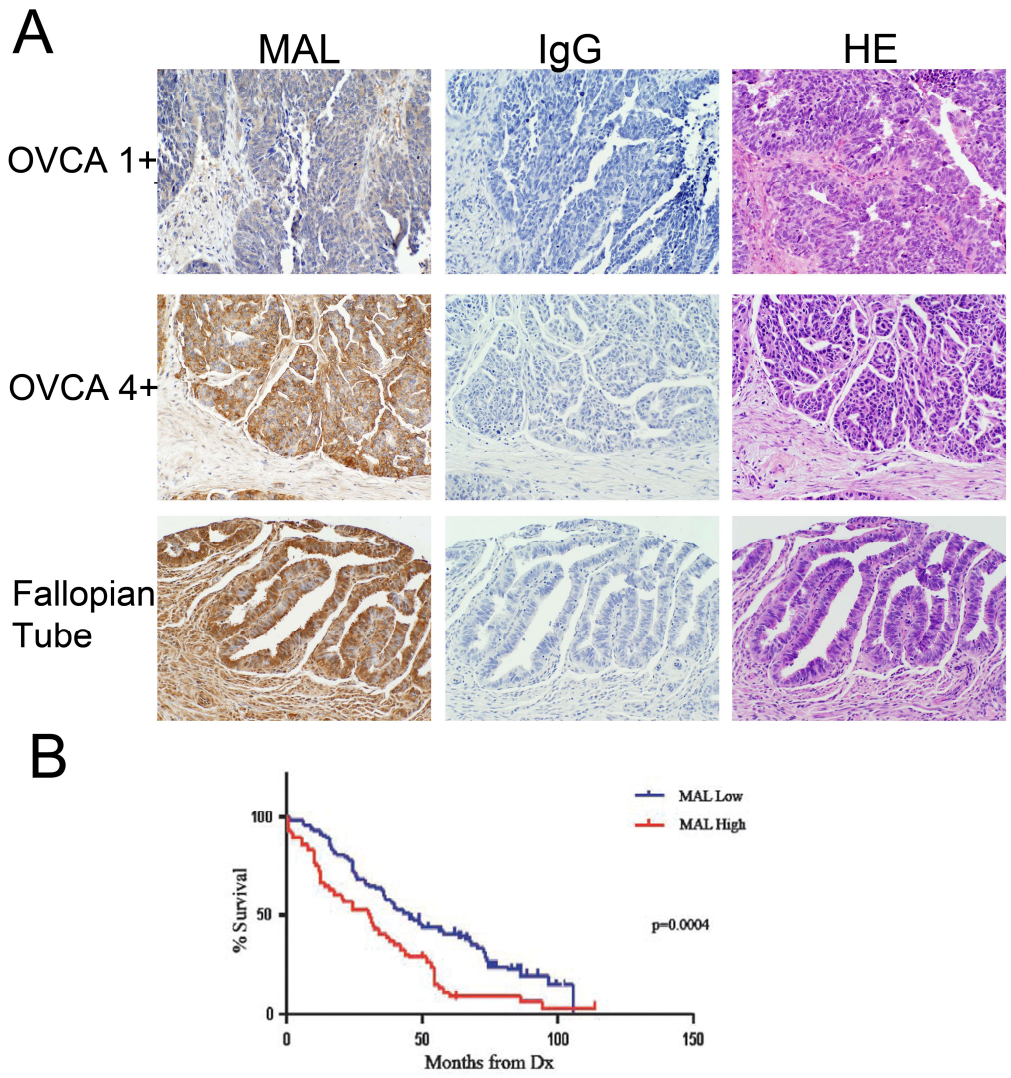

Figure 6-1. Immunodetection of MAL protein in primary ovarian tissues and relation to disease outcome. A. Examples of immunohistochemical detection of the MAL protein in two advanced serous ovarian cancers and a benign fallopian tube with negative control (mouse IgG) and H&E-stained parallel sections. Examples of weak (1+) and strong (4+) expression are shown. **B.** Kaplan-Meier survival curves for 144 late stage

serous ovarian cancer patients stratified by MAL staining using 1+ as a threshold to define high versus low expression (*P*=0.0004).

Table 4. Cox multivariate analysis by survival in advanced ovarian cancer

Variable	Hazard Ratio	*P*
Clinical response (CR vs. other)	0.15	<0.0001
MAL expression (≥1)	1.9	0.004
Stage (IV vs. III)	1.5	0.13
Race (black vs. white)	0.71	0.24
Debulking status (suboptimal vs. optimal)	1.3	0.34
Age (continuous)	1.0	0.91

Abbreviation: CR, complete response.

6.2.2 Characterizing the effects of altered MAL expression in ovarian cancer cell lines

Given that high MAL expression is associated with poor prognosis in ovarian cancer, we are interested in investigating the biological consequences of knocking down MAL expression in this cancer type. Specifically, to determine if altering MAL expression has any effect on the phenotype of ovarian cancer cell lines. Similar to the primary ovarian cancer tumors, we observed variable MAL protein expression in a panel of ovarian cancer cell lines (Fig. 6-2A). Since the SKOV8 cell line had high levels of MAL by western blot analysis, we chose this cell line to perform our MAL shRNA knockdown experiments. By western blot analysis we observed a substantial reduction of MAL protein levels in shMAL clone #2 (Fig. 6-2B); this clone will be used in subsequent *in vitro* studies. Furthermore, since the MAL protein was undetectable in SKOV4 cells by immunoblot analysis, we stably overexpressed the MAL-V5 protein or a pcDNA vector control in this cell line (Fig. 6-2C). We intend to utilize these two stable ovarian cancer cell lines in future *in vitro* studies in order to gain a better understanding of the dynamics of MAL expression in the ovary in comparison to the breast.

Fig. 6-2.

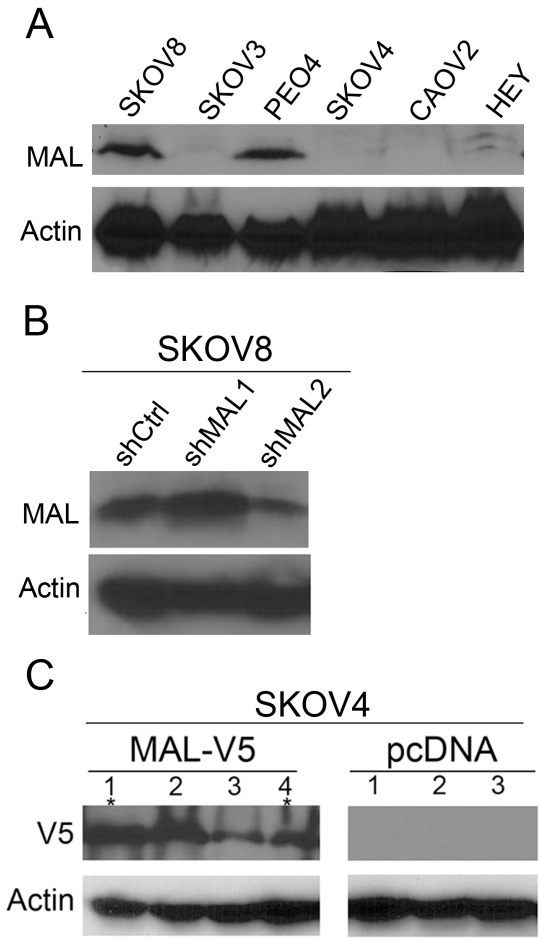

Figure 6-2. Variable MAL protein levels in ovarian cancer cell lines. A. Western blot analysis detecting MAL protein levels in whole cell lysates from the indicated ovarian cancer cell lines. **B.** Western blot analysis verifying reduction of MAL expression in SKOV8 cells stably transfected with either a non-silencing control (shCtrl) plasmid of shRNA directed at the MAL gene (shMAL). The shMAL2 clone will be used in subsequent studies. **C.** Western blots showing the stable expression of the MAL-V5 protein or a vector control in SKOV4 ovarian cancer cells.

6.3 Discussion

The availability of a specific monoclonal antibody that can be used to detect the MAL protein *in situ* allowed us to further investigate the expression of this gene with respect to ovarian cancer outcome. Staining a large set of advanced serous cancers unselected for disease outcome, we found that high level of the MAL protein was associated with shorter survival. These results further support the expression array analysis and highlight the biological significance of the MAL protein in both breast and ovarian cancer. An interesting paradox observed in our results is that while loss of MAL expression is associated with breast cancer, in ovarian cancer overexpression of the same protein correlated with poor survival. Using the same monoclonal MAL antibody utilized in our studies, Marazuela *et al.* surveyed the range of MAL expression in a panel of human tissues and found that MAL expression is very tissue- and cell-type specific (16). Even within the same tissue type certain cells showed high MAL expression while in other cells, MAL was absent. Moreover, when examining the literature for MAL expression in malignant cells, both down regulation and overexpression of mRNA and protein are associated with cancer progression (23, 24, 30, 96).

Further consideration of the differences in MAL expression in breast versus ovarian cancer raises the possibility that MAL is acting as both a tumor suppressor and an oncogene. Given the function of MAL in directing membrane trafficking, it is possible that the differences in the effects of MAL expression in transformed cells reflects a

variation in the type of proteins that rely on MAL for cellular transport for that particular cell type. For example, if MAL is involved in transporting a protein that functions in increasing cell proliferation in ovarian cells while in breast cells it transports anti-proliferative proteins, both overexpression and loss of expression could potentially contribute to a malignant phenotype. It has previously been demonstrated that both increased and decreased MAL expression results in aberrant protein sorting. In Madin-Darby canine kidney (MDCK) cells, overexpression of MAL disturbed cell morphology by increasing apical delivery while expression of anti-sense RNA directed against MAL caused accumulation in the Golgi and impaired apical transport of different apical protein markers (17). Thus, the differing roles of MAL as a potential tumor suppressor gene and an oncogene could be largely due to divergent roles in protein sorting in breast and ovarian cells.

The traditional view of ovarian carcinogenesis has been that various tumors are all derived from the ovarian surface epithelium and that subsequent metaplastic changes results in the development of the different cell types including serous, endometreoid, clear cell, mucinous, and transitional cell (128). However, the normal ovary has no components that resemble the tumors. The more advanced serous ovarian tumors, on the other hand, morphologically resemble the epithelia of the fallopian tube. Therefore, an opposing theory has been proposed by several groups suggesting that the majority of high-grade serous ovarian carcinomas are derived from the fallopian tube

(129-131). By immunohistochemistry we show that benign fallopian tube epithelium have abundant expression of the MAL protein whereas ovarian surface epithelial cells have no detectable protein. Based on this evidence, it is therefore plausible that high MAL expression in ovarian cancers is more indicative of the level of expression seen in the tissue where the tumor cells originated and not an increase in expression in the ovarian surface epithelium. This would indicate that aberrant function and not expression of the MAL protein contributes to ovarian cancer progression.

Furthermore, since our immunohistochemical studies showed high MAL protein levels in patients with shorter survival after diagnosis; it is plausible that aberrant MAL expression and/or function in these patients has an effect on overall survival by influencing patient response to chemotherapy therefore affecting survival. A recent study published by our collaborators comparing the IC50 of cisplatin to MAL mRNA expression in a panel of ovarian cancer cell lines, found that MAL transcript levels were higher in resistant cell lines (P=0.04) (29), suggesting that MAL expression may serve as a marker for platinum resistance in ovarian cancer. Our forthcoming experiments will involve using our stable ovarian cancer cell lines to examine the consequences of aberrant MAL expression with respect to response to platinum-based chemotherapeutics alone or in combination with EGFR-targeted therapies.

Given the obvious differences in MAL expression in the ovary compared to the breast, conducting a panel of *in vitro* biological assays in ovarian cancer cell lines will

give us a broader perspective of what role MAL plays in carcinogenesis. We have developed two stable ovarian cancer cell lines either overexpressing the MAL-V5 protein or with reduced MAL expression due to transfection with shRNA directed against MAL. These cell lines will be used in future studies to examine the effect of MAL on common tumor-promoting characteristics including proliferation, cell motility, invasion, and anchorage-independent growth.

In summary, our data identifies the MAL protein as a significant independent predictor of survival in advanced serous ovarian cancer patients. Moreover, the stable MAL knockdown and overexpressing ovarian cancer cells developed will be utilized in future *in vitro* experiments. Prospective mechanistic studies are warranted to get a better understanding of the implications of high MAL expression in the biology of ovarian cancer.

7. Summary

The studies presented in this dissertation sought to examine the role of the MAL (myelin and lymphocyte) protein in both breast and ovarian cancer. Using bisulfite genomic sequencing and methylation-specific PCR, we have demonstrated that the MAL promoter CpG island is frequently methylated in breast cancer leading to transcriptional silencing (132). The majority of breast cancer cells lines used in this study and 69% of the primary breast cancers analyzed exhibited aberrant promoter methylation while normal breast epithelial cells were largely unmethylated. In methylated breast cancer cell lines, treatment with the methylation inhibitor DAC was able to reactivate MAL expression to a level comparable to what was seen in normal epithelial cells (132).

A thorough examination of the pattern of methylation within the MAL promoter, including the methylation status of 71 CpG dinucleotides, revealed a sharp transition in the methylation profile. Our sequence analysis determined that the area of differential methylation between normal and cancer cells was confined to the proximal promoter region, approximately 356 bp upstream of the start of transcription (132). The transition point we have defined may represent the 5'-boundary of the functional MAL promoter.

Utilizing a monoclonal antibody specific for the MAL protein we conducted immunohistochemical analysis on a panel of primary breast tumors and attempted to correlate MAL protein levels with common pathologic features. Categorizing 122 primary cancers based upon the absence or presence of staining in malignant epithelial

cells, we found no significant correlations with standard clinico-pathologic parameters (132). However, in the subgroup of patients who did not receive adjuvant chemotherapy (>40%), absence of MAL protein expression was highly associated with shorter disease-free survival (P=0.003). Thus, within the group of patients that traditionally do not receive adjuvant chemotherapy (e.g., patients who are older, hormone positive and node negative), lack of MAL protein expression might identify a subset that would benefit from receiving adjuvant chemotherapy.

In order to determine the biological consequences of loss of MAL expression during breast carcinogenesis, we conducted several *in vitro* experiments using breast cell lines stably overexpressing the MAL-V5 protein or depleted of endogenous MAL using shRNA. We found that exogenous expression of MAL in breast cell lines that did not express the endogenous MAL protein resulted in decreased cell proliferation, motility, reduced cell invasion through Matrigel and suppressed anchorage-independent growth in soft agar. However, knocking down MAL expression in the non-tumorigenic telomerase immortalized DU99 cell was not sufficient to cause substantial tumorigenic changes. Based on these findings, it appears that loss of the MAL protein in breast epithelial cells is a contributing and not a causative factor in breast cancer development.

We also examined the effect of MAL expression on the sensitivity of EGFR-overexpressing, triple-negative breast cancer cell lines to the EGFR tyrosine kinase inhibitor AG1478. We found that exogenous expression of MAL in MD468 and BT20

breast cancer cells increased the sensitivity of these cells to AG1478. Inhibition of EGFR with AG1478 caused a greater induction of apoptosis, decrease in cell growth, and cell cycle arrest in MAL-expressing cells compared to the vector control. Furthermore, this increase in sensitivity with MAL expression was accompanied by a marked decrease in phosphorylated Akt levels that possibly accounts for the observed increase in caspase 3/7 activation. Based on sucrose gradient fractionation data showing that MAL expression was able to alter the composition of membrane rafts and exclude signaling molecules from those same membrane microdomains, we could speculate that MAL's ability to affect cellular signaling is likely mediated through its membrane raft altering functions. However, future experiments will allow us to further elucidate the mechanism of action by which MAL expression enhances sensitivity to AG1478.

To further understand the role of MAL in ovarian cancer development, we utilized immunohistochemical analysis to evaluate MAL protein expression in a series of 144 late-stage serous cancers with known outcome. In this cohort of patients, we found that high-level expression of MAL was associated with shorter survival (31). We also found positive MAL staining in the normal fallopian tube but absence of MAL staining in ovarian surface epithelial cells. There is currently a debate in the field of ovarian cancer research as to whether fallopian tube epithelial cells or ovarian surface epithelial cells give rise to ovarian cancers. Thus, future experiments are warranted to determine whether high MAL levels in advanced serous ovarian cancer cells is reflective of an

overexpression compared to the ovarian surface epithelium, or due to the fact that they originated from the fallopian tube. In either case, it is apparent that the MAL protein has a significant role in the pathogenesis of ovarian cancer.

Taken together, our data provides substantial evidence that aberrant expression and function of the MAL protein in breast and ovarian epithelial cells contributes to cancer progression. The practical applications of this work are multi-faceted. Studies have shown that it is possible to detect hypermethylation of tumor suppressor genes in the serum from patients with DCIS and all grades and stages of invasive breast cancer (69). Thus, detecting MAL promoter methylation in combination with other tumor suppressor genes that are frequently methylated in breast cancer (e.g., RASSF1A and APC), is a potential approach that could be utilized to improve current early detection strategies. Also, the current use of methylation inhibitors in clinical trials to treat cancer suggests a future utility for MAL promoter methylation as a means of identifying patients who might respond to global methylation inhibitors such as decitabine.

A frequent obstacle encountered when treating cancer is identifying the population of patients that would benefit from a given therapy. With respect to both breast and ovarian cancer, the MAL protein appears to be a relevant predictive factor with regards to benefit from chemotherapy. In breast cancer, older patients, patients with smaller tumors, and patients who are node negative or hormone receptor positive are not likely to receive adjuvant chemotherapy. Based on our immunohistochemistry

results, absence of MAL expression in this subset of patients identifies a population that would benefit from receiving adjuvant chemotherapy. Additionally, patients who present with the more aggressive triple-negative (ER-, PR-, HER2/neu-) form of breast cancer, therapeutic options are often limited and treatment with standard chemotherapies often results in relapse. As a result, identifying molecular features of the triple-negative tumor types that would make them more vulnerable to cytotoxic therapy is extremely important. Our work demonstrates that expression of the MAL protein in triple-negative breast cancer cell lines is associated with an increased sensitivity to EGFR tyrosine kinase inhibition leading to downregulation of Akt activation. Therefore, it is plausible that triple-negative breast cancer patients who express the MAL protein might benefit from EGFR-targeted therapies. The availability of a high quality monoclonal antibody specific for the MAL protein provides a means with which to screen tumor expression as a way to gauge response and/or benefit from chemotherapy.

References

1. Institute NC. Cancer Topics/Breast. 2010 [cited 01/07/2010]; Available from: http://www.cancer.gov/cancertopics/types/breast

2. Allred DC, Mohsin SK, Fuqua SA. Histological and biological evolution of human premalignant breast disease. Endocr Relat Cancer 2001;8(1):47-61.

3. Ma XJ, Salunga R, Tuggle JT, *et al.* Gene expression profiles of human breast cancer progression. Proceedings of the National Academy of Sciences of the United States of America 2003;100(10):5974-9.

4. Osborne C, Wilson P, Tripathy D. Oncogenes and tumor suppressor genes in breast cancer: potential diagnostic and therapeutic applications. Oncologist 2004;9(4):361-77.

5. Fresno Vara JA, Casado E, de Castro J, Cejas P, Belda-Iniesta C, Gonzalez-Baron M. PI3K/Akt signalling pathway and cancer. Cancer Treat Rev 2004;30(2):193-204.

6. Gasco M, Shami S, Crook T. The p53 pathway in breast cancer. Breast Cancer Res 2002;4(2):70-6.

7. Santen RJ, Song RX, McPherson R, *et al.* The role of mitogen-activated protein (MAP) kinase in breast cancer. The Journal of steroid biochemistry and molecular biology 2002;80(2):239-56.

8. Segota E, Bukowski RM. The promise of targeted therapy: cancer drugs become more specific. Cleve Clin J Med 2004;71(7):551-60.

9. Alonso MA, Weissman SM. cDNA cloning and sequence of MAL, a hydrophobic protein associated with human T-cell differentiation. Proceedings of the National Academy of Sciences of the United States of America 1987;84(7):1997-2001.

10. Martin-Belmonte F, Kremer L, Albar JP, Marazuela M, Alonso MA. Expression of the MAL gene in the thyroid: the MAL proteolipid, a component of glycolipid-enriched membranes, is apically distributed in thyroid follicles. Endocrinology 1998;139(4):2077-84.

11. Millan J, Alonso MA. MAL, a novel integral membrane protein of human T lymphocytes, associates with glycosylphosphatidylinositol-anchored proteins and Src-like tyrosine kinases. European journal of immunology 1998;28(11):3675-84.

12. Zacchetti D, Peranen J, Murata M, Fiedler K, Simons K. VIP17/MAL, a proteolipid in apical transport vesicles. FEBS letters 1995;377(3):465-9.

13. Puertollano R, Alonso MA. MAL, an integral element of the apical sorting machinery, is an itinerant protein that cycles between the trans-Golgi network and the plasma membrane. Molecular biology of the cell 1999;10(10):3435-47.

14. Sanchez-Pulido L, Martin-Belmonte F, Valencia A, Alonso MA. MARVEL: a conserved domain involved in membrane apposition events. Trends Biochem Sci 2002;27(12):599-601.

15. Schaeren-Wiemers N, Bonnet A, Erb M, *et al.* The raft-associated protein MAL is required for maintenance of proper axon--glia interactions in the central nervous system. The Journal of cell biology 2004;166(5):731-42.

16. Marazuela M, Acevedo A, Adrados M, Garcia-Lopez MA, Alonso MA. Expression of MAL, an integral protein component of the machinery for raft-mediated apical transport, in human epithelia. J Histochem Cytochem 2003;51(5):665-74.

17. Cheong KH, Zacchetti D, Schneeberger EE, Simons K. VIP17/MAL, a lipid raft-associated protein, is involved in apical transport in MDCK cells. Proceedings of the National Academy of Sciences of the United States of America 1999;96(11):6241-8.

18. Martin-Belmonte F, Puertollano R, Millan J, Alonso MA. The MAL proteolipid is necessary for the overall apical delivery of membrane proteins in the polarized epithelial Madin-Darby canine kidney and fischer rat thyroid cell lines. Molecular biology of the cell 2000;11(6):2033-45.

19. Martin-Belmonte F, Arvan P, Alonso MA. MAL mediates apical transport of secretory proteins in polarized epithelial Madin-Darby canine kidney cells. The Journal of biological chemistry 2001;276(52):49337-42.

20. Kamsteeg EJ, Duffield AS, Konings IB, *et al.* MAL decreases the internalization of the aquaporin-2 water channel. Proceedings of the National Academy of Sciences of the United States of America 2007;104(42):16696-701.

21. Hatta M, Nagai H, Okino K, *et al.* Down-regulation of members of glycolipid-enriched membrane raft gene family, MAL and BENE, in cervical squamous cell cancers. The journal of obstetrics and gynaecology research 2004;30(1):53-8.

22. Overmeer RM, Henken FE, Bierkens M, *et al.* Repression of MAL tumour suppressor activity by promoter methylation during cervical carcinogenesis. The Journal of pathology 2009;219(3):327-36.

23. Mimori K, Shiraishi T, Mashino K, *et al.* MAL gene expression in esophageal cancer suppresses motility, invasion and tumorigenicity and enhances apoptosis through the Fas pathway. Oncogene 2003;22(22):3463-71.

24. Beder LB, Gunduz M, Hotomi M, *et al.* T-lymphocyte maturation-associated protein gene as a candidate metastasis suppressor for head and neck squamous cell carcinomas. Cancer Sci 2009;100(5):873-80.

25. Tracey L, Villuendas R, Ortiz P, *et al.* Identification of genes involved in resistance to interferon-alpha in cutaneous T-cell lymphoma. The American journal of pathology 2002;161(5):1825-37.

26. Hsi ED, Sup SJ, Alemany C, *et al.* MAL is expressed in a subset of Hodgkin lymphoma and identifies a population of patients with poor prognosis. American journal of clinical pathology 2006;125(5):776-82.

27. Lind GE, Ahlquist T, Kolberg M, *et al.* Hypermethylated MAL gene - a silent marker of early colon tumorigenesis. J Transl Med 2008;6:13.

28. Buffart TE, Overmeer RM, Steenbergen RD, *et al.* MAL promoter hypermethylation as a novel prognostic marker in gastric cancer. British journal of cancer 2008;99(11):1802-7.

29. Lee PS, Teaberry VS, Bland AE, *et al.* Elevated MAL expression is accompanied by promoter hypomethylation and platinum resistance in epithelial ovarian cancer. Int J Cancer 2009.

30. Berchuck A, Iversen ES, Lancaster JM, *et al.* Patterns of gene expression that characterize long-term survival in advanced stage serous ovarian cancers. Clin Cancer Res 2005;11(10):3686-96.

31. Berchuck A, Iversen ES, Luo J, *et al.* Microarray analysis of early stage serous ovarian cancers shows profiles predictive of favorable outcome. Clin Cancer Res 2009;15(7):2448-55.

32. Brown DA, London E. Functions of lipid rafts in biological membranes. Annu Rev Cell Dev Biol 1998;14:111-36.

33. Simons K, van Meer G. Lipid sorting in epithelial cells. Biochemistry 1988;27(17):6197-202.

34. van Meer G, Simons K. Lipid polarity and sorting in epithelial cells. J Cell Biochem 1988;36(1):51-8.

35. Simons K, Ikonen E. Functional rafts in cell membranes. Nature 1997;387(6633):569-72.

36. Pike LJ. Rafts defined: a report on the Keystone Symposium on Lipid Rafts and Cell Function. Journal of lipid research 2006;47(7):1597-8.

37. Galbiati F, Razani B, Lisanti MP. Emerging themes in lipid rafts and caveolae. Cell 2001;106(4):403-11.

38. Hancock JF. Lipid rafts: contentious only from simplistic standpoints. Nat Rev Mol Cell Biol 2006;7(6):456-62.

39. Brown DA, London E. Structure of detergent-resistant membrane domains: does phase separation occur in biological membranes? Biochemical and biophysical research communications 1997;240(1):1-7.

40. Munro S. Lipid rafts: elusive or illusive? Cell 2003;115(4):377-88.

41. Edidin M. The state of lipid rafts: from model membranes to cells. Annu Rev Biophys Biomol Struct 2003;32:257-83.

42. Lasserre R, Guo XJ, Conchonaud F, *et al.* Raft nanodomains contribute to Akt/PKB plasma membrane recruitment and activation. Nature chemical biology 2008;4(9):538-47.

43. Pike LJ, Han X, Gross RW. Epidermal growth factor receptors are localized to lipid rafts that contain a balance of inner and outer leaflet lipids: a shotgun lipidomics study. The Journal of biological chemistry 2005;280(29):26796-804.

44. Chen X, Resh MD. Cholesterol depletion from the plasma membrane triggers ligand-independent activation of the epidermal growth factor receptor. The Journal of biological chemistry 2002;277(51):49631-7.

45. Lambert S, Vind-Kezunovic D, Karvinen S, Gniadecki R. Ligand-independent activation of the EGFR by lipid raft disruption. The Journal of investigative dermatology 2006;126(5):954-62.

46. Roepstorff K, Thomsen P, Sandvig K, van Deurs B. Sequestration of epidermal growth factor receptors in non-caveolar lipid rafts inhibits ligand binding. The Journal of biological chemistry 2002;277(21):18954-60.

47. Schley PD, Brindley DN, Field CJ. (n-3) PUFA alter raft lipid composition and decrease epidermal growth factor receptor levels in lipid rafts of human breast cancer cells. The Journal of nutrition 2007;137(3):548-53.

48. Liu Y, Sun R, Wan W, *et al.* The involvement of lipid rafts in epidermal growth factor-induced chemotaxis of breast cancer cells. Molecular membrane biology 2007;24(2):91-101.

49. Anton O, Batista A, Millan J, *et al.* An essential role for the MAL protein in targeting Lck to the plasma membrane of human T lymphocytes. J Exp Med 2008;205(13):3201-13.

50. Band V, Zajchowski D, Kulesa V, Sager R. Human papilloma virus DNAs immortalize normal human mammary epithelial cells and reduce their growth factor requirements. Proceedings of the National Academy of Sciences of the United States of America 1990;87(1):463-7.

51. Davis P, Bazar K, Huper G, Lozano G, Marks J, Iglehart JD. Dominance of wild-type p53-mediated transcriptional activation in breast epithelial cells. Oncogene 1996;13(6):1315-22.

52. Silva JM, Li MZ, Chang K, *et al.* Second-generation shRNA libraries covering the mouse and human genomes. Nature genetics 2005;37(11):1281-8.

53. Grunau C, Clark SJ, Rosenthal A. Bisulfite genomic sequencing: systematic investigation of critical experimental parameters. Nucleic acids research 2001;29(13):E65-5.

54. Huang Z, Wen Y, Shandilya R, Marks JR, Berchuck A, Murphy SK. High throughput detection of M6P/IGF2R intronic hypermethylation and LOH in ovarian cancer. Nucleic acids research 2006;34(2):555-63.

55. Brown DA, Rose JK. Sorting of GPI-anchored proteins to glycolipid-enriched membrane subdomains during transport to the apical cell surface. Cell 1992;68(3):533-44.

56. Debnath J, Muthuswamy SK, Brugge JS. Morphogenesis and oncogenesis of MCF-10A mammary epithelial acini grown in three-dimensional basement membrane cultures. Methods (San Diego, Calif 2003;30(3):256-68.

57. Momparler RL. Cancer epigenetics. Oncogene 2003;22(42):6479-83.

58. Baylin SB, Esteller M, Rountree MR, Bachman KE, Schuebel K, Herman JG. Aberrant patterns of DNA methylation, chromatin formation and gene expression in cancer. Human molecular genetics 2001;10(7):687-92.

59. Domann FE, Futscher BW. Flipping the epigenetic switch. The American journal of pathology 2004;164(6):1883-6.

60. Graff JR, Herman JG, Myohanen S, Baylin SB, Vertino PM. Mapping patterns of CpG island methylation in normal and neoplastic cells implicates both upstream and downstream regions in de novo methylation. The Journal of biological chemistry 1997;272(35):22322-9.

61. Tomatsu S, Orii KO, Islam MR, *et al.* Methylation patterns of the human beta-glucuronidase gene locus: boundaries of methylation and general implications for frequent point mutations at CpG dinucleotides. Genomics 2002;79(3):363-75.

62. Jones PA, Baylin SB. The fundamental role of epigenetic events in cancer. Nature reviews 2002;3(6):415-28.

63. Huang E, Cheng SH, Dressman H, *et al.* Gene expression predictors of breast cancer outcomes. Lancet 2003;361(9369):1590-6.

64. Huang KT, Dobrovic A, Fox SB. No evidence for promoter region methylation of the succinate dehydrogenase and fumarate hydratase tumour suppressor genes in breast cancer. BMC Res Notes 2009;2:194.

65. Ostrow KL, Park HL, Hoque MO, *et al.* Pharmacologic unmasking of epigenetically silenced genes in breast cancer. Clin Cancer Res 2009;15(4):1184-91.

66. Leon SA, Shapiro B, Sklaroff DM, Yaros MJ. Free DNA in the serum of cancer patients and the effect of therapy. Cancer research 1977;37(3):646-50.

67. Stroun M, Anker P, Maurice P, Lyautey J, Lederrey C, Beljanski M. Neoplastic characteristics of the DNA found in the plasma of cancer patients. Oncology 1989;46(5):318-22.

68. Esteller M, Sanchez-Cespedes M, Rosell R, Sidransky D, Baylin SB, Herman JG. Detection of aberrant promoter hypermethylation of tumor suppressor genes in serum DNA from non-small cell lung cancer patients. Cancer research 1999;59(1):67-70.

69. Dulaimi E, Hillinck J, Ibanez de Caceres I, Al-Saleem T, Cairns P. Tumor suppressor gene promoter hypermethylation in serum of breast cancer patients. Clin Cancer Res 2004;10(18 Pt 1):6189-93.

70. Deng G, Song GA, Pong E, Sleisenger M, Kim YS. Promoter methylation inhibits APC gene expression by causing changes in chromatin conformation and interfering with the binding of transcription factor CCAAT-binding factor. Cancer research 2004;64(8):2692-8.

71. Tada Y, Brena RM, Hackanson B, Morrison C, Otterson GA, Plass C. Epigenetic modulation of tumor suppressor CCAAT/enhancer binding protein alpha activity in lung cancer. Journal of the National Cancer Institute 2006;98(6):396-406.

72. Schug J. TESS: Transcription Element Search Software on the WWW. http://wwwcbilupenedu/tess; 1997.

73. Comb M, Goodman HM. CpG methylation inhibits proenkephalin gene expression and binding of the transcription factor AP-2. Nucleic acids research 1990;18(13):3975-82.

74. Ballestar E, Wolffe AP. Methyl-CpG-binding proteins. Targeting specific gene repression. European journal of biochemistry / FEBS 2001;268(1):1-6.

75. Ballestar E, Paz MF, Valle L, *et al.* Methyl-CpG binding proteins identify novel sites of epigenetic inactivation in human cancer. The EMBO journal 2003;22(23):6335-45.

76. Lin X, Nelson WG. Methyl-CpG-binding domain protein-2 mediates transcriptional repression associated with hypermethylated GSTP1 CpG islands in MCF-7 breast cancer cells. Cancer research 2003;63(2):498-504.

77. Magdinier F, Wolffe AP. Selective association of the methyl-CpG binding protein MBD2 with the silent p14/p16 locus in human neoplasia. Proceedings of the National Academy of Sciences of the United States of America 2001;98(9):4990-5.

78. Deng G, Peng E, Gum J, Terdiman J, Sleisenger M, Kim YS. Methylation of hMLH1 promoter correlates with the gene silencing with a region-specific manner in colorectal cancer. British journal of cancer 2002;86(4):574-9.

79. Tugores A, Rubio T, Rancano C, Alonso MA. A tandem array of Sp-1 sites and a reverse initiator element are both required for synergistic transcriptional activation of the T-cell-specific MAL gene. DNA and cell biology 1997;16(3):245-55.

80. Issa JP, Garcia-Manero G, Giles FJ, *et al.* Phase 1 study of low-dose prolonged exposure schedules of the hypomethylating agent 5-aza-2'-deoxycytidine (decitabine) in hematopoietic malignancies. Blood 2004;103(5):1635-40.

81. Santini V, Kantarjian HM, Issa JP. Changes in DNA methylation in neoplasia: pathophysiology and therapeutic implications. Annals of internal medicine 2001;134(7):573-86.

82. Szyf M, Pakneshan P, Rabbani SA. DNA demethylation and cancer: therapeutic implications. Cancer letters 2004;211(2):133-43.

83. Wei M, Grushko TA, Dignam J, *et al.* BRCA1 promoter methylation in sporadic breast cancer is associated with reduced BRCA1 copy number and chromosome 17 aneusomy. Cancer research 2005;65(23):10692-9.

84. Hanahan D, Weinberg RA. The hallmarks of cancer. Cell 2000;100(1):57-70.

85. Widschwendter M, Jones PA. DNA methylation and breast carcinogenesis. Oncogene 2002;21(35):5462-82.

86. Dammann R, Yang G, Pfeifer GP. Hypermethylation of the cpG island of Ras association domain family 1A (RASSF1A), a putative tumor suppressor gene from the 3p21.3 locus, occurs in a large percentage of human breast cancers. Cancer research 2001;61(7):3105-9.

87. Shivakumar L, Minna J, Sakamaki T, Pestell R, White MA. The RASSF1A tumor suppressor blocks cell cycle progression and inhibits cyclin D1 accumulation. Molecular and cellular biology 2002;22(12):4309-18.

88. Dreijerink K, Braga E, Kuzmin I, *et al.* The candidate tumor suppressor gene, RASSF1A, from human chromosome 3p21.3 is involved in kidney tumorigenesis. Proceedings of the National Academy of Sciences of the United States of America 2001;98(13):7504-9.

89. Graff JR, Herman JG, Lapidus RG, *et al.* E-cadherin expression is silenced by DNA hypermethylation in human breast and prostate carcinomas. Cancer research 1995;55(22):5195-9.

90. Gould Rothberg BE, Bracken MB. E-cadherin immunohistochemical expression as a prognostic factor in infiltrating ductal carcinoma of the breast: a systematic review and meta-analysis. Breast cancer research and treatment 2006;100(2):139-48.

91. Schuck S, Simons K. Polarized sorting in epithelial cells: raft clustering and the biogenesis of the apical membrane. Journal of cell science 2004;117(Pt 25):5955-64.

92. Bilder D. Epithelial polarity and proliferation control: links from the Drosophila neoplastic tumor suppressors. Genes & development 2004;18(16):1909-25.

93. Liu H, Radisky DC, Bissell MJ. Proliferation and polarity in breast cancer: untying the Gordian knot. Cell cycle (Georgetown, Tex 2005;4(5):646-9.

94. Wang W, Huper G, Guo Y, Murphy SK, Olson JA, Jr., Marks JR. Analysis of methylation-sensitive transcriptome identifies GADD45a as a frequently methylated gene in breast cancer. Oncogene 2005;24(16):2705-14.

95. Bickel PE, Scherer PE, Schnitzer JE, Oh P, Lisanti MP, Lodish HF. Flotillin and epidermal surface antigen define a new family of caveolae-associated integral membrane proteins. The Journal of biological chemistry 1997;272(21):13793-802.

96. Marazuela M, Alonso MA. Expression of MAL and MAL2, two elements of the protein machinery for raft-mediated transport, in normal and neoplastic human tissue. Histology and histopathology 2004;19(3):925-33.

97. Patra SK, Bettuzzi S. Epigenetic DNA-methylation regulation of genes coding for lipid raft-associated components: a role for raft proteins in cell transformation and cancer progression (review). Oncol Rep 2007;17(6):1279-90.

98. Vermeer PD, Einwalter LA, Moninger TO, *et al.* Segregation of receptor and ligand regulates activation of epithelial growth factor receptor. Nature 2003;422(6929):322-6.

99. Simons K, Toomre D. Lipid rafts and signal transduction. Nat Rev Mol Cell Biol 2000;1(1):31-9.

100. Hitosugi T, Sato M, Sasaki K, Umezawa Y. Lipid raft specific knockdown of SRC family kinase activity inhibits cell adhesion and cell cycle progression of breast cancer cells. Cancer research 2007;67(17):8139-48.

101. van Rheenen J, Achame EM, Janssen H, Calafat J, Jalink K. PIP2 signaling in lipid domains: a critical re-evaluation. The EMBO journal 2005;24(9):1664-73.

102. Yuan TL, Cantley LC. PI3K pathway alterations in cancer: variations on a theme. Oncogene 2008;27(41):5497-510.

103. Baillat G, Siret C, Delamarre E, Luis J. Early adhesion induces interaction of FAK and Fyn in lipid domains and activates raft-dependent Akt signaling in SW480 colon cancer cells. Biochimica et biophysica acta 2008.

104. Zhuang L, Lin J, Lu ML, Solomon KR, Freeman MR. Cholesterol-rich lipid rafts mediate akt-regulated survival in prostate cancer cells. Cancer research 2002;62(8):2227-31.

105. Arcaro A, Aubert M, Espinosa del Hierro ME, *et al.* Critical role for lipid raft-associated Src kinases in activation of PI3K-Akt signalling. Cellular signalling 2007;19(5):1081-92.

106. Mineo C, Gill GN, Anderson RG. Regulated migration of epidermal growth factor receptor from caveolae. The Journal of biological chemistry 1999;274(43):30636-43.

107. Prenzel N, Fischer OM, Streit S, Hart S, Ullrich A. The epidermal growth factor receptor family as a central element for cellular signal transduction and diversification. Endocr Relat Cancer 2001;8(1):11-31.

108. Ellis AG, Doherty MM, Walker F, *et al.* Preclinical analysis of the analinoquinazoline AG1478, a specific small molecule inhibitor of EGF receptor tyrosine kinase. Biochemical pharmacology 2006;71(10):1422-34.

109. Han Y, Caday CG, Nanda A, Cavenee WK, Huang HJ. Tyrphostin AG 1478 preferentially inhibits human glioma cells expressing truncated rather than wild-type epidermal growth factor receptors. Cancer research 1996;56(17):3859-61.

110. Zhu XF, Liu ZC, Xie BF, *et al.* EGFR tyrosine kinase inhibitor AG1478 inhibits cell proliferation and arrests cell cycle in nasopharyngeal carcinoma cells. Cancer letters 2001;169(1):27-32.

111. Bianco R, Shin I, Ritter CA, *et al.* Loss of PTEN/MMAC1/TEP in EGF receptor-expressing tumor cells counteracts the antitumor action of EGFR tyrosine kinase inhibitors. Oncogene 2003;22(18):2812-22.

112. She QB, Solit D, Basso A, Moasser MM. Resistance to gefitinib in PTEN-null HER-overexpressing tumor cells can be overcome through restoration of PTEN function or pharmacologic modulation of constitutive phosphatidylinositol 3'-kinase/Akt pathway signaling. Clin Cancer Res 2003;9(12):4340-6.

113. Hollestelle A, Elstrodt F, Nagel JH, Kallemeijn WW, Schutte M. Phosphatidylinositol-3-OH kinase or RAS pathway mutations in human breast cancer cell lines. Mol Cancer Res 2007;5(2):195-201.

114. Li X, Luwor R, Lu Y, Liang K, Fan Z. Enhancement of antitumor activity of the anti-EGF receptor monoclonal antibody cetuximab/C225 by perifosine in PTEN-deficient cancer cells. Oncogene 2006;25(4):525-35.

115. Marty B, Maire V, Gravier E, *et al.* Frequent PTEN genomic alterations and activated phosphatidylinositol 3-kinase pathway in basal-like breast cancer cells. Breast Cancer Res 2008;10(6):R101.

116. Alonso MA, Millan J. The role of lipid rafts in signalling and membrane trafficking in T lymphocytes. Journal of cell science 2001;114(Pt 22):3957-65.

117. Kabouridis PS, Magee AI, Ley SC. S-acylation of LCK protein tyrosine kinase is essential for its signalling function in T lymphocytes. The EMBO journal 1997;16(16):4983-98.

118. Ringerike T, Blystad FD, Levy FO, Madshus IH, Stang E. Cholesterol is important in control of EGF receptor kinase activity but EGF receptors are not concentrated in caveolae. Journal of cell science 2002;115(Pt 6):1331-40.

119. Waugh MG, Lawson D, Hsuan JJ. Epidermal growth factor receptor activation is localized within low-buoyant density, non-caveolar membrane domains. Biochem J 1999;337 (Pt 3):591-7.

120. Remacle-Bonnet M, Garrouste F, Baillat G, Andre F, Marvaldi J, Pommier G. Membrane rafts segregate pro- from anti-apoptotic insulin-like growth factor-I receptor signaling in colon carcinoma cells stimulated by members of the tumor necrosis factor superfamily. The American journal of pathology 2005;167(3):761-73.

121. Stockmans G, Deraedt K, Wildiers H, Moerman P, Paridaens R. Triple-negative breast cancer. Curr Opin Oncol 2008;20(6):614-20.

122. Schneider BP, Winer EP, Foulkes WD, *et al.* Triple-negative breast cancer: risk factors to potential targets. Clin Cancer Res 2008;14(24):8010-8.

123. Lee JS, Kim SY, Kwon CH, Kim YK. EGFR-dependent ERK activation triggers hydrogen peroxide-induced apoptosis in OK renal epithelial cells. Arch Toxicol 2006;80(6):337-46.

124. Bast RC, Jr., Hennessy B, Mills GB. The biology of ovarian cancer: new opportunities for translation. Nat Rev Cancer 2009;9(6):415-28.

125. Schuijer M, Berns EM. TP53 and ovarian cancer. Human mutation 2003;21(3):285-91.

126. Niikura H, Sasano H, Sato S, Yajima A. Expression of epidermal growth factor-related proteins and epidermal growth factor receptor in common epithelial ovarian tumors. Int J Gynecol Pathol 1997;16(1):60-8.

127. Sewell JM, Macleod KG, Ritchie A, Smyth JF, Langdon SP. Targeting the EGF receptor in ovarian cancer with the tyrosine kinase inhibitor ZD 1839 ("Iressa"). British journal of cancer 2002;86(3):456-62.

128. Kurman RJ, Shih Ie M. The origin and pathogenesis of epithelial ovarian cancer: a proposed unifying theory. Am J Surg Pathol 2010;34(3):433-43.

129. Dubeau L. The cell of origin of ovarian epithelial tumours. Lancet Oncol 2008;9(12):1191-7.

130. Salvador S, Gilks B, Kobel M, Huntsman D, Rosen B, Miller D. The fallopian tube: primary site of most pelvic high-grade serous carcinomas. Int J Gynecol Cancer 2009;19(1):58-64.

131. Levanon K, Crum C, Drapkin R. New insights into the pathogenesis of serous ovarian cancer and its clinical impact. J Clin Oncol 2008;26(32):5284-93.

132. Horne HN, Lee PS, Murphy SK, Alonso MA, Olson JA, Jr., Marks JR. Inactivation of the MAL gene in breast cancer is a common event that predicts benefit from adjuvant chemotherapy. Mol Cancer Res 2009;7(2):199-209.

Biography

Hisani N. Horne

Born: Beaufort, SC
September 27, 1982

Education

Duke University Graduate School, Durham, NC, Graduate Student

Department of Pathology, August 2005 – present

Cell and Molecular Biology Program, August 2004 – present

Hampton University, Hampton, VA

Bachelor of Science, Summa Cum Laude, May 2004

Publications

Manuscripts

Horne HN, Murphy SK, Hsueh M, Sheehy O, Alonso MA, Olson JA ad Marks JR. 2010. Exogenous expression of the MAL protein in triple-negative breast cancer cell lines confers sensitivity to EGFR-targeted therapy. *In preparation.*

Horne HN, Lee PS, Murphy SK, Alonso MA, Olson JA and Marks JR. 2009. Inactivation of the MAL gene in breast cancer is a common event that predicts benefit from adjuvant chemotherapy. Molecular Cancer Research. 7(2): 199-209.

Berchuck A, Iversen ES, Luo J, Clarke JP, **Horne H**, et al. 2009. Microarray analysis of early stage serous ovarian cancers demonstrates profiles predictive of favorable outcome. Clinical Cancer Research. 15(7): 2448-2455.

Brylawski BP, Cohen SM, **Horne H**, Irani N, Cordeiro-Stone M, and Kaufman, DG. 2004. Transitions in replication timing in a 340 kb region of human chromosomal r-band 1p36.1. J Cell Biochem 92: 755-769.

Conference Talks and Posters

Horne HN, Lee PS, Murphy SK, Alonso MA, Olson JA and Marks, JR. 2008. Biological Consequences of Aberrant MAL Expression in Breast Cells. Abstract for poster presentation, Duke University Graduate Student Research Symposium, Durham, NC.

Horne HN, Lee P, Murphy SK, and Marks JR 2007. Hypermethylation of the MAL gene promoter in breast cancer. Abstract for poster presentation, American Association for Cancer Research Annual Meeting, Los Angeles, CA.

Horne HN, Murphy S and Marks JR. 2006. Hypermethylation of the MAL gene promoter in breast cancer. Abstract for poster presentation, Duke University Graduate Student Research Symposium, Durham, NC.

Horne HN and Kaufman DG. 2004. Replication timing map of a 145 kb region of human chromosomal band 1p36.1. Abstract for oral presentation, 9th Biennial Symposium on Minorities, the Medically Underserved and Cancer, Washington D.C.

Principal Honors/Awards

NIH/NIGMS Ruth L. Kirschstein National Research Service Award – 2007

American Association for Cancer Research Minority Scholar Award – 2007

Duke University Endowment Fellowship – 2004

Alpha Kappa Alpha Sorority, Incorporated National Scholar Award – 2004

NIGMS Minority Access to Research Careers (MARC) Scholar – 2002